CARBON DIOXIDE CAPTURE METHODS FOR INDUSTRIAL SOURCES: A LITERATURE REVIEW, ENERGY EFFICIENCY AND FEASIBILITY STUDY

By

Khalid Osman

BSc. Eng. (Chemical)

University of KwaZulu Natal, South Africa

Submitted in fulfilment of the academic requirements for the degree of Master of Science in Engineering to the Faculty of Engineering, School of Chemical Engineering, University of KwaZulu-Natal, Durban.

December 2010

Supervisor: Prof. D. Ramjugernath

Co-Supervisor: Dr. C. Coquelet

PREFACE

The work presented in this dissertation was carried out in the Thermodynamic Research Unit in the School of Chemical Engineering at the University of KwaZulu-Natal, Durban, from February 2009 to November 2010 under the supervision of Professor D. Ramjugernath and Doctor C. Coquelet. This thesis is submitted as the full requirement for the degree of Master of Science in Engineering, Chemical Engineering.

I, Khalid Osman, therefore declare that:

(i) The research reported in this dissertation, except where otherwise indicated, is my original work.

(ii) This dissertation has not been submitted for any degree or examination at any other university.

(iii) This dissertation does not contain other persons' data, pictures, graphs or other information, unless specifically acknowledged as being sourced from other persons.

(iv) This dissertation does not contain other persons' writing, unless specifically acknowledged as being sourced from other researchers. Where other written sources have been quoted, then:

a) Their words have been re-written but the general information attributed to them has been referenced.

b) Where their exact words have been used, their writing has been placed inside quotation marks, and referenced.

(v) Where I have reproduced a publication of which I am an author, co-author or editor, I have indicated in detail which part of the publication was actually written by myself alone and have fully referenced such publications.

(vi) This dissertation does not contain text, graphics or tables copied and pasted from the Internet, unless specifically acknowledged, and the source being detailed in the dissertation and in the References sections.

_____

K. Osman

As the candidate's supervisor, I, Prof. D. Ramjugernath, approve this dissertation for submission.

_____

Professor D. Ramjugernath

As the candidate's co-supervisor, I, Dr. C. Coquelet, approve this dissertation for submission.

_____

Dr. C. Coquelet

ACKNOWLEDGEMENTS

بسم الله الرحمن الرحيم

"In the name of God, the Beneficient, the Merciful"

I take this opportunity to acknowledge the following people who have made an invaluable contribution, directly or indirectly, to the completion of this work:

i. My supervisors, Professor D. Ramjugernath of the University of KwaZulu Natal, South Africa, and Dr. C. Coquelet of Mines-Paristech, Fontainebleau, France, for their invaluable guidance, provision, and support.
ii. The National Research Foundation of South Africa for financial assistance.
iii. David Kawesha of SASOL Ltd. for industrial information related to my work.
iv. The laboratory staff of Mines-Paristech, Fontainebleau, France, for their technical assistance for the experimental aspects of this work. This includes Eric Booneart, Waheed Afzal, Javeed Awan, Veronica Belandria, Elise El Ahmar, Alan Valtz, and Albert Chareton, who made my work and stay in France a successful and pleasant experience.
v. Samuel Ayodele Iwarere for assistance in the modelling aspects of this work.
vi. My family, fellow postgraduate colleagues, and friends.
vii. And importantly, my mum, Zubaida Bibi Osman, dad, Essa Osman, and grandfather, Osman Mohammed Essop, for their unyielding love, support, encouragement, motivation, and belief in me even in the most difficult of times in this work, and in my life. I stand tall today only because I stand on the shoulders of giants. I will always love you.
viii. Finally, my Lord, Creator and Sustainer, Allah (Almighty and Glorious is He) and His exalted messenger, Muhammed (Upon whom be peace), who have made my life and continued success a reality.

"Therefore glory be unto Him, in Whose Hands is the dominion of all things, and unto Him is our return" – Quran (36:83).

ABSTRACT

In order to reduce the rate of climate change, particularly global warming, it is imperative that industries reduce their carbon dioxide (CO_2) emissions.

A promising solution of CO_2 emission reduction is Carbon dioxide Capture and Storage (CCS) by sequestration, which involves isolating and extracting CO_2 from the flue gases of various industrial processes, and thereafter burying the CO_2 underground.

The capture of CO_2 proved to be the most challenging aspect of CCS. Thus, the objective of this research was to identify the most promising solution to capture CO_2 from industrial processes. The study focussed on capturing CO_2 emitted by coal power plants, coal-to-liquids (CTL) and gas-to-liquids (GTL) industries, which are common CO_2 emitters in South Africa.

This thesis consists firstly of an extensive literature review detailing the above mentioned processes, the modes of CO_2 capture, and the various CO_2 capture methods that are currently being investigated around the world, together with their benefits and drawbacks in terms of energy penalty, CO_2 loading, absorption rate, capture efficiency, investment costs, and operating costs. Modelling, simulation, and pilot plant efforts are also described.

The study reviewed many CO_2 capture techniques including solvent absorption, sorbent capture, membrane usage, hydrate formation, and newly emerging capture techniques such as enzyme based systems, ionic liquids, low temperature cryogenics, CO_2 anti-sublimation, artificial photosynthesis, integrated gasification steam cycle (IGSC), and chemical looping combustion

The technique of solvent absorption was found to be the most promising for South African industries. Vapour-liquid-equilibrium (VLE) measurements of solvent absorption using amine blends were undertaken, using blends of methyl-diethanol amine (MDEA), diethanol amine (DEA) and water (H_2O) with composition ratios of 25: 25: 50 wt% and 30: 20: 50 wt% respectively, and with CO_2 and N_2 gases at CO_2 partial pressures of 0.5 to 10.5 bar. Experiments were conducted under system pressures of 5 to 15 bar and temperatures of 363.15 and 413.15 K, using a static analytic apparatus. CO_2 liquid loading results were analysed and discussed.

The experimental data were regressed in Matlab (R2009b) using the Posey-Tapperson-Rochelle model and the Deshmukh-Mather model. The Matlab programmes are presented along with the regressed binary interaction and model parameters. The accuracy of model predictions are discussed.

Thereafter an Electrolyte-NRTL model regression and simulation of the absorption process was conducted using Aspen Plus V 7.1. for flue gas compositions, solvent compositions, temperature, and pressure conditions similar to that of process operating conditions. CO_2 loading, design factors, CO_2 recovery, and CO_2 purity results were analysed and compared

where appropriate, with experimental results. Finally a general preliminary energy efficiency and cost analysis was conducted based on the simulation results.

The main conclusions reached are that the amine solvent blend containing 25:25:50 wt% of MDEA:DEA:H_2O, produced higher CO_2 loadings for its respective system conditions than other solvents studied and those found in literature. However, absorption of CO_2 was found to be highly dependent on system temperature and pressure.

The Deshmukh-Mather model provided higher accuracy than the Posey-Tapperson-Rochelle model, producing CO_2 loading predictions with a relative error not exceeding 0.04%, in 1.5 to 3 minutes using a dual core processor.

Aspen absorption simulations provided significantly lower CO_2 loading results than those experimentally obtained, due to the low contact time achieved and higher temperature dependence in the proposed absorption process. Process improvements were highlighted and implemented to increase CO_2 recovery and purity. Energy penalty values were found to be higher than those found in literature, but room for process and design improvement was identified and recommendations were given. Investment cost estimates were found to be justifiable and within reason. Limitations of the simulation were also identified and discussed.

TABLE OF CONTENTS

Section **Page**

Section **Page**

Section **Page**

APPENDICES

LIST OF FIGURES

Figure **Page**

Chapter 1

Chapter 2

Chapter 3

Chapter 4

Figure **Page**

Figure **Page**

Appendix A:

Figure **Page**

Appendix B:

Appendix E:

LIST OF TABLES

Table **Page**

Chapter 2

Chapter 3

Appendix A

Appendix B

Table **Page**

Appendix D

Appendix F

Appendix G

Table **Page**

Appendix H

NOMENCLATURE

x : Liquid mole fraction

y : Vapour mole fraction

X : Liquid mole fraction in charged solvent

P : Total system pressure (bar)

P_i : Partial pressure of component i (bar)

H_i : Henry's constant of component i

T : System temperature (K)

V: Volume (cm^3)

V_C^V : Vapour volume in cell (cm^3)

V_C^L: Liquid volume in cell (cm^3)

P_{CO2}^1 : Pressure of CO_2 cylinder before charging (bar)

P_{CO2}^2 : Pressure of CO_2 cylinder after charging (bar)

n : Number of moles (mol)

m : Mass (kg)

M : Molar mass (g/mol)

L : CO_2 loading

v : Molar volume (dm^3/mol)

v_T^V : Total molar volume (dm^3/mol)

K : Equilibrium constant

Z : Electric charge

$B_{i,j}$: Binary interaction parameter between molecular and ionic species that exist in the system.

F = Faraday's Constant (C/mol)

N_A = Avogadro number (mol^{-1})

C = Species concentration

G : Gibb's energy

g^E : Excess Gibb's energy

Greek Letters:

ρ : Density (g/cm^3)

γ_i : Activity coefficient of species i

α : CO_2 gas loading (mol CO_2/mol gas)

ρ_{CO2} : Density of CO_2 in cylinder (g/cm^3)

ε_O = Vacuum permittivity (F/m)

Subscripts

i, j : Components/species

k : Reaction number

m, m' : Molecular species;

a, a', a'' : Anion species;

c, c', c'' : Cation species;

CO_2 : Carbon dioxide

S : Solvent

T : Total

C : Equilibrium cell

Superscripts

V : Vapour

L : Liquid

1 : Before charging into equilibrium cell

2 : After charging into equilibrium cell.

1. INTRODUCTION

Climate change is inevitable. It is affected by naturally occurring factors such as El Nino, volcanism and solar radiation. This change in climate is often slow, hence most species on earth can adapt to such changes. However, if climate change occurs too quickly, it may have disastrous effects.

The primary climate change problem that currently prevails is the issue of global warming, which refers to a rise in the overall temperature at the surface of the earth. The past 30 years have seen a global temperature increase of 0.2 K per decade (Hansen et al., 2006).

The reason for this increase in the earth's surface temperature is the increasing concentrations of carbon dioxide (CO_2) gas in the earth's atmosphere. Atmospheric CO_2 traps heat from the sun, resulting in an increased global temperature, in the same way as heat is trapped in a greenhouse by the glass, metal, or plastic structure that encloses it. For this reason, the trapping of heat by atmospheric CO_2, is commonly known as the greenhouse effect, and CO_2 is referred to as a greenhouse gas.

While there are many other gases that result in a greenhouse effect, CO_2 receives the most attention because it exists in far higher concentrations than other greenhouse gases. In 2008, the CO_2 concentration in the atmosphere stood at 383.9 ppm (CDIAC, 2008), a 37 % increase since the beginning of the industrial revolution of the late 18^{th} century. A further consequence of this increasing CO_2 concentration is that the pH of the earth's oceans has decreased by 0.1 units since the industrial revolution (Mongabay, 2008). This threatens marine life, while global warming caused by the greenhouse effect results in increasing sea levels due to melting polar ice. A change of this nature and pace is a danger to many species on earth, including mankind. A solution to reduce this rapid climate change is thus important.

The primary cause of high CO_2 emissions, and the resultant increase in CO_2 concentration, is the burning of fossil fuels. Most countries throughout the world are dependent on fossil fuels for their daily operation. The transportation sector, electricity sector, and all other processes requiring extreme heating or mechanical operation use fossil fuels, and in doing so, emit CO_2 to varying degrees. It is estimated that 29 381 Mt (mega tonnes) of CO_2 was emitted worldwide in 2008, a sharp increase from 15 643 Mt in 1971 (IEA, 2010).

It was found that 78 to 83 % of CO_2 emissions ultimately stem from the burning of fossil fuels to generate electricity, while as much as 9 % account from petrochemical production and gas processing worldwide (Figueroa et al., 2007). If these industries can reduce their CO_2 emissions, the impact on global warming would be highly significant.

The ultimate long term solution to this problem is a divergence from the use of fossil fuels and a change towards cleaner sources of energy, such as wind, hydro or geothermal power. This radical change, however, requires much capital expenditure and research, which many developing nations cannot afford.

A promising alternative solution for the above mentioned industries to reduce CO_2 emissions, especially in the short term, is carbon dioxide capture and storage (CCS) by sequestration. This idea entails the direct capture of CO_2 from power plants and other industrial flue gases, its compression and transportation, and finally its subsequent underground sequestration. Refer to Figure 1-1 below for an illustration:

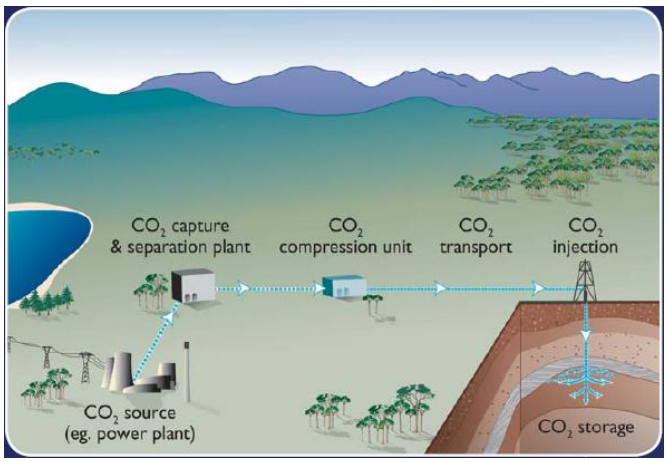

Figure 1-1: Illustration of Carbon Dioxide Capture and Storage by Sequestration (CCS) (IPCC, 2004)

As Figure 1-1 illustrates, sequestration involves the compression, transport and injection of CO_2 underground. Compression may be done using compressors and refrigeration techniques. The cheapest way to transport CO_2 is through pipelines. The CO_2 needs to be injected through permeable and porous rock and trapped in cap rock or fault trap formations (IPCC, 2004). South Africa can fortunately accommodate this procedure. The Vryheid and Katberg formation are good sites to store CO_2, for millions of years (Surridge, 2005).

Most of the costs for this process are attributed to the capture and separation of CO_2 from the industrial CO_2 source, before it can be compressed, transported, and stored (IEA, 2004). Hence, much research into techniques of capturing CO_2 in an energy efficient and feasible manner needs to be conducted.

The aim of this study was to identify all options for CO_2 capture from the flue gases that are emitted by various industrial processes, and to further identify the most feasible option suited to major industrial CO_2 emitting processes in developing nations, particularly South Africa.

Carbon dioxide capture and storage is a relatively new concept to developing countries and South Africa is no exception. The objective of this study was thus to conduct an extensive literature review of all CO_2 capture processes, current and new. Upon choosing the best method of CO_2 capture, experimentation, data modelling, and simulations were conducted to confirm its applicability to South African industries.

This study focuses on CO_2 capture from flue gases that are emitted from coal power plants, coal-to-liquids Fischer Tropsch (CTL-FT) plants and gas-to-liquids Fischer Tropsch (GTL-FT) plants, which are the main emitters of CO_2 in South Africa (Surridge, 2005 and (Figueroa et al., 2007). Although not the main focus, the study is also applicable to natural gas processing.

It is estimated that 42.9 % of CO_2 is emitted by coal industries worldwide, while 19.9% of CO_2 is emitted by gas industries (IEA, 2010). The importance of this study is hence not only limited to South African industries, but to all coal and gas industries worldwide.

This thesis first presents a detailed literature review regarding the above-mentioned industries, the factors that influence the implementation of CO_2 capture, and the various CO_2 capture techniques that are currently being investigated around the world.

Upon completion of this research, it was found that solvent absorption using amine blends showed the most promise as a viable CO_2 capture technique for South African industries. Further literature review into this technique commenced, detailing the theoretical background of amine absorption, measurements that were made regarding the technique, modelling of absorption measurements, and simulations of solvent absorption that were attempted by various literature sources.

A programme of measurement was set up and VLE data were measured for the absorption of CO_2 in amine solvent blends of methyl-diethanol amine (MDEA), diethanol amine (DEA), and H_2O, at various CO_2 partial pressures and at temperatures of 363.15 K and 413.15 K.

The VLE measurements were then modelled in Matlab V. R2009b using the Posey-Tapperson-Rochelle model and the Deshmukh-Mather model.

Finally a basic simulation of the solvent absorption process was conducted in Aspen Plus Engineering Suite, using the Electrolyte Non-Random Two Liquid (Elec-NRTL) model, to predict the overall efficiency of the process for CO_2 capture, and provide an indication of the capital cost, energy penalty and feasibility of solvent absorption as a CO_2 capture technique.

The results of all above-mentioned endeavours are presented and discussed in this thesis. Recommendations are made in each aspect of this thesis, while conclusions are summarized at the end of the discussion.

2. LITERATURE REVIEW

Carbon dioxide capture and storage by sequestration (CCS) is at present not a popular concept in South African industries (Surridge, 2005). CCS projects have been spearheaded mainly by developed countries, with success being achieved particularly in pilot plants in Austria (Knudsen et al., 2008) and the Netherlands (VNS, 2008).

An extensive literature review detailing all the available options under investigation is required to keep South African industries informed and up to date on the various developments and progress made regarding CCS, particularly carbon dioxide (CO_2) capture techniques which would require the most participation on the part of these various industries. Another objective of this review is to determine the CO_2 capture technique that would be best suited and most promising for industries in developing nations such as South Africa.

As mentioned before, the primary emitters of greenhouse gases such as CO_2 in South Africa are the coal power plants, coal-to-liquids (GTL), and gas-to-liquids (GTL) processes. It is of urgent concern to develop CCS in light of these industries, to reduce South Africa's carbon footprint substantially. This chapter begins with a review of the above-mentioned processes. A CO_2 capture process has to be installed within these above-mentioned processes.

Three CO_2 capture modes were identified, where CO_2 capture processes can be installed within CTL, GTL and coal power plant processes. These modes are Post Combustion/Reaction CO_2 capture (flue gases are treated for CO_2 after the combustion/reaction process), Pre-Combustion/Reaction CO_2 capture (CO_2 capture occurs upstream of the reaction/combustion process), and Oxy-fuel Combustion (combustion occurs in the presence of pure O_2 instead of air, producing a CO_2:H_2O stream which can be easily separated). These capture modes are discussed in detail in this chapter.

Thereafter, concerns regarding the installation of CO_2 capture processes are summarized. These concerns are related mainly to safety, energy efficiency and feasibility of the process in question.

The following section of this chapter addresses, in detail, the various CO_2 capture techniques that are currently under development. This includes relatively well-developed techniques such as solvent absorption, sorbent usage, membrane usage, and hydrate formation, as well as newly emerging techniques such as enzyme based systems, ionic liquids, low temperature cryogenics, CO_2 anti-sublimation, artificial photosynthesis, integrated gasification steam cycle, and chemical looping combustion.

Each capture technique was researched and analysed with respect to its applicability to the industries mentioned above, its benefits and drawbacks, its degree of development and resultant

availability of comprehensive information, and on whether the technique has been implemented successfully on an industrial or pilot scale plant. Important data drawn from the review of these techniques are presented as well.

Upon reviewing all CO_2 capture techniques, it would be shown that solvent absorption using amine solvents is the best solution for CO_2 capture in South African industries. The reasons for this choice are discussed in this chapter. Thereafter, a detailed literature review is presented, focussing on this technique. A programme of measurement was drawn up to obtain VLE data for a gas mixture of CO_2 and N_2, and a solvent mixture of methyl-diethanol amine (MDEA), diethanol amine (DEA), and H_2O. This is done to investigate the amount of CO_2 that could be absorbed by the solvent and hence separated from the gas mixture. The programme of measurement is presented in this chapter.

The modelling of the data obtained, are discussed thereafter, focussing on the use of the Posey-Tapperson-Rochelle model, the Deshmukh-Mather model, and the Electrolyte-Non-Random Two Liquid (Elec-NRTL) model. The theory behind these models is discussed in detail.

Finally, a simulation using Aspen Plus Engineering suite was attempted, in order to obtain an indication of the technique's success and feasibility in an industrial situation. A literature review of Aspen simulations regarding solvent absorption is presented in this chapter. The chapter concludes with a brief description of the particular simulations that were conducting in this study.

2.1 A review of coal power plants

A good understanding of the main CO_2 emitting industries in South Africa is required in order to find successful solutions to lowering their emissions. This section discusses coal power plant processes.

There are two main categories of coal power plants: Pulverised coal (PC) power plants and Integrated Gasification Combined Cycle (IGCC) power plants.

2.1.1 Pulverised coal power plants

Refer to Figure 2-1. Coal is conveyed to a bunker using a conveyor belt or hopper. From the bunker, the coal is pulverised and then blasted into the furnace where it burns in the presence of air. The resulting gas being emitted drives turbines. The gas is then treated to remove ash and sulphurous compounds.

In the original setup (i.e. without CO_2 capture), the stack gas is emitted at the end as shown. However, with CO_2 capture, a capture process may be installed after the stack to treat the flue gas to remove CO_2. This downstream processing of flue gas is known as post-combustion capture, which will be explained in Section 2.3.1.

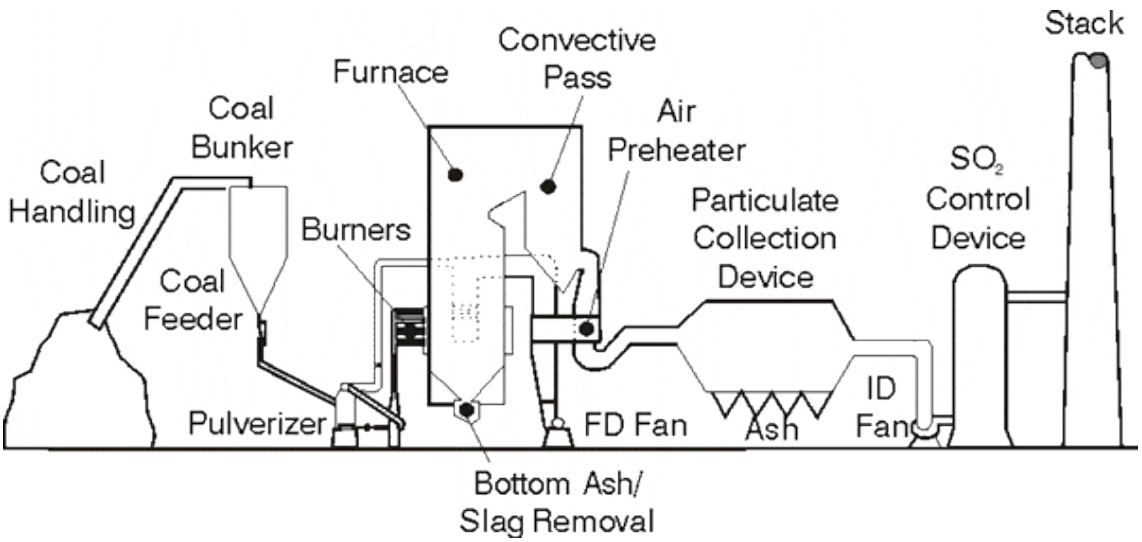

Figure 2-1: Illustration of a Typical Pulverised Coal Combustion Process (CARC, 2008)

2.1.2 Integrated Gasification Combined Cycle (IGCC) power plants

Refer to Figure 2-2. The process differs quite significantly from PC fired power plants. Coal is sent to a gasifier to produce syngas, which is a mixture of CO, CO_2, and H_2 gas. The syngas is then treated for impurities such as dust and sulphurous compounds. Thereafter the syngas is sent to a shift converter, to increase the hydrogen content by the following reaction:

$$CO + H_2O \rightarrow CO_2 + H_2 \qquad \text{(R2-1)}$$

(393.15 – 623.15 K; 150 bar) (Kanniche and Bouallou, 2007)

The CO_2 gas is then separated and H_2 gas drives turbines and is then emitted through a stack.

The IGCC process with CO_2 capture, by lab experiments and cost prediction (Gielen, 2003), is claimed to be more cost effective by 25 - 40 %, since the syngas streams have relatively high CO_2 concentration. Hence the construction of IGCC plants in the future, as opposed to PC plants, seems promising.

CO_2 capture may occur after shift conversion, as a post-combustion/reaction capture process.

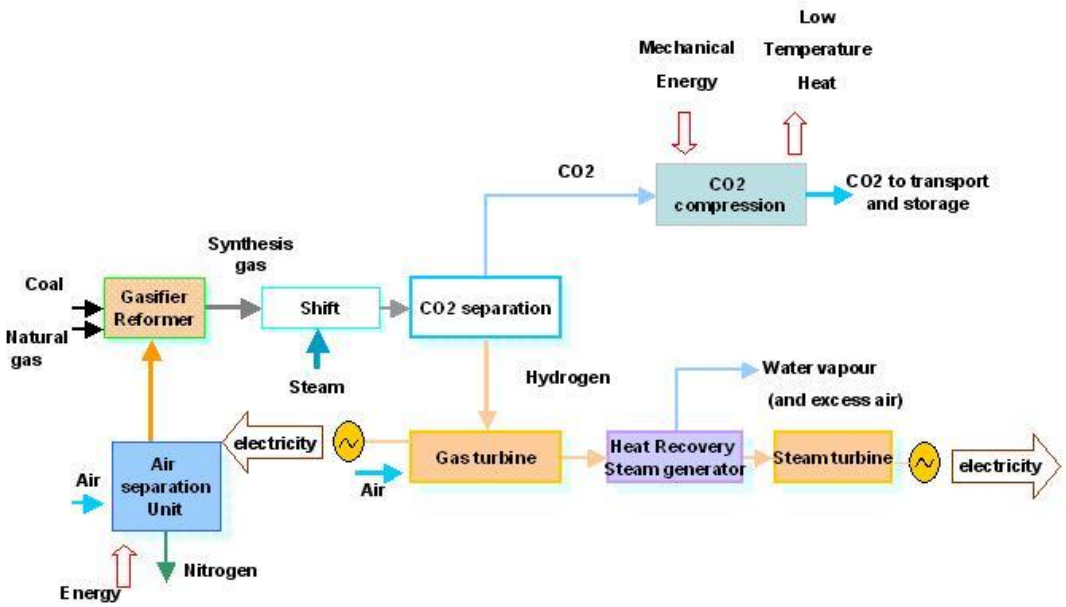

Figure 2-2: Integrated Gasification Combined Cycle Illustration (ENCAP, 2008)

2.2 A review of CTL and GTL processes

As an alternative to producing fuel from crude oil, coal-to-liquid (CTL) processes convert coal into liquid products such as petroleum and paraffins. Gas-to-liquid (GTL) processes achieve the same products with the use of natural gas, composed primarily of methane.

South Africa has become a pioneer in coal and natural gas processes due to the abundance of these natural resources in the region. However, CTL and GTL industries, together with coal power plants, have become the highest emitters of CO_2 in South Africa (Surridge, 2005). A good understanding of these processes is essential in order to obtain viable solutions for reducing CO_2 emissions.

2.2.1 The coal-to-liquids (CTL) process

The CTL process has some similarities to the IGCC process, but the aim is different. IGCC processes aim to produce electricity, while CTL processes aim to produce liquid hydrocarbons. Refer to Figure 2-3.

In the CTL process, coal is gasified, creating syngas of primarily CO, H_2 and some CO_2. Although not shown in Figure 2-3, the syngas is often sent to a shift converter (as for IGCC in Figure 2-2) to increase the H_2 content for hydrogenation, at the expense of excess CO. CO_2 is formed as a by-product. Thereafter the syngas is treated for impurities.

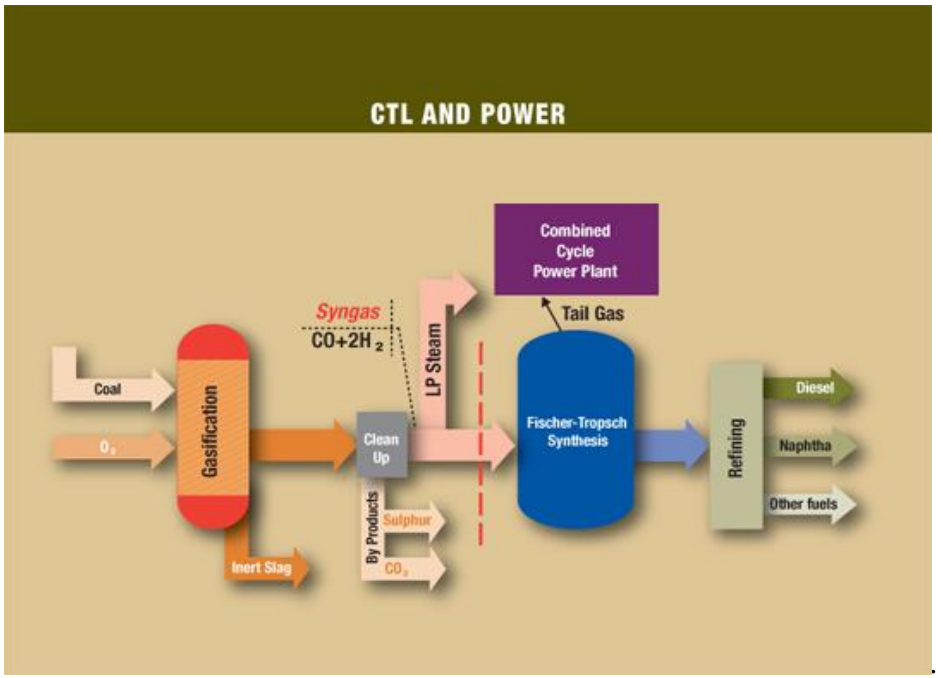

Figure 2-3: A Coal-to-Liquids Process Illustration (Altona, 2008)

In the absence of CO_2 capture, it is only sulphurous and nitrogenous compounds that are removed. However, some techniques for sulphur removal can also remove CO_2, but to a limited degree (~0.15 % of total CO_2 (Van Bibber et al., 2007).

Once the syngas is treated, it is sent to a Fischer Tropsch (FT) reactor for conversion to hydrocarbons, by the following general reaction:

$$CO + 2.15H_2 \rightarrow \text{hydrocarbons} + H_2O \qquad \text{(R2-2)}$$

The type of FT reactor (Low Temperature (393.15 K) or High Temperature (623.15 K)), the operating conditions, and the catalyst dictate the reactions that occur and the specific hydrocarbon products formed, as well as if any CO_2 may be formed as well. The H_2/CO ratio is typically 2.15 (Dry, 2002). Cobalt catalysts ensure dominance of reaction R2-2. If iron based catalysts are used, the water gas shift reaction (R2-1) occurs to a greater extent, albeit still lower than R2-2 (Dry, 2002).

2.2.2 The gas-to-liquids (GTL) process

Refer to Figure 2-4. The GTL process involves the treatment of natural gas and thereafter conversion to hydrocarbons. The treatment of the natural gas differs depending on its composition. Generally, the natural gas is sent to a reformer. Air is generally used during reforming but the use of pure O_2 gas is also an option. Reforming is done to produce syngas, a mixture of CO, CO_2 and H_2. The syngas is sent to a Fischer Tropsch reactor to produce liquid hydrocarbons.

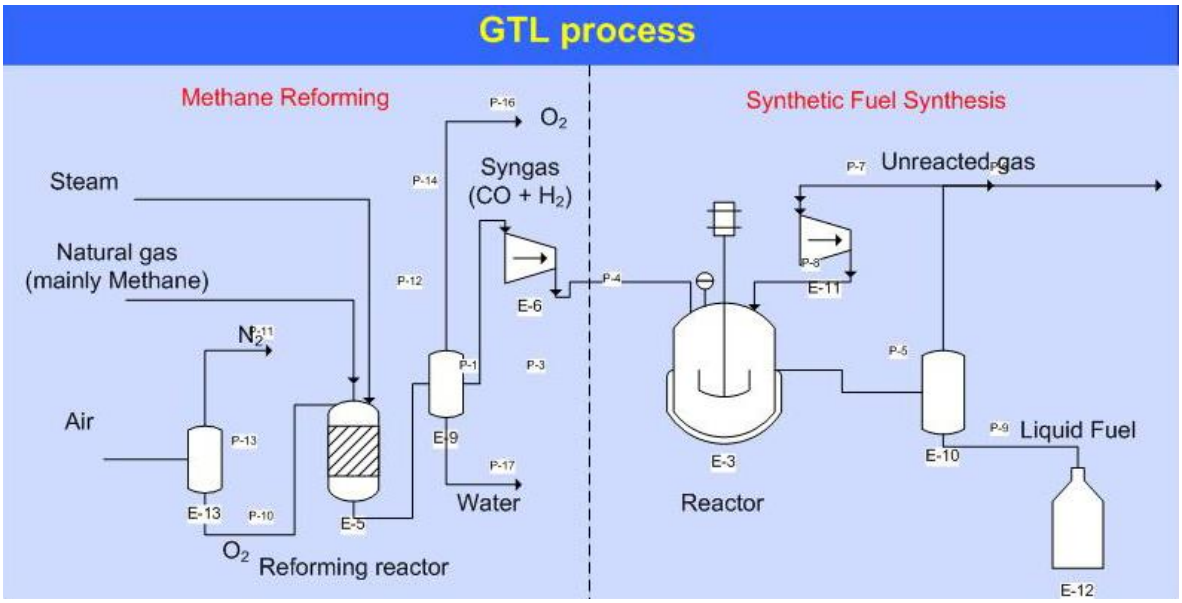

Figure 2-4: A Gas-to-Liquids Process Illustration (CSFRU, 2008)

CTL and GTL processes can be modified or retro-fitted in many different ways to reduce CO_2 emission. There are three modes of CO_2 capture: Post Combustion/Reaction Capture, Pre-Combustion/Reaction Capture, and Oxyfuel Combustion Capture.

2.3 Basic capture modes

The modes of CO_2 capture refer either to the location in an industrial process where CO_2 gas may be isolated and removed, or changes in combustion/reaction processes that allow CO_2 to be removed more efficiently. A good understanding of these modes is imperative, as many CO_2 capture techniques under investigation can only be applied successfully in certain modes of operation. Three main capture modes are discussed in this section, along with the benefits and drawbacks of these modes.

2.3.1 Post-combustion/reaction capture

This capture mode involves the treatment of flue gas that is being emitted from the combustion process. In Figures 2-1 and 2-2, CO_2 capture would take place after the stack, for a PC fired and IGCC power plant respectively.

For CTL and GTL processes (Figures 2-3 and 2-4 respectively), the flue gas emitted from the FT reactor, is treated.

The capture process is installed generally after desulphurisation and denitrogenation of the flue gas. This location of installation is advantageous as the capture process does not alter the rest of the process in terms of product purity and process parameters. The disadvantage is that the CO_2

composition of the emitted flue gas is typically low (<15 vol% (Descamps et al., 2008)). The pressure is also often as low as atmospheric pressure. This makes CO_2 capture difficult and often inefficient. Due to the low pressure, much energy is needed for CO_2 compression thereafter.

2.3.2 Pre-combustion/reaction capture

Pre-combustion capture refers to the capture of CO_2 upstream of the combustion/reaction process. This mode is applicable only to IGCC, CTL and GTL processes. Refer to Figure 2-2. For IGCC, pre-combustion capture generally occurs during the syngas cleanup process, after shift conversion. Depending on the syngas, this cleanup may entail denitrification and desulphurisation before CO_2 capture.

Refer to Figure 2-3. Pre-reaction capture is shown after gasification for CTL processes. If shift conversion is included in the process, then the syngas cleanup will occur after it. For GTL processes, the location of CO_2 capture varies. It can occur after reforming or after separation of CO_2. In all cases, the capture occurs before the FT reaction process.

The main advantage of pre-combustion/reaction capture is that the syngas stream to be treated typically contains a high concentration of CO_2 (> 15 %). This is reported to provide easier CO_2 capture. The capture process can have greater energy efficiency and hence a lower running cost (IEA, 2007).

The sad truth is that the CTL and GTL processes are not common worldwide and IGCC processes are comparatively new, with some modifications still being in the research phase. Most power plants are PC power plants. To change such processes to IGCC to accommodate pre-combustion capture, would require an extremely high capital investment. As previously mentioned however, IGCC is claimed to be more cost effective due to the high CO_2 concentration in the syngas. The development and optimisation of IGCC is expected to provide further interest in the industrial application of pre-combustion/reaction capture.

Another disadvantage with employing capture techniques in pre-combustion/reaction mode is that the syngas is treated before combustion/reaction. This changes the conditions of the feed to the combustor/reactor. These altered conditions need to be accommodated in the process. It is for this reason that pre-combustion/reaction capture has not generally been preferred to post-combustion/reaction even in CTL and GTL processes.

2.3.3 Oxyfuel combustion capture

Oxyfuel combustion refers to the burning of coal in pure (or nearly pure) oxygen, as opposed to air. It is a modification of the conventional PC power plant.

Refer to Figure 2-5 (EON, 2007). Air is first passed through as air separation unit (ASU). Usually cryogenic air separation is employed. From the ASU, oxygen is burned with coal in a combustor. The flue gas emanating from combustion is treated for CO_2.

The advantage of burning coal in pure oxygen is that the flue gas stream that emanates from the combustor consists mainly of CO_2 and water vapour (Figueroa et al., 2007). CO_2 can be separated from the water by partial condensation of the flue gas stream, and thereafter compressed and transported. The added advantage is that the CO_2 concentration in the flue gas is relatively high (Davison, 2006), assisting in increasing capture efficiency. CO_2 capture occurs after combustion.

The increased capture efficiency is offset by the energy needed to produce pure oxygen. Air separation requires increased energy. Moreover, oxyfuel combustion alters the conventional pulverised coal combustion process. This modification requires increased capital investment, which deters its use. Thus, oxyfuel combustion shall only be feasible in the long term, for new power plants.

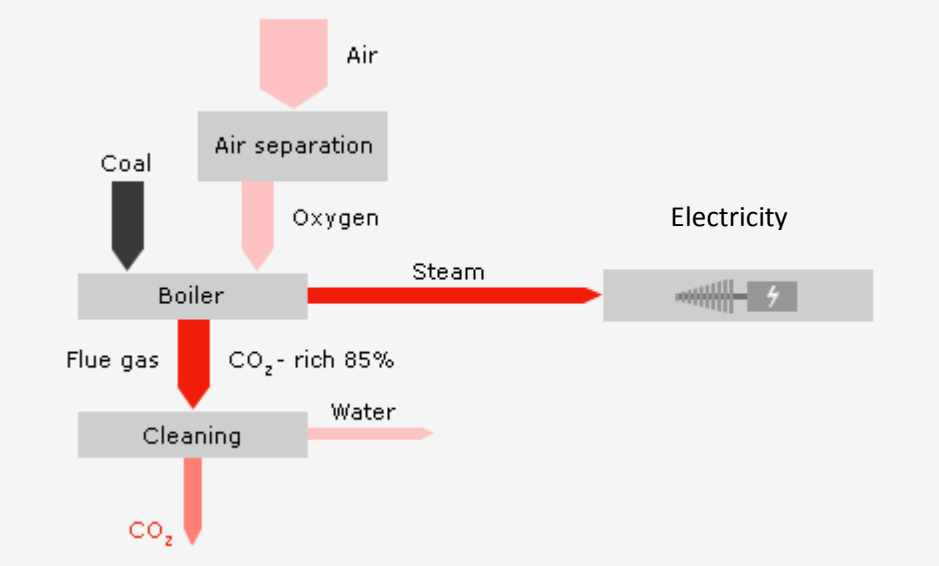

Figure 2-5: An Oxy-fuel Combustion Process Illustration (EON, 2007)

2.4 Concerns regarding CO_2 capture techniques

There are many different techniques that can be used to capture CO_2 from flue gas (or syngas) streams. However, many of these techniques have not been found to be feasible thus far. Davison (2006) and GPA (2004) have summarised a few factors affecting capture technologies. The issues affecting the feasibility and implementation of capture techniques can be summarized as follows:

- The investment cost of purchasing and installing capture equipment. If the operating cost of the capture process is promising, then the venture may seem encouraging despite the initial

capital expenditure.

- The amount of space available to safely accommodate the capture equipment.
- The cost of solvents, membranes etc. (if any) associated with the capture of CO_2. This is of particular importance if the solvents or membranes used cannot be regenerated over a substantial number of cycles.
- The properties of solvents. This regards issues of safety with handling and corrosion with equipment.
- The amount of energy required to support the capture process. This includes heat energy, often provided by steam, and compression energy for CO_2 transportation after capture and separation. Some capture methods also require refrigeration. The amount of energy needed forms the largest aspect of operating costs.
- The complexity of the technique. Higher complexity generally means higher energy usage, higher investment costs, larger space, and sometimes substantial change to downstream processing efficiency (this depends on the mode of capture).
- The degree of development of the capture technique and the associated certainty of estimates (capital and operating costs, safety aspects etc.). A highly complex process also introduces substantial doubt in the accuracy of cost estimates and hence the success of the venture, which is ultimately a deterrent to investors.
- The overall operating cost of CCS is the ultimate deciding factor as to whether the capture technique will be feasible or not. A technique having a high energy penalty, and hence a high operating cost, can reduce overall plant feasibility substantially. An inherently unsafe technique requires extra safety measures and further monitoring by personnel, which may require extra employment. If the operating costs are too high, plant output can be decreased or products will be produced at substantially higher costs, effectively making a company less competitive.

The success of the implementation of CCS depends on the optimisation of the above factors. The purpose of this study was to perform an extensive literature review to identify the most promising capture techniques that can be implemented on CTL, GTL and coal combustion processes, especially in South Africa. The experimentation and associated efficiency study shall be designed once such techniques are identified, in order to prove their success.

2.5 CO_2 capture techniques

This section contains details regarding the various CO_2 capture techniques that are currently being investigated around the world. The theory of these techniques, the developmental maturity, the benefits, and drawbacks of these techniques are discussed.

2.5.1 Solvent absorption

The technique of solvent absorption entails the use of liquid solvents to absorb CO_2 from the flue gas. Refer to Figure 2-6 (Figueroa et al., 2007). Flue gas passes through an absorber counter-currently with a solvent, which absorbs CO_2. The treated flue gas may then be emitted to the atmosphere and the solvent goes to a stripper where it is heated to release the CO_2. A flash can be used instead of a stripper if CO_2 concentrations are high in the solvent. The CO_2 is compressed and transported and the solvent, now regenerated, is recycled to the absorber.

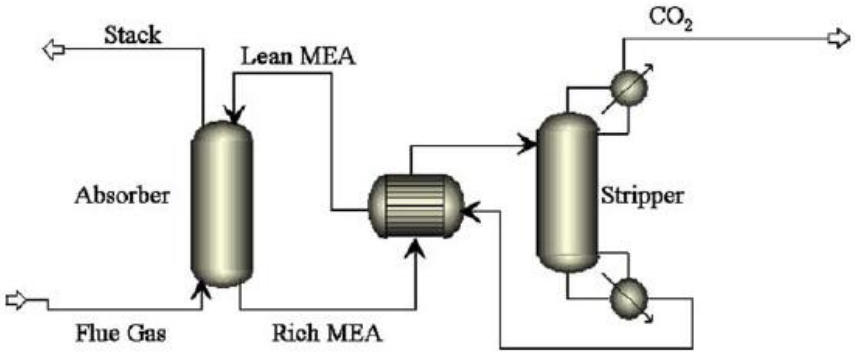

Figure 2-6: An Illustration of a Typical Solvent Absorption Process (Figueroa et al., 2007)

There are two categories of solvents: chemical solvents and physical solvents. There are also hybrid solvents, which are mixtures of chemical and physical solvents, as well as blends, which are mixtures of two or more solvents of the same nature.

2.5.1.1 Chemical solvents

With chemical solvents, CO_2 is absorbed and exists as another compound in the solvent, and only becomes CO_2 again, upon regeneration of the solvent (reactive absorption). Ammonia (NH_3) was the first solvent under investigation. It was found to be corrosive and the required saturation pressure was too high (Figueroa et al., 2007). Today, the most popular chemical solvents are amine based, although many carbonate solvents are researched as well. Common amine based solvents being researched are Mono-ethanolamine (MEA), Di-ethanolamine (DEA), and Methyl-di-ethanolamine (MDEA). They absorb CO_2 in the following overall manner:

$$CO_2 + 2R_2NH \longleftrightarrow R_2NH_2^+ + R_2NCOO^- \qquad \text{(R2-3)}$$ (Miller et al., 2005, pg 377)

The reaction is exothermic. Regeneration is done by heating the CO_2 rich solvent and hence reversing the reaction, in a stripper. Kinetics are provided by Manuel et al., 1998. Other amine solvents under investigation are tabulated below along with popular amine solvents (GPA, 2004 and Mamun et al., 2005).

Table 2-1: Amine Solvents and Abbreviated Name	
Amine Solvent	**Abbreviation**
Mono-ethanolamine	MEA
Di-ethanolamine	DEA
Methyl-di-ethanolamine	MDEA
Di-Glycol Amine	DGA
Tri-ethanol Amine	TEA
Methyl Mono-ethanol Amine	MMEA
Amino-Ethyl-Ethanol Amine	AEEA
Ethyl Amino-ethanol	EMEA
Butyl Amino-ethanol	BEA

The advantage of amine solvents is that absorption can be efficient even at low CO_2 composition of the flue gas (< 15 wt%). This makes chemical solvent absorption applicable not only in pre-combustion/reaction mode, but also in post-combustion/reaction mode. Moreover, the absorption rate is comparatively high. A lead additive can be added for greater efficiency when high CO_2 concentrations prevail in the flue gas.

The general disadvantages of amine solvents are: their sensitivity to contaminants in the flue gas such as NO_X and SO_X, as well as O_2 gas; their arguably limited absorption capacity and regeneration stability; the corrosiveness of their reaction products; and most importantly their high regeneration energy (France, 2007).

Such disadvantages do not apply to all amine solvents. Secondary and tertiary amines such as MDEA, DEA, and DGA are less corrosive and have higher CO_2 loading and regeneration properties than MEA, a primary amine (GPA, 2004). However, this is offset by lower absorption rates. Some secondary and tertiary solvents are also more selective to SO_2, COS and other pollutants and in some cases degrade upon contact with such pollutants. This degradation is often reversible however, and the solvent can be regenerated in a reclaimer unit, as with DEA and MDEA.

Ammonia is also a competing solvent. Alstom Ltd has made much progress in researching the use of aqueous ammonia. The advantage is that it is much less sensitive to contaminants such as NO_X, SO_X and O_2, and can even simultaneously absorb these gases along with CO_2. There is also less degradation during regeneration, which means that the solvent can be used over more cycles than amine solvents such as MEA (Steeneveldt et al., 2006).

Carbonate based solvents (Knuutila et al., 2008) are also gaining popularity. Sodium carbonate is already used for flue gas desulphurisation. Equipment and systems may be optimised to allow for efficient CO_2 capture as well. The advantage is that it can simultaneously absorb SO_2 and CO_2. It is reported to be less corrosive. The reaction with CO_2 is as follows:

$$CO_3^{2-} + H_2O + CO_2 \rightarrow 2HCO_3^- \quad \text{(R2-4)}$$

Potassium carbonate is also a popular carbonate based solvent. Mamun (2005) presents absorption rates and CO_2 loading for potassium carbonate. This solvent is particularly useful when combined with other solvents.

The disadvantage is the comparatively lower absorption rate and its lack of efficiency with low CO_2 concentrated flue gases. Thus the use of this solvent is limited to pre-combustion mode, where the CO_2 concentration of syngas is relatively high. Carbonate based solvents also have a greater tendency to precipitate and if equipment is not cleaned more regularly than usual, damage may occur. Extra capital and labour costs result from the need to account for this.

Another class of amine solvents under investigation are sterically hindered amines. These solvents are organic compounds with a primary amine functional group attached to a tertiary carbon atom. Secondary amine groups attached to secondary carbon atoms also form hindered amines. Exxon (Nerula and Ashraf, 1987) and Mitsubishi Heavy Industries (Steeneveldt et al., 2006) are at the forefront of its development. This steric hindrance causes unstable carbamate ions to form upon reaction with CO_2, unlike normal amines which form stable carbamate ions. This increases the absorption capacity by 20 - 40 % for hindered amines.

Popular hindered amine solvents are KS-1, a product of MHI, and 2-amine-2-methyl-1-propanol (AMP) and Flexsorb (R), a product of Exxon.

2.5.1.2 Physical solvents

With physical solvents, absorption of CO_2 merely entails a reconfiguration or rearrangement of the solvent molecules to accommodate CO_2 molecules. The industrial process is the same as with chemical absorption. The difference is that physical solvent regeneration processes may vary depending on the solvent.

Common physical solvents are Selexol® (Union Carbide), methanol and Sulfinol® (Shell) (Gielen, 2003).

Selexol is made up of a polyethylene glycol derivative. It was developed by Union Carbide Corporation and has many advantages. Selexol solvent can absorb CO_2, water and sulphur compounds. The solvent is reported to be applicable at ambient pressure, does not degrade appreciably and is stable.

The disadvantage is that the solvent can also absorb valuable paraffins, olefins, and aromatics. The operating temperature is also limited, from 255.15 K to ambient.

Methanol can also be used as a solvent. However, its operating conditions are demanding. Due to the high volatility of methanol, the absorption process can only be run between 200.15 and 238.15 K (GPA, 2004), with an operating pressure of 20 bar (IEA, 2004).

2.5.1.3 Hybrid solvents

Hybrid solvents are blends of physical and chemical solvents. The motive of trying to blend these two types of solvents, is to combine the best features of these types and minimise their flaws. It is an attempt to produce a solvent that has the high absorption rates and capabilities of chemical solvents to absorb at low CO_2 concentrations, and the high loading, low regeneration energy, low corrosiveness and high stability of physical solvents.

A hybrid solvent showing promising performance is the Sulfinol solvent. This solvent is actually a mixture of sulfolane, water, and either MDEA or Di-Isopropanol Amine (DIPA). This means that the solvent acts as a chemical solvent to a small extent.

The advantage of this solvent is that H_2S, CO_2, COS and CS_2 are absorbed simultaneously. The process is claimed to have high gas loadings and non-corrosiveness. It is also claimed to reduce CO_2 concentration of flue gas to as low as 50 ppm. Regeneration may be done using a flash vessel rather than a stripper, hence the energy penalty is lower (Nerula and Ashraf, 1987).

The disadvantage is that there is also co-absorption of hydrocarbons, which could mean loss of product or reactants if the process has entrainment problems. A reclaimer may also be needed to recover degraded solvent and the CO_2 entrained in it, making the absorption process more complex and likely more expensive.

The Amisol hybrid solvent was researched and developed in the 1960s by Lurgi Ltd. The most developed Amisol solvent is a mixture of aliphatic alkyl amines, di-isopropyl amine (DIPAM), and diethyl amine (DETA). Previous mixtures used MEA and DEA as well. With this solvent, absorption is optimum at 308.15 K and regeneration is typically done at 353.15 K. Due to this close range of temperature, a lean/rich heat exchanger is not needed. However, the existing gas has to undergo water washing and the water needs to undergo distillation to retrieve entrained methanol, since methanol is highly volatile and may easily be lost in the gas stream.

The Amisol solvent is reported to be non-corrosive and can also absorb sulphurous compounds such as HCN, COS and mercaptans, and can reduce CO_2 concentration in the flue gas to as low as 5 ppm.

The disadvantage however, is that the solvent can also absorb hydrocarbons and hence result in a loss of product. The flue gas must be treated for this before absorption occurs, making CO_2 capture an overall complicated procedure.

The common issue with hybrid solvents is their low selectivity (Duc et al., 2007). This is advantageous in the sense that other pollutants can be captured along with CO_2. On the other hand, it is disadvantageous as hydrocarbon products or reactants are lost to the solvent. (Chatti et al., 2005).

2.5.1.4 Blended solvents

It is often advantageous to blend two or more solvents of the same type in order to optimise absorption. This idea is popular for amine solvents. Primary, secondary and tertiary amines have different benefits and drawbacks for use in absorption. Primary amines such as MEA are known to have high absorption rates (Nerula and Ashraf, 1987). Due to their high corrosiveness, they are heavily diluted with water, to concentrations as low as 30 wt%. Since water has a relatively high specific heat capacity (4.187 kJ/kg.K), the overall heat capacity of the solvent is increased and the regeneration energy of the solvent becomes exorbitant.

To remedy the problem, tertiary amines such as MDEA are added. This replaces some water, hence reducing the overall heat capacity of the solvent. The corrosiveness is also reduced since MDEA is a tertiary amine and hence much less corrosive. Moreover, the addition of a tertiary amine also enables the solvent to absorb other pollutants such as H_2S, SO_2 and other sulphurous compounds (Coquelet and Richon, 2007). This is how such amines are combined to obtain the benefits of all types of amine solvents.

From the literature review, it was found that MEA+MDEA blends were most popularly researched. Ritter et al. (2006) showed that the capture energy required when using MEA alone, is 3.14 GJ/ton CO_2 while when MEA in combination with MDEA is used, the energy required is 2.2 GJ/ton CO_2. MEA:MDEA blend ratios are suggested by Chakravarti et al. (2001) to be 10 to 20% MEA with 20 to 40 % MDEA.

The same can be done with other amines. MDEA has also been blended with MMEA and piperazine additives (Mamun et al., 2006). MMEA and piperazine are reported to accelerate the reaction between MDEA and CO_2. Such effects were studied with 5 and 10 mol% concentrations of piperazine and MMEA. MMEA at 10 mol% concentration and piperazine at 5 mol% concentration were particularly successful in increasing the solubility and rate of absorption of CO_2 in MDEA. A study by Mamun et al. (2005) produced absorption curves for MDEA blended with MEA, AEEA, and PZ. MDEA + PZ, as well as MDEA + AEEA showed better performance than MDEA + MEA blends. However, none of these blends had higher absorption rates than unblended MEA solvent.

Solvent blending is not limited to amine solvents. Mamun et al. (2005) has studied the blending of potassium carbonate with MEA. Absorption data were tabulated for different concentrations

of MEA. In this particular study however, the performance of such a blend in terms of CO_2 loading and absorption rate was proven to be low in comparison to other complete amine blends. The performance was much lower than the use of diluted MEA solvent.

The advantage of absorption processes is that the concept is comparatively the most developed and hence estimates are relatively accurate. The process can be retrofitted in post-combustion/reaction mode, and can hence have little or no effect on the rest of the process, with the exception of energy requirements. On the other hand, it can be used in pre-combustion/reaction mode, to take advantage of higher CO_2 concentrations and achieve greater efficiency.

The method is highly flexible, two or more solvents can be combined to increase efficiency. The method can be combined with other absorption techniques as well. The process is relatively simple and requires a comparatively smaller space. Most solvents are regenerable.

The disadvantage is the high energy penalty associated with the capture method. Energy is needed in the form of heat for regeneration, as well as cooling of the solvent, since the absorption rate decreases with increasing temperature. Absorption processes of this nature can account for as much as 40 % (Kanniche and Bouallou, 2007)**,** of the total plants energy requirements. Hence, operating costs are appreciable. Moreover, many solvents, especially physical solvents, are only feasible when treating flue gas containing a high CO_2 concentration, and hence can only be applied to pre-combustion. Some solvents are also particularly expensive.

Absorption processes are currently the most researched and closest to commercialisation of all capture techniques. Austria and Netherlands have managed to set up pilot plants in 2008 (VNS, 2008 and Knudsen et al., 2008).

2.5.2 Dry regenerable sorbents for CO_2 capture

Another way to remove CO_2 is to pass the flue gas/syngas through a reactor full of dry sorbents. The sorbent can absorb, or adsorb CO_2 and then be regenerated using a temperature swing. Refer to Figure 2-7 for an illustration of the technique. Flue gas is first cooled and then passed through a carbonation reactor, where CO_2 is absorbed/adsorbed. Depending on the sorbent, water vapour from the flue gas may also get removed with the CO_2. The CO_2 rich sorbent is then passed to a regenerator where it is heated to remove the CO_2. If there is water vapour present, then the stream passes through a condenser to separate water from CO_2. Recycle loops vary for different process designs.

The sorbents are usually in the form of pellets in a fluidised bed. These pellets are then transported to the regenerator. Porous solids in a fixed bed may also be used but there is downtime between carbonation and regeneration. This problem is solved by using two reactor

units. One may perform carbonation while the other performs regeneration. However, this switch in duties often leads to irregular operation with non-uniform results.

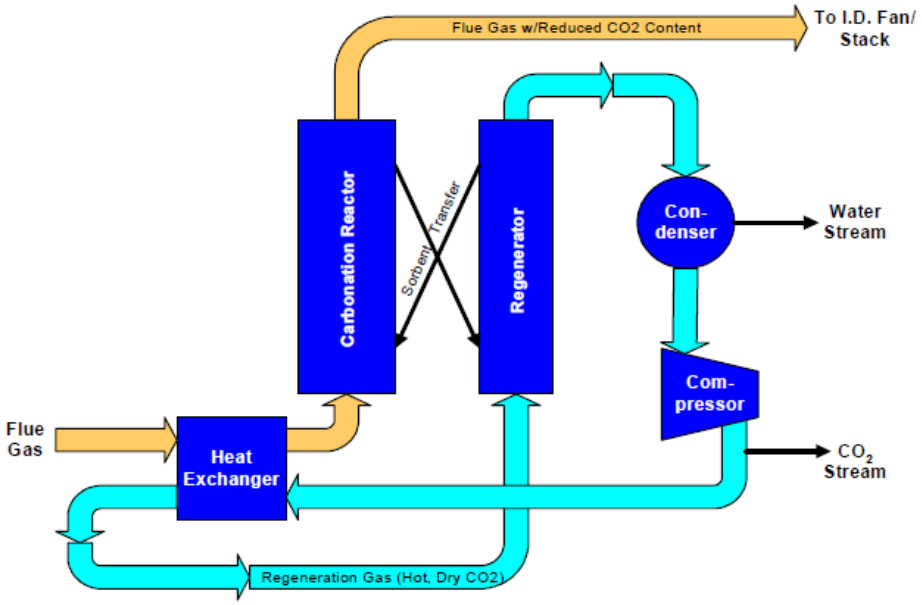

Figure 2-7: An illustration of a Sorbent Capture Process (Green et al., 2004)

Common sorbents used are activated coal, solid calcium, sodium and potassium carbonate, but there are many variations. Sodium and potassium carbonate were among the first investigated sorbents for use in CO_2 capture.

The general reactions for sodium carbonate are: (Green et al., 2004)

$$Na_2CO_3(s) + CO_2(g) + H_2O(g) \leftrightarrow 2NaHCO_3(s) \quad \text{(R2-5)}$$

$$\Delta H_r^o = -32.4 \text{ kcal/mol } CO_2$$

$$Na_2CO_3(s) + 0.6\ CO_2(g) + 0.6\ H_2O(g) \leftrightarrow 0.4[Na_2CO_3 \bullet 3NaHCO_3(s)] \quad \text{(R2-6)}$$

$$\Delta H_r^o = -32.5 \text{ kcal/mol } CO_2$$

The carbonation reaction occurs typically between 333.15 K and 353.15 K, while regeneration occurs between 393.15 K and 473.15 K.

Green et al. (2004) reported 90 % CO_2 capture during a single cycle. Multicycle operation proved to be fruitless because of rearrangement of sodium carbonate pellets in the bed during the first cycle. Graphs by Green et al. (2004) show significantly lower change in dimensionless weight when the sorbents are used for as little as 5 cycles.

The problem with sorbents such as Na_2CO_3 is that it reacts irreversibly with contaminants by the following reactions:

$$Na_2CO_3(s) + 2HCl(g) \rightarrow 2NaCl(s) + CO_2(g) + H_2O(g) \quad \text{(R2-7)}$$

$$Na_2CO_3(s) + SO_2(g) + \tfrac{1}{2}\ O_2(g) \rightarrow Na_2SO_4(s) + CO_2(g) \quad \text{(R2-8)}$$

An evidently worse result is that the sorbent reacts to form more CO_2, hence doing more harm than good. For this reason, highly efficient denitrification and desulphurisation of the flue gas has to be accomplished before CO_2 capture.

Dimensionless weight tests were done by Green et al. (2004), as well as Lee et al. (2008) regarding the effect of carbonation temperature, CO_2 and H_2O concentration in the flue gas and the effect of calcination temperature. The tests proved that the initial adsorption rate and dimensionless weight of the sorbents decreased as carbonation temperature increased. It was concluded that adsorption is feasible within the temperature range of adsorption rate and CO_2 loading was higher when the flue gas had high CO_2 concentration, however caking of the sorbent occurred when H_2O concentrations were too high. The problem could be alleviated by using zeolites. Also shown, is the effect of SO_X contaminants. The adsorption rate is significantly reduced and lower change in dimensionless weight of the sorbent was observed.

Other sorbents are Trona T-50, which has showed good absorption performance but poor reproducibility. Sodium bicarbonate was also studied as a sorbent source. The treatment of the sodium bicarbonate (i.e. The source of the sodium carbonate and its associated impurities, the degree of calcination to remove the volatile impurities, and the calcinations temperature) dictates the type of sorbent that will be formed. SBC#1, SBC#2 and SBC#3 sorbents were formed and studied in Green et al. (2004). Their properties are also provided.

The reactions for potassium carbonate sorbent are (Zhao et al., 2008):

$$K_2CO_3(s)+ 1.5H_2O(g)\leftrightarrow K_2CO_3 \cdot 1.5H_2O(s) \quad \text{(R2-9)}$$

$$K_2CO_3(s)+CO_2(g)+H_2O(g)\leftrightarrow 2KHCO_3(s) \quad \text{(R2-10)}$$

$$2K_2CO_3(s)+CO_2(g)+ 2.5H_2O(g)\leftrightarrow K_4H_2(CO_3)_3 \cdot 1.5H_2O(s) \quad \text{(R2-11)}$$

$$K_4H_2(CO_3)_3 \cdot 1.5H_2O(s)+CO_2(g)\leftrightarrow 4KHCO_3(s)+0.5H_2O(g) \quad \text{(R2-12)}$$

CO_2 capture of 85 % was reported. The sorbent resisted attrition for the 5 cycles in which it was tested. The tests were done in the absence of contaminants however.

Green et al. (2004) also made a study on potassium carbonate in a fluidised bed carbonation reactor. The advantage was that adsorption continued at temperatures over 383.15 K, which is higher than what sodium carbonate can adsorb under. Adsorption was slow however. After 30 minutes, 50 % of the CO_2 in the flue gas was still not recovered. Moreover pipe plugging was reported. The combining of K_2CO_3 with 40 % alumina support corrected the pipe plugging. The sorbent resisted attrition for over 5 cycles. Temperature profiles and carbon dioxide removal curves are presented in Green et al. (2004).

There are many other sorbents that are made by combining different materials such as supports, inorganic binders, organic additives as dispersants, water as solvent, a defoamer, and organic

binders. Lee et al. (2008) has developed many solvents such as Sorb N2A, N2B, N2C, NX, NH, and NX30. Sodium carbonate and sodium hydrogen carbonate is a key ingredient in these sorbents. Sorbent properties such as pH, viscosity, porosity, and density are also provided. Attrition and thermogravimetric results are presented. The effect of calcination and carbonation temperature was also studied. It was claimed that the NX30 sorbent showed better adsorption performance than all other sorbents, including sodium carbonate and sodium hydrogen carbonate as well as MEA solvent. Regeneration was done at 393.15 K. The only uncertainty is that the flue gas synthesized had no contaminants.

The advantages of sorbent usage are that some sorbents can be used at higher temperatures than many solvents. Moreover, some sorbents can achieve 99 % CO_2 capture from flue gas more easily than many other capture techniques can (Green et al., 2004). Capture can be efficient at low CO_2 concentrations, but is much more efficient at higher concentrations. There are also claims of lower regeneration energy required for some sorbents. In some cases, water is also absorbed and can be recycled as steam for usage as a heat utility (Green et al., 2004).

The main challenge facing sorbent usage is the expensive nature of solids handling. Equipment is usually large, complete with conveyors or compressed air blast loops. Cost of solids handling, dust elimination and mechanical strengthening is potentially high. The sorbents also need to meet certain attrition resistance requirements. Water is particularly destructive to many sorbents, especially carbonate sorbents, where attrition is enhanced when water is present. Alumina supports are a popular idea to increase attrition resistance, but they are expensive. Other additives, inorganic and organic, are also an option but need further research.

Comprehensive research into the performance and feasibility of sorbents has thus far remained elusive, due to much time being taken on research into optimising sorbent attrition resistance and other properties for multi-cycle CO_2 capture.

2.5.3 Membrane usage for CO_2 capture

Membranes can be used as a gas pre-treatment step to remove impurities before CO_2 capture, or for the capture process itself, or in combination with solvents to increase capture efficiency (Figueroa et al., 2007). A membrane contactor with solvent is illustrated in Figure 2-8.

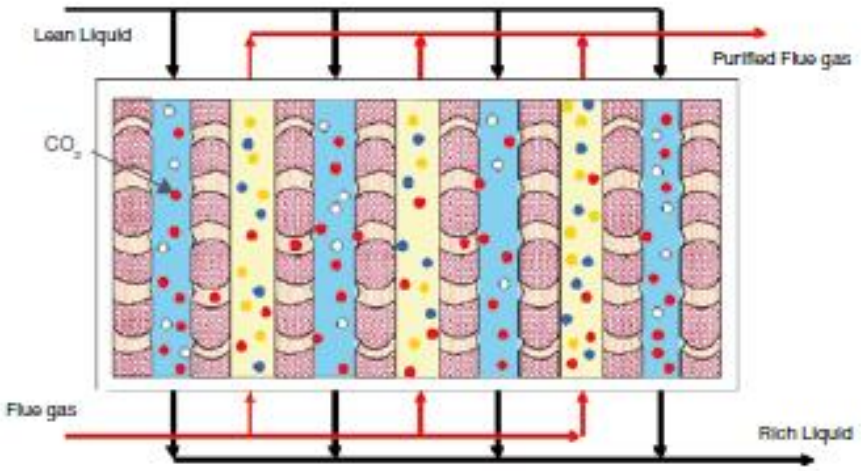

Figure 2-8: An Illustration of a Membrane Contactor with solvent (NETL, 2007)

Flue gas enters the membrane inlet chambers. The CO_2 passes through the membrane material and is absorbed by the solvent on the other side of the membrane material. In this case a plate and frame is illustrated. Rotary filters can be used to facilitate continuous operation without much downtime. Common membranes include polymer, ceramic, silica, and zeolite membranes. Some membranes are fragile and are hence supported by alumina supports.

The University of New Mexico is currently investigating zeolite (crystalline alumino silicate) membranes (Figueroa et al., 2007). The main advantage that was found is its resistance to degradation for temperatures up to 673.15 K. Moreover, zeolites are fairly well researched and are already in use in other industries and for other purposes such as Fischer-Tropsch reactions and as molecular sieves. Zeolites are claimed to be useful when separating CO_2 from a CO_2+N_2 gas stream. However, the effect of more complex gas mixtures that include contaminants is still uncertain.

Silica membranes can separate CO_2 from a CO_2+CH_4 gas stream. Inorganic silica membranes are reported to be capable of separating CO_2 from O_2, N_2 and SO_2. Amine solvents are used to increase selectivity. This membrane can be used even when the CO_2 concentration is low (<15 wt%). The only problem is that the tiny pores of the membrane eventually get blocked by the solvent.

Ceramic membranes are becoming increasingly popular, especially with IGCC processes and oxy-fuel combustion. Ceramic porous membranes, as well as Pd-ceramic membranes can be used to separate H_2 from gas streams, for combustion. CO_2 and other contaminants are trapped in the membrane (Steeneveldt et al., 2006). As far as CO_2 capture and isolation is concerned, the membrane is reported to be able to operate at higher temperatures than polymer membranes. The drawback however, is that the membrane has very low selectivity. CO_2 recovery can be as

low as 7 % (IEA, 2004). Multistage operation thus becomes a necessity. This is an expensive option.

Membrane Technology and Research (MTR) Inc. are among the many companies that are studying polymer membranes (Figueroa et al., 2007). The advantage is that this type of membrane has comparatively high selectivity to CO_2. CO_2 recovery is as high as 57 %. This significantly reduces the number of cycles necessary for membrane filtration of flue gas. Another advantage is that the polymer membranes are comparatively thin, requiring less membrane area. The only problem that arises, is that a thin membrane has a high risk of breakage under high pressure. This is adequately compensated by using alumina supports (Meisen and Shuai, 1997).

Polyether-polyamide copolymer membranes are studied at MTR. The membrane can also be used for post combustion at low CO_2 concentrations.

Polybenzimidazole (PBI) membranes are researched by the U.S. Department of Energy (DOE) and were found to have good stability for temperatures up to 673.15 K. Tests were done over 400 days to prove such stability (Figueroa et al., 2007).

The use of liquid membranes is also of increasing interest. The National Energy Technology Laboratory (NETL) of the U.S.A. is one of the drivers of this research. With liquid membranes, the gas dissolves and diffuses into liquid in the pores of solid supports. Since the gas molecules do not have to diffuse into the solid state, diffusion through the liquid in the pores is fast.

An increasingly researched idea is combining membranes with solvents. Gas is passed on one side of the membrane and CO_2 permeates through and then gets absorbed in a solvent on the other side of the membrane. The solvent acts as a sweep fluid and increases separation rate. Teng and Tondeur (2006) provides efficiency results for the combined use of membranes and MEA solvent. The type of membrane was not specified however. Another idea mentioned by Steeneveldt et al. (2006) is combining polymeric membrane usage with DEA solvent. Meisen and Shuai (1997) states that the advantage of combining solvents and membranes is that the equipment needed for CO_2 capture is more compact and perhaps requires lower capital expenditure. The International Energy Agency (IEA), an organisation comprising 28 member states, has published general tabulated data for the combination of solvents and membranes (IEA, 2004).

The advantage of using a membrane such as the one illustrated in Figure 2-8, is that there are no moving parts. Hence the method is simple and less maintenance is required. If solvents are not used, then regeneration heat is not needed. The method is particularly efficient if the flue gas is being emitted at high pressure. Solvents are used to facilitate a high CO_2 removal rate.

The disadvantage is that the usage of membranes alone is very inefficient, because the membrane material is at present not well researched. A balance between permeability and selectivity has not been optimized. Hence current capture methods involving the use of membranes alone are performed as multistage operations to achieve the desired CO_2 removal, which results in high capital costs. If the pressure of the flue gas is too low, then energy for compression is needed to overcome the large pressure drop across membranes. This is expensive. Hence membrane usage alone has the highest energy penalty: capture rate ratio. Moreover, the fact that the membrane equipment does not move can also be disadvantageous as a boundary layer may cover the stationary membrane and reduce efficiency from then on.

On the other hand, the use of solvents with membranes is claimed to have the lowest energy penalty: capture rate (Teng and Tondeur, 2006). The use of membranes combined with solvents is fairly well researched. A pilot plant in the Netherlands was constructed in 2008 to accommodate solvents and membranes (Knudsen et al., 2008).

2.5.4 CO_2 capture by hydrate formation

Gas hydrates are crystalline inclusion compounds. They form when water molecules bond, by hydrogen bonding, to form cage like structures into which other molecules can be trapped (Jadhawar et al., 2006). This formation is facilitated through low temperature (268.15 - 298.15 K) and extremely high pressure (30 - 500 bar) conditions. Figure 2-9 (Jadhawar et al., 2006), shows how hydrates are formed on a molecular level. CO_2 and water are frozen together forming a slurry hence the CO_2 molecules get trapped. The captured CO_2 molecules are released upon heating the slurry thus breaking the ice cages.

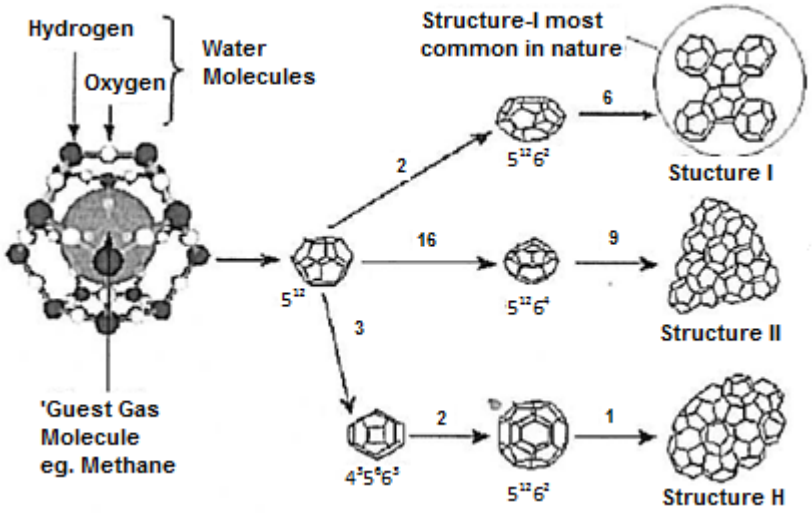

Figure 2-9: Illustration of Guest Molecule Trapped inside Water Molecule, forming Hydrates (Jadhawar et al., 2006)

The advantage of hydrate formation is that water is used as the solvent. 99 % CO_2 recovery can

be achieved and at relatively low CO_2 concentrations (Chatti et al., 2005). One volume of hydrate can store as much as 35 volumes of CO_2 (Duc et al., 2007).

Additives are used to lower the hydrate formation pressure. Duc et al. (2007) reported the successful use of tetra-n-butyl ammonium bromide (TBAB) and tetrahydrofuran (THF) for CO_2 capture in the steel making industry. Hydrate formation pressures were reduced from approximately 50 bar to approximately 3 bar by TBAB, at temperatures ranging from 279 - 290 K. Linga et al. (2007) suggested the use of propane as an additive, for gas streams containing high concentrations of H_2.

Studies on THF were conducted by Linga et al. (2007). Experimentation found that THF reduced the hydrate formation pressure from 84 to 5 bar, for CO_2+N_2 gas mixtures of varying composition. The test was done at a temperature of 275.15 K. Moreover, there is also evidence that THF also decreases the induction time, which means that hydrate crystals begin to form more quickly. The drawback however, is that the rate of overall gas consumption over time is significantly lower. This may prove to be a serious problem when trying to employ hydrates in continuous mode.

Silica gel porous beads are also reported to improve the efficiency of hydrate processes, by Park et al. (2006). 30 nm diameter pores were contained in the beads.

There is also research being done combining membranes with hydrates, either to remove impurities and achieve effective capture rates, or as a polishing step for CO_2 capture (Linga et al., 2007). Linga et al. (2007) presents process flow diagrams of combining hydrate processes and membranes. Hydrates are used in two or three cycles and membranes are utilised at the end for final product separation.

The disadvantage is that the handling of hydrates can be difficult. Such slurries can lead to pipeline plugging. Pipeline inspection gauges need to be used often. Alternatively, it is reported that methanol or glycol can be used to inhibit pipeline plugging. The capture process is viable in batch mode but some papers claim that the process is highly complex when continuous mode is accommodated. Duc et al. (2007) shows the complexity of continuous multistage operation in simulation.

The use of hydrates is still in the research phase. No pilot plants have been established yet. It is likely that batch processes will be investigated first, with continuous processes following thereafter.

2.5.5 New ideas of CO_2 capture

There have been many other ideas proposed for CO_2 capture. Some are novel while others do not seem promising at all. Some have undergone preliminary research but others are still being

pondered upon theoretically without any evidence of research being commenced or results being released.

2.5.5.1 Enzyme based systems

Enzymes achieve CO_2 capture and release by mimicking mammalian respiratory systems. They are used as a liquid membrane, through which flue gas passes.

Carbozyme Ltd. is pursuing this research. Carbonic Anhydrase (CA) enzyme is used as the liquid membrane, trapped in hollow fibre supports through which flue gas must pass. Refer to Figure 2-10 (Figueroa et al., 2007) below. Flue gas containing N_2, O_2, and CO_2 passes through a liquid membrane (CA) suspended by a fibre support. CO_2 hydrates and permeates through the membrane as carbonic acid at a higher rate than N_2 and O_2 and is swept out the other side, often using sweep gas. 90 % CO_2 recovery is claimed.

Regeneration of the enzyme is done at ambient conditions. There is a significant reduction in energy penalty due to the comparatively low heat of absorption for the CA liquid. Dissolution rate of CO_2 is limited by the rate of aqueous CO_2 hydration. CA is used to catalyse hydration. 600 000 molecules of CO_2 can be hydrated per molecule of CA (Trachtenberg et al., 1999).

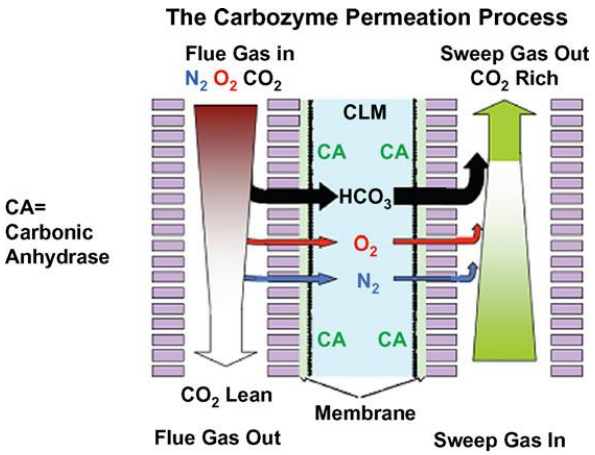

Figure 2-10: CO_2 Separation using Carbonic Anhydrase (Figueroa et al., 2007)

The drawbacks of enzyme usage is summarised by Figueroa et al. (2007) to be the limitations at membrane boundary layers, pore wetting, surface fouling, loss of enzyme activity long-term operation uncertainty, and scale-up uncertainties.

2.5.5.2 CO_2 capture using ionic liquid solvents

Ionic liquids refer to salt solutions containing organic cations and inorganic/organic anions that interact with CO_2 molecules. The ionic liquid is used as a liquid membrane or as a solvent. In

fact, it is a special type of physical solvent.

The benefit of these liquids is that they can absorb CO_2 efficiently at temperatures of up to several hundred degree Celsius. This means that hot flue gas doesn't need to be cooled before it is treated for CO_2 recovery. It is also claimed that less heat is required for regeneration (Figueroa et al., 2007).

The National Energy Technology Laboratory (NETL) and the University of Notre Dame are spearheading researching efforts for ionic liquids to be used in the simultaneous removal of CO_2 and SO_2, as well as the separation of CO_2 from H_2 (Figueroa et al., 2007).

The drawback regarding the use of ionic liquids is the cost of the liquid. This is due to the low commercial availability of ionic liquids. Moreover, a physical constraint is that the viscosity of ionic liquids is comparatively high compared to conventional solvents (Figueroa et al., 2007). This will amount to high operating costs, particularly circulation costs. Some lead based ionic liquids have also been found to be corrosive.

2.5.5.3 Cryogenics

This technique involves the cooling of the flue gas until CO_2 condenses and was investigated briefly by the Intergovernmental Panel on Climate Change (IPCC, 2004). This is merely a proposed idea. No performance data were found to be published.

The benefit of this technique is that capture and compression can be easily integrated into one process. The drawback is that its feasible application is very limited. The flue gas composition has to be such that CO_2 is the most or least volatile component in the flue gas. The flue gas has to be at relatively low temperature and high pressure. If this is not the case, then refrigeration and compression costs will be expensive and is likely to be unfeasible. This penalty can be overcome if other utilities are available at the plant and pinch technology is applied.

2.5.5.4 CO_2 anti-sublimation

A more popular method than cryogenics, is CO_2 anti-sublimation. This technique involves cooling the flue gas to below its triple point, and then converting the CO_2 in the gas directly to the solid phase.

Clodic et al. (2005) presents a detailed description of the process. A refrigerant is used for the freezing process. The freezing temperatures are dependent on the CO_2 concentration in the flue gas, and vary from 194.65 K for 100 vol% CO_2, to 136.45 K for 0.1 vol% CO_2 in the flue gas. The solid CO_2 can be used to cool the recycled refrigerant for continuous operation. Depending

on the conditions and energy saving methods employed, CO_2 may be stored in a solid or gaseous phase.

Clodic et al. (2005) also present experimental measurements and comparisons with convention absorption processes using MEA solvent. The results show a 17 - 27 % lower energy penalty in comparison to MEA absorption.

A pilot plant has been developed in the Netherlands, commissioned by the government under CATO programme (VNS, 2008). The pilot plant can be used to study various CO_2 capture techniques, including CO_2 anti-sublimation.

2.5.5.5 Artificial photosynthesis

Solar energy can be used to burn CO_2 in the flue gas at 2673.15 K to create hydrocarbons. This not only relieves CO_2 emissions but also in principle increases hydrocarbon product yield.

Although it is an intriguing idea, the drawback is that much surface area is required to harness the solar energy for this purpose (Science Daily, 2009). Space is indeed finite and limited for CO_2 capture processes to be integrated into the plant. There has not been any analysis to determine how much space is required.

Another idea that seems more likely to be successful, is the use of a plasma reactor to heat the CO_2. Plasma cracking occurs under pyrolysis conditions i.e. in the absence of oxides. This is likely to take up less space but the energy penalty is still expected to be high due to the operating temperature required (IPCC, 2004).

While the use of artificial photosynthesis as a CO_2 capture technique is unlikely, the process may find much use as an alternative to CO_2 sequestration. Captured CO_2 from other industries may be sent to a solar power plant which may harness solar energy to produce hydrocarbons from CO_2.

2.5.5.6 Integrated gasification steam cycle (IGSC)

This is a new process developed through research by a consortium consisting of Siemens, MAN Turbo, CO_2 Global and Imperial College in the United Kingdom. This process is claimed to have very little or no energy penalty as waste energy is put to good use (Griffiths, 2008).

Refer to Figure 2-11. Coal is burnt in two stages. Coal is first gasified in a quench gasifier. Only 40 % of the oxygen that is needed for complete combustion is used. Water is also added as a temperature moderator and as a reactant with carbon and carbon oxides to produce hydrogen. The result is a syngas containing equal proportions of carbon monoxide and hydrogen as well as

10 % O_2, at a temperature of 1573.15 - 1773.15 K. Combustion is completed in a fired expander. Water is again used to regulate the temperature. The benefit of this, it that the gas stream produced has increased CO_2 concentration. The fired expander consists of a burner mounted annularly to a commercial gas turbine to generate power. This expander has no air compressor. The expanded combustion gases are sent to a heat recovery steam generation system (HRSG). Steam is produced here, by cooling the combustion gases. This steam can drive a turbine for additional power. The gases are cooled to the dew point and then sent to a desaturator to condense the water using cooling water. Water is recovered and a CO_2+SO_2 gas stream is isolated for capture. The energy recovered in the desaturator can drive a low pressure turbine. Further details are given in Griffiths (2008).

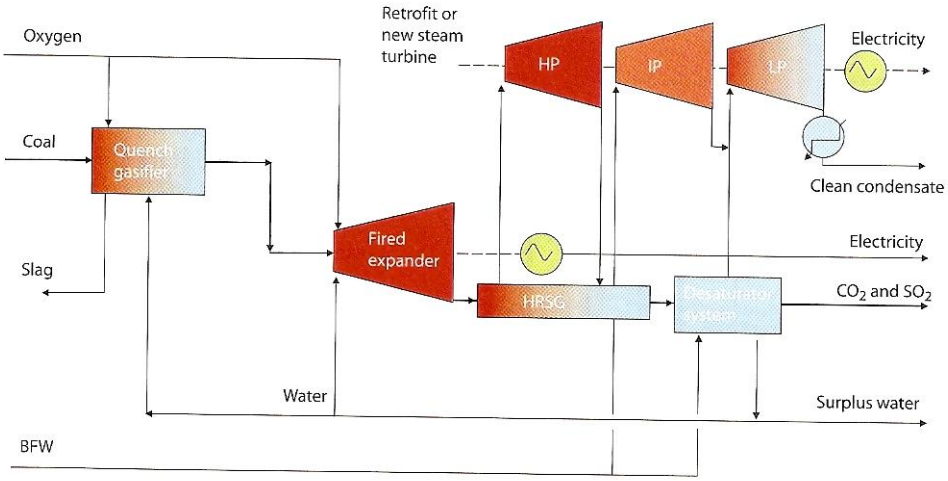

Figure 2-11: Integrated Gasification Steam Cycle Illustration (Griffiths, 2008)

The main advantage of this process is its efficient heat recovery and usage. High quality heat can be recovered from the HRSG and desaturator to drive turbines. Conventional equipment can be used to build this process. With the exception of the fired expander and perhaps the quench gasifier, there are no high end technological requirements for this process to work. Conventional turbines are used and simple heat recovery and desaturator units are used.

As far as CO_2 capture is concerned, the advantage is that CO_2 and SO_2 are produced together. By using applicable solvents, both these components can be simultaneously captured and stored. If CO_2 is desired in isolation, then an SO_2 selective solvent is needed. The gas stream is claimed to be at high pressure which would reduce CO_2 compression costs. In principle, 100 % of CO_2 can be captured, and with an overall efficiency of up to 60 % more than conventional power plants with CCS. There are even claims that power generation capacity is increased when compared to plants even without CCS.

The process is well thought out for power generation using coal but there are claims that natural gas can also be used. There is no mention of CTL and GTL processes however, which suggests that this process may only be beneficial to the power generation sector. Further research is required to confirm this.

There are many great claims regarding this process. However, the uncertainty of estimates is easily revealed upon further literature study. The process is extremely new. The method was only released in January 2009. Thus far, there has been no evidence of a study done by any other companies or research institutions, other than the consortium that developed this technique. The process seems to need pure oxygen, yet no mention is made as to whether this was taken into account in the cost and efficiency analysis. The technique is highly underdeveloped and in great need of further research.

2.5.5.7 Chemical looping combustion

This is a new oxyfuel combustion technique that uses oxygen derived from metal oxides. Refer to Figure 2-12. Two fluidised bed reactors are typically used. Metal based compound (Me) is oxidised with air to form an oxide of the compound (MeO) in the first reactor. This reactor is commonly known as the air reactor (Figueroa et al., 2007). A hot flue gas is produced:

Air Reactor: $O_2 + 2Me \rightarrow 2MeO$.....(R2-13)

This is how flue gas can be used to produce steam and drive a turbine that runs a generator.

The MeO gas is then sent to a second reactor, known as the reducer. Here, the gas is reduced to its initial state by the fuel. For this reason, the reducer is also known as the fuel reactor:

Fuel Reactor: $C_nH_{2m} + (2n + m)MeO \rightarrow nCO_2 + mH_2O + (2n+m)Me$.....(R2-14)

The result is a flue gas mixture of high CO_2 concentration that can undergo CO_2 capture (Figueroa et al., 2007). Whatever the capture method used, it would have an inherent advantage due to the high CO_2 concentration (31 % (NETL, 2007) in the flue gas. In this case CO_2 capture will be done in Post-combustion mode.

Chemical looping can also be applied to IGCC processes and CTL processes. NETL (2007) studied its application to CTL processes. Iron Oxide (Fe_2O_3) is used as the oxygen carrier. Syngas (CO and H_2), as well as light hydrocarbons from the tail gas of the FT reactor, are reacted with Fe_2O_3 in a fuel reactor:

$3CO + Fe_2O_3 \leftrightarrow 3CO_2 + 2Fe$ $\Delta H = -18362$ kJ/mole (R2-15)

$3H_2 + Fe_2O_3 \leftrightarrow 3H_2O + 2Fe$ $\Delta H = 28790$ kJ/mole (R2-16)

$$C_2H_4 + 2Fe_2O_3 \leftrightarrow 4Fe + 2CO_2 + 2H_2O \quad \Delta H = 88535 \text{ kJ/mole} \qquad \text{(R2-17)}$$

CO_2, H_2O and reduced iron is produced. The reduced iron can be reacted with steam to produce more H_2 for use in the FT reactor. This reaction occurs in a fuel reactor:

$$3Fe + 4H_2O \leftrightarrow Fe_3O_4 + 4H_2 \qquad \Delta H = -44.668 \text{ kJ/mole} \qquad \text{(R2-18)}$$

It is reaction (R2-18) that produces H_2 for recycle and hence relieving the need for a shift converter. The water gas shift (WGS) reaction is not needed. This result is advantageous as capital and operating costs is lowered. The Fe_3O_4 is recycled to the fuel reactor pneumatically using air. This pressurised air transport not only transports the Fe_3O_4, but also oxidises it to form Fe_2O_3.

$$4Fe_3O_4 + O_2 \leftrightarrow 6Fe_2O_3 \qquad \Delta H = -219.229 \text{ kJ/mole} \qquad \text{(R2-19)}$$

It is evident that reaction (R2-19) is highly exothermic. It can thus be concluded that the pneumatic conveyance serves to transport, oxidise and heat the solid Fe_2O_3. This heat acts as a primary source of energy to reduce Fe_2O_3 to Fe in the fuel reactor. Refer to Figure 2-12 for an industrial illustration. Selexol capture systems can then be used to capture CO_2.

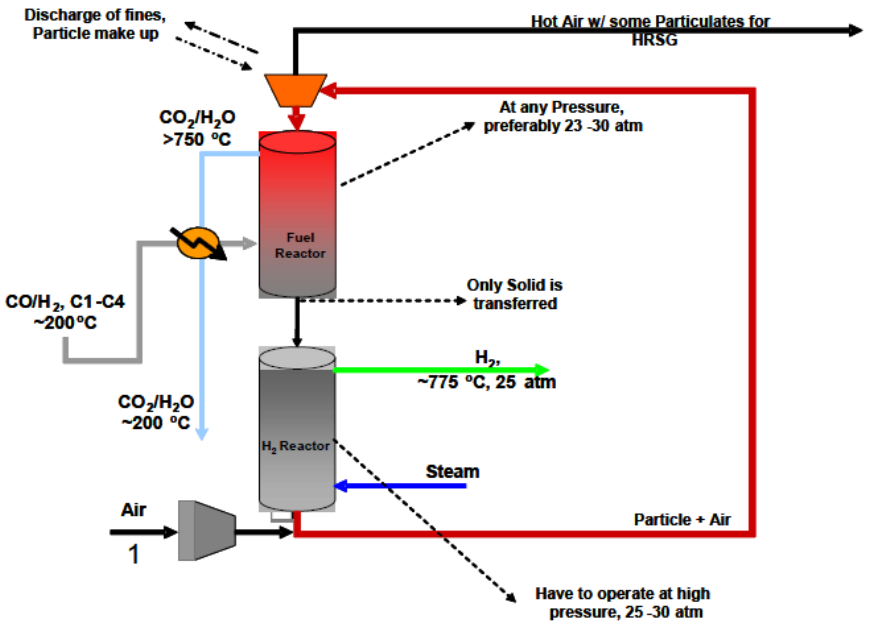

Figure 2-12: Chemical Looping Combustion Illustration (NETL, 2007)

There are some potential advantages of using chemical looping combustion. H_2 can be produced to achieve a good CO/H_2 ratio for FT synthesis, without the need of a shift converter. The flue gas stream emitted contains mainly CO_2 and H_2O. H_2O can be removed by condensation and the resultant CO_2 stream is of relatively high pressure, which reduces compression costs. If,

depending on the process, other components are present in the flue gas and condensation is inadequate, then other capture methods can be used. Selexol solvent and MDEA are popular suggestions (Figueroa et al., 2007). Capture would be easier and more energy efficient due to the relatively higher CO_2 concentration. High quality waste heat is produced during oxidation of Fe_3O_4 and is useful in the fuel reactor.

Costs related to chemical looping integration are summarised in NETL (2007). A gasifier of 180 m^3 was assumed. The fuel reactor was assumed to be 210 m^3 and the hydrogen reactor was 180 m^3.

A comparison of capital costs was done. The study showed that the capital cost for building a new plant with chemical looping is actually lower than the conventional CTL plant. This is due to lower cost of an MDEA CO_2 capture unit in comparison to a two stage Selexol unit, lower compression costs and FT recycle and no shift conversion. NETL (2007) also claims, using a simulation, that an increase of 10 % in liquid product occurs, due to the abundance of H_2 created during reaction 4. The process is 3 % more efficient than conventional CTL processes.

IEA (2004) has concluded that electricity production costs for a plant using chemical looping, is lower than that of conventional IGCC processes. Chemical looping is also applicable to GTL processes, with power plant efficiencies estimated to be up to 54 %, 14 % higher than conventional power plants currently in use (Griffiths, 2008). Estimates of capital investment costs, operating costs, overall costs and capture efficiency are provided by IEA (2004).

Chemical looping is the most developed and most promising of all new speculative technologies. Its disadvantages are the uncertainty of estimates due to the lack of further development made. Research thus far has only been made through lab experiments and computer simulations. There has been no pilot plant testing of chemical looping.

While such disadvantages will be overcome in good time, other disadvantages are related to the fact that chemical looping significantly alters the overall process, which is a greater challenge to overcome. The alteration is not so significant when chemical looping is applied to an oxy-fuel combustion process. However, chemical looping significantly alters IGCC and PC combustion processes, as well as CTL and GTL processes. Many downstream processes will have to be re-evaluated and their conditions altered and re-optimised to ensure the success of chemical looping integration. Although chemical looping is an attractive option for new plants, the feasibility of its integration into existing plants remains uncertain.

Another disadvantage is the potentially expensive and dangerous impact of solids handling. It can be costly and a safety hazard to circulate hot solid oxides continuously. Extra precaution

needs to be taken. Moreover, more metal oxides need to be investigated for their durability for continuous usage in a recirculation loop.

2.6 Useful quantitative data obtained from the literature review

Useful numerical data were extracted from all literature sources consulted. Important data have been made available as presented in Table 2-2. Data in Table 2-2 are given in units as expressed in their title category, unless otherwise stated.

Table 2-2: Data Obtained from the Literature				
Reference	**Technique**	**Energy Penalty (GJ/ton CO_2)**	**Max CO_2 loading at temp. (mol CO_2/mol solvent)**	**Absorption Rate (mol/L/s)**
IEA, 2007	Absorption General	-	-	-
Mamun, 2005	Blended Absorption	-	0.26 - 0.56	2E-05 to 43E-5
Descamps et al., 2004	Blended Absorption	-	-	-
Oexmann et al., 2008	Blended Absorption	2.44 to 3.07	-	-
Nerula and Ashraf, 1987	Blended Absorption		21.5	8.1 to 8.4 rel. to MDEA
GPA, 2004	Blended Absorption	245 - 280kJ/L lean sol.	0.72 - 1.02	-
France, 2007	Blended Absorption	-	-	-
Mamun et al., 2005	Chemical Absorption	-	0.3 - 0.83	2E-05 to 43E-05
Coquelet and Richon, 2007	Chemical Absorption	-	0.15 - 1	-
Descamps et al., 2004	Chemical Absorption	2.4 to 3.14	-	-
Nerula and Ashraf, 1987	Chemical Absorption	3.16	-	-
Singh et al., 2003	Chemical Absorption	-	-	-
Nerula and Ashraf, 1987	Chemical Absorption	3.8	18.8 to 60 vol/vol	-
Teng and Tondeur, 2006	Chemical Absorption	28 to 33 % inc.	-	-
Knuutila et al., 2008	Chemical Absorption	3.2 to 7.4	-	-
GPA, 2004	Chemical Absorption	220-360 kJ/L lean sol.	0.2 - 0.4	-
Knudsen et al., 2008	Chemical Absorption	3.5 - 3.7	-	-
Leci, 1997	Chemical Absorption	-	-	-
Alie et al., 2004	Chemical Absorption	3.08	-	-
IEA, 2004	Chemical Absorption	-	-	-
Rodgers et al., 1998	Chemical Absorption	-	0.05 - 0.1	-
Kim and Svendsen, 2007	Chemical Absorption	-	-	-
Hook, 1997	Chemical Absorption	-	0.6 - 0.8	-
Kanniche and Bouallou, 2007	Chemical Absorption	-	-	-
France et al., 2007	Chemical Absorption	4	-	-
Mamun et al., 2005	Physical Absorption	3.4	-	-
Nerula and Ashraf, 1987	Physical Absorption	-	30 - 55 vol/vol	-
IEA, 2004	Physical Absorption	-	-	-
Kanniche and Bouallou, 2007	Physical Absorption	-	-	-
GPA, 2004	Physical Absorption	-	-	-
GPA, 2004	Hybrid Absorption	100 - 210kJ/L lean sol.	-	-

Table 2-2: Data Obtained from the Literature (Continued)					
Reference	**Flue Gas Information**	**α_{rich} (mol CO_2/mol amine)**	**α_{lean}(mol CO_2/mol amine)**	**α_{diff} (mol CO_2/mol amine)**	**Heat of Absorption (kJ/mol CO_2)**
IEA, 2007	-	-	-	-	-
Mamun, 2005	10 vol% CO_2, 90 N_2	-	-	-	-
Descamps et al., 2004	-	-	-	-	70 - 84
Oexmann et al., 2008	15.9 vol% CO_2 - 335.15 K	1.01 - 1.447	1.013 - 1.261	0.088 - 0.186	-
Nerula and Ashraf, 1987	8.5 to 12 vol% CO_2	-	-	-	-
GPA, 2004	311.15 K	0.8 - 1.1	0.08	-	-
France, 2007	40-393.15 K. 1- 10 bar, 20 % CO_2	2mol/L sol	1.6mol/L sol	-	90
Mamun et al., 2005	10 vol% CO_2, 90 N_2	-	-	-	-
Coquelet and Richon, 2007	1 to 3 bar pressure	-	-	-	-
Descamps et al., 2004	-	-	-	-	62 - 85
Nerula and Ashraf, 1987	15.9 vol% CO_2- 335.15 K	1.612	1.331	0.281	-
Singh et al., 2003	13 - 15 % CO_2				-
Nerula and Ashraf, 1987	8.5 to 12 vol% CO_2	0.5	0.15	0.35	-
Teng and Tondeur, 2006	-	-	-	-	-
Knuutila et al., 2008	13.5 mol% CO_2 - 318.15 K	-	-	-	-
GPA, 2004	311.15 K	0.35 - 0.73	0.08 to 0.2	-	-
Knudsen et al., 2008	12 %CO_2 47^{o}C with contaminant	-	-	-	-
Leci, 1997	-	-	-	-	-
Alie et al., 2004	15 vol% CO_2	-	-	-	-
IEA, 2004	-	-	-	-	-
Rodgers et al., 1998	3 bar partial pressure	-	-	-	-
Kim and Svendsen, 2007	3 bar	-	-	-	80 - 115
Hook, 1997	4.7 vol%CO_2	0.6	0.2	-	-
Kanniche and Bouallou, 2007	0 - 25 vol% CO_2	-	-	-	-
France et al., 2007	40- 393.15 K. 1-10 bar, 20 % CO_2	2.6 mol/L sol	0.5- 2.4 mol/L sol	-	60 - 95
Mamun et al., 2005	10 vol% CO_2, 90 N_2	-	-	-	-
Nerula and Ashraf, 1987	8.5 to 12 vol% CO_2	-	-	-	-
IEA, 2004	-	-	-	-	-
Kanniche and Bouallou, 2007	0 - 25 vol% CO_2	-	-	-	-
GPA, 2004	-	-	0.007	-	-
GPA, 2004	311.15 K	-	-	-	-

Table 2-2: Data Obtained from the Literature (Continued)						
Reference	**Overall Plant energy increase (%)**	**Capture Efficiency (%)**	**Overall Plant Efficiency (%)**	**Investment Cost ($/kW)**	**Capture Cost ($/ton CO_2)**	**Operating Cost (Percentage inc.)**
IEA, 2007	9.4 - 11.7	-	33.6 - 35.9	229M€	-	-
Mamun, 2005	-	-	-	-	-	-
Descamps et al., 2004	-	-	-	-	-	-
Oexmann et al., 2008	-	90	-	-	-	-
Nerula and Ashraf, 1987	-	-	-	-	-	-
GPA, 2004	-	-	-	-	-	-
France, 2007	-	-	-	-	-	-
Mamun et al., 2005	-	-	-	-	-	-
Coquelet and Richon, 2007	-	-	-	-	-	-
Descamps et al., 2004	3.3 - 4.3%	90.8 - 98	-	-	-	-
Nerula and Ashraf, 1987	-	90	36.40%	10.9 M€	-	-
Singh et al., 2003	-	65	-	27M$/year	55	28M$/year
Nerula and Ashraf, 1987	-	95	-	-	-	-
Teng and Tondeur, 2006	-	90	28 to 29	-	-	-
Knuutila et al., 2008	-	43 - 92	30 - 66	-	-	-
GPA, 2004	-	-	-	-	-	-
Knudsen et al., 2008	-	90	-	-	-	-
Leci, 1997	65%	-	-	1842$/kW	50% inc.	35%
Alie et al., 2004	-	-	-	-	-	-
IEA, 2004	-	85	31	1850$/kW	24	-
Rodgers et al., 1998	-	-	-	-	-	-
Kim and Svendsen, 2007	-	-	-	-	-	-
Hook, 1997	-	-	-	-	-	-
Kanniche and Bouallou, 2007	-	88	28 - 30	-	-	-
France et al., 2007	-	-	-	-	-	-
Mamun et al., 2005	-	-	-	-	-	-
Nerula and Ashraf, 1987	-	-	-	-	-	-
IEA, 2004	-	85	40 - 51	800-1635	20-25	-
Kanniche and Bouallou, 2007	-	85	30 - 33	53%inc	-	59%
GPA, 2004	-	90	34.2	-	-	-
GPA, 2004	-	-	-	-	-	-

2.7 Discussion of the literature data

From the data of the literature review, a few conclusions are immediately evident.

Absorption techniques are substantially more researched and developed than other capture techniques. Chemical absorption is particularly well developed, with amine and carbonate solvents receiving the most interest. While hybrid solvents are mentioned often and theoretically well explained, data for such a technique still seems scarce. Absorption using physical solvents is fairly well researched, but data are not as comprehensively found as that for chemical solvents.

Blended absorption, although not the most researched, show the most promising results. Low energy penalty values were reported by Nerula and Ashraf (1987), as well as GPA (2004), in comparison to most energy penalty measurements reported for chemical and physical absorption. Moreover, relatively higher CO_2 loading measurements were reported in comparison to other capture techniques. Lower absorption rates were reported by Descamps et al. (2004), in comparison to chemical and physical solvents, which contributes to the lower energy penalty observed.

The drawback found, is the lower capture efficiency for blended absorption in comparison to what chemical absorption can potentially achieve. Cyclic solvent capacity (α) is also comparatively much lower, which may be the reason for lower capture efficiencies. Another current drawback is the lack of costing data available for blended absorption.

It is quite evident that solvent absorption is the most researched compared to other CO_2 capture techniques which lack sufficient data. A fatal drawback of some techniques is the complete lack of data available for absorption rates, CO_2 loading, capture efficiency and cyclic capacity. Energy penalty is often only found expressed as a percentage increase rather than absolute values. The most data reported for these other techniques, were data for the technique of combining membranes with absorption. Data reported by IEA (2004) and Teng and Tondeur (2006) show highly optimistic CO_2 capture costs and investment costs, and comparatively higher overall efficiencies.

Data for hydrate and sorbent based capture techniques are disappointingly scarce. This may be due to the lack of development of hydrate processes at present. Much investigation needs to be done to optimise hydrate formation conditions and selectivity, by using additives such as TBAB and THF. Current data for such investigations are abundantly available in reports such as Jadhawar et al., 2006. Once this challenge is overcome, more valuable simulations may be done using hydrates.

The fundamental drawback of sorbent usage is the low attrition resistance and hence low durability of sorbents for long term usage. Only once this is overcome, can more valuable measurements be taken and its prospects for use in CO_2 capture be more optimistic.

Cost data are abundantly available for general cases of post, pre, and oxyfuel combustion/reaction modes, for IGCC and PC power plants. Data for CTL, GTL and other non-electricity production plants seems scarce however. Results show high investment costs for IGCC and oxyfuel combustion power plants. This is due to other units that need to be installed for IGCC to be successful, such as gasifiers and shift converters. Expensive cryogenic air separation units are needed to accommodate oxyfuel combustion, which also increases the plant operating costs considerably.

2.8 The choice of capture method

The factors mentioned in previous sections have influenced the decision as to which capture method to investigate further. Solvent absorption is noted for its versatility in application. Depending on the solvent, it can be applied to all combustion modes and for all coal processes. Many of its applications require relatively simple retrofit techniques and do not disturb the rest of the process.

Solvent absorption is applicable to coal combustion, CTL and GTL processes, and are comparatively efficient in many cases where incoming gas conditions are unfavourable.

Another factor which cannot be ignored is the maturity of the technique. Solvent absorption is the most researched capture technique, possessing the most quantitative data to enable accurate decision making on its application. As noted in the literature review results, key information such as efficiency and cost estimates can be drawn, which is a necessity when deciding to invest in its application. In comparison, other techniques lack the data and hence the required certainty of decision making.

With such abundant data, it requires much less research on the part of individual companies which choose to incorporate CO_2 capture and storage. This has financial benefits, which is of greater importance to a developing country such as South Africa, compared to developed nations. The importance of this aspect is further explained by Gibbons et al. (2007) and Surridge (2005).

Hence the choice of capture method to investigate further in this study is solvent absorption. The next issue regards which aspect of solvent absorption to study further in particular.

As mentioned before, physical solvents are not well researched compared to chemical solvents.

There are also stricter limitations to their operating conditions. Nerula and Ashraf (1987) studied the performance of methanol at different temperatures, as well as Selexol® , NMP and Flour solvents. Descamps et al. (2005) studied the performance of Methanol at different temperatures. Kanniche and Bouallou (2007) studied Selexol®. Hybrid solvents are not well researched

Amine absorption is a relatively well developed technology that is already in use in industry for applications such as denitrification and acid gas desulphurisation processes.

There has been much research done in the application of single amines of different concentration. Mamun et al. (2005) has done low pressure solubility and absorption rate measurements for MEA, MMEA, EMEA, MDEA, BEA, AEEA, and PZ solvents of different solvent concentrations and CO_2 partial pressures. Dicko et al. (2010) measured CO_2 solubilities of up to 3 bar partial pressure in 50 wt% MDEA at temperatures up to 393.15 K. Kanniche and Bouallou (2007) considered MEA, MDEA, and DEA solvents at 30 wt% concentration. Oexmann et al. (2007) considered the use of potassium carbonate for absorption at 335.15 K. Nerula and Ashraf (1987) did a vast study on MEA, MDEA, DEA, and K_2CO_3 solvents of different concentration.

Knudsen et al. (2008) studied the absorption capacity of MEA and Castor 2 solvent. Rodgers et al. (1998) measured the solubility of MDEA at pressures up to 3 bar and temperatures up to 323.15 K. Measurements with MEA and AEEA were also done at different temperatures by Kim and Svendson (2007). The performance of hindered amines such as AMP and Alkazid were measured by Hook (1997).

It is thus safe to conclude that chemical absorption using single amines, is already well researched.

Another promising idea is the use of amine blends. The literature review results presented in Table 2-2 show that the technique appears to have comparatively good efficiency in CO_2 absorption. Many blended solvents have been shown to have higher solubilities and absorption rates than single amine solvents.

The technique of using solvent blends also provides added versatility and provides avenues to reach a better compromise between absorption capacity and absorption rate, especially when blending primary amines with secondary or tertiary amines. Although it is still an emerging technique, there is substantial data available for comparison. Mamun et al. (2006) obtained solubility data for MDEA, BEA, AEEA, and MEA blends. Kanniche and Bouallou (2007) focussed on MEA+MDEA of different blend ratios and solvent concentrations. Oexmann et al. (2008) obtained loading data for potassium carbonate + PZ blends of different concentrations.

Therefore, further research into the use of blended amine solvents was undertaken. There is abundant information regarding the use of MEA+MDEA blends. Kaewsichen et al. (2001) have obtained solubility data for MEA+MDEA blends at 25 - 393.15 K and CO_2 partial pressures from 0.1 - 10 bar. Comparatively less data are available for MDEA+DEA blends, which are also of great interest. Data are typically limited in temperature range and often recorded for low CO_2 partial pressures. Kundu and Bandyopadhyay (2006) studied and obtained vapour-liquid equilibrium (VLE) data for MDEA+DEA blends in MDEA:DEA compositions of 1.5: 28.5, 3: 27, and 4.5: 25.5 (wt%), at CO_2 partial pressures of up to 1 bar and temperatures up to 323.15 K. Murrieta-Guivara et al. (1998) published VLE data for CO_2 in MDEA: DEA blends of ratios 15: 10, 20: 10, 10: 20, and 35: 10 (wt%) at temperatures from 30 - 393.15 K. CO_2 partial pressures ranged from 3 - 30 bar.

It was decided that more VLE measurements could be done to contribute to the investigation of MDEA: DEA blends for use as CO_2 capture solvents. System conditions of these measurements were decided based on industrial operating conditions, as well as the novelty of these systems.

Since the temperature of flue gas in South African coal industries is typically 413.15 K (Kawesha, 2009), it was decided to investigate whether it would be feasible to treat the gas for CO_2 removal without lowering this temperature. To compare efficiencies, a temperature of 363.15 K was also studied.

One of the advantages stated regarding secondary and tertiary amines, was their relatively low corrosiveness. Many papers did not exploit this advantage and investigated solvent weight fractions of not more than 30 wt%. Murrieta-Guivara et al. (1998) was one of the few sources investigating solvent concentrations of up to 45 wt%. This study focussed on solvent concentrations of 50 wt%. Two solvent blend ratios were studied: 25 wt% MDEA + 25 wt% DEA + 50 wt% Water, and 30 wt% MDEA + 20 wt% DEA + 50 wt% water.

The total system pressures studied were 5 and 15 bar. The gas mixture was CO_2 + N_2. CO_2 partial pressures studied were 0.5, 1.5, 3.5, 4.5, and 10.5 bar. This partial pressure range covers a wide range of industrial applications. It can also be used to investigate whether compressing the flue gas (which is usually at pressures close to atmospheric in South African coal industries) is necessary or whether such compression need not apply.

A programme of measurement was set up, consisting of four main systems. The details of each measurement are described in Table 2-3:

Table 2-3: Programme of Measurement					
System	**Solvent Composition**	**System Temperature (K)**	**Data point**	**System Pressure (bar)**	**PCO_2 (bar)**
1	25 (wt%) MDEA : 25 (wt%) DEA : 50 (wt%) H_2O	363.15	1	15	0
			2	10	0
			3	5	0
			4	15	1.5
			5	5	0.5
			6	5	1.5
			7	15	4.5
			8	5	3.5
			9	15	10.5
2	25 (wt%) MDEA : 25 (wt%) DEA : 50 (wt%) H_2O	413.15	10	15	0
			11	5	0.5
			12	15	1.5
			13	15	4.5
			14	5	1.5
			15	5	0
			16	15	10.5
			17	5	3.5
3	30 (wt%) MDEA : 20 (wt%) DEA : 50 (wt%) H_2O	363.15	18	5	0.5
			19	15	1.5
			20	15	10.5
			21	15	4.5
			22	5	3.5
			23	5	1.5
			24	5	0
			25	15	0
4	30 (wt%) MDEA : 20 (wt%) DEA : 50 (wt%) H_2O	413.15	26	5	0.5
			27	15	1.5
			28	15	10.5
			29	5	1.5
			30	5	0
			31	15	0
			32	5	3.5
			33	15	4.5

The experimental procedure for the above mentioned measurements is described in Chapter 3, while results of the experimentation are discussed in Chapter 4. The obtained data are available in Appendix A and B, and related calculations of CO_2 loading in the solvent are explained in Appendix C.

2.9 Theoretical background of solvent absorption using amine solvent blends

The data obtained from the literature review suggested that solvent absorption is most likely to be the best option to consider for CO_2 capture. A good understanding of solvent absorption was necessary to further investigate its use and applicability to industrial processes.

As mentioned in Section 2.8, solvent blends of MDEA + DEA + H_2O were to be investigated for CO_2 absorption. As previously explained in Section 2.5.1.1, MDEA and DEA are chemical solvents. These solvents react with CO_2 in order to absorb it. The reaction mechanism of absorbing CO_2 using these two solvents, is complex. Blending these solvents introduces further complications to the reaction mechanism, since DEA is a secondary amine while MDEA is a tertiary amine.

The general reactions occurring would be: (Mamun et al., 2005, and Austgen et al., 1991)

CO_2 phase change: $CO_2\ (g) \leftrightarrow CO_2\ (aq)$ (R2-20)

Dissociation of H_2O: $2H_2O \leftrightarrow OH^- + H_3O^+$ (R2-21)

Dissociation of CO_2: $2H_2O + CO_2 \leftrightarrow H_3O^+ + HCO_3^-$ (R2-22)

Dissociation of Bicarbonate ion: $H_2O + HCO_3^- \leftrightarrow CO_3^{2-} + H_3O^+$ (R2-23)

Reactions (R2-20) to (R2-23) are common for all amines. Thereafter, the reaction mechanism differs. Primary and secondary amines undergo zwitterion formation mechanisms, while tertiary amines undergo alternative reaction mechanisms. Reaction mechanisms for DEA and CO_2 are as follows:

Zwitterion formation: $CO_2 + R^1R^2NH \leftrightarrow R^1R^2NH^+COO^-$ (R2-24)

Zwitterion deprotonation by a base: $R^1R^2NH^+COO^- + B \leftrightarrow R^1R^2NCOO^- + BH^+$ (R2-25)

The mechanism for MDEA differs from DEA as tertiary amines cannot react with CO_2 directly. The MDEA acts as a base for CO_2 to react with hydroxide in solution according to the following reaction mechanism (Mamun et al., 2005):

Dissociation of Amine: $R^1R^2R^3N + H_2O \leftrightarrow R^1R^2R^3NH^+ + OH^-$ (R2-26)

Hydroxide reaction: $CO_2 + OH^- \leftrightarrow HCO_3^-$ (R2-27)

Overall reaction ((R2-26) and (R2-27) combined):

$CO_2 + R^1R^2R^3N + H_2O \leftrightarrow R^1R^2R^3NH^+ + HCO_3^-$ (R2-28)

The above reactions were also documented in Osman et al. (2010). Equilibrium constant and Henry constant parameters for these reactions, pertaining to MDEA and DEA, are provided in Table D5 of Appendix D. Mamun et al. (2005) claimed that other minor reactions also occur,

such as formation of dicarbamate and dissociation of diprotonated amine. These reactions were neglected in this study.

2.10 Modelling of solvent absorption

The modelling of solvent absorption is imperative. This provides parameters for extrapolation and estimation of CO_2 partial pressures or CO_2 loading (depending on the model) over a broader range of systems. Aside from this benefit, models can be programmed into simulation packages such as Aspen-Plus Engineering Suite, so that an industrial simulation of solvent absorption can be performed. Highly developed models are already programmed into simulation packages. The modelling of measured solvent absorption data provides more accurate model parameters for use in these simulation packages.

There have been many proposed models for determining the CO_2 loading in solvents. These models were designed to account for the reaction mechanisms that occur as explained in Section 2.9. Simple models attempt to reduce the number of reactions that are accounted for, in order to simplify the calculation. With significant advances in computing speed, the use of more comprehensive models, offering greater accuracy in predictions, are becoming increasingly popular.

The first comprehensive model was by Klyamer et al. (1973), which used an activity coefficient approach for the excess Gibbs free energy. It assumed chemical reaction equilibrium in the liquid phase. It was also one of the first models to include the Debye-Huckel term which accounted for the non-ideality of solutions containing ionic solutes due to long range electrostatic interactions between ions. Activity coefficients were considered equal for each species and depended only on ionic strength as expressed in the Debye-Huckel limiting law. Species interaction was not considered (Weiland et al., 1993).

The Kent-Eisenberg model was thereafter developed and was found to be useful for single amine solutions. All non-idealities in the system were accounted for in the equilibrium constant (K) values (Benamor and Aroua, 2005). Certain non-idealities were ignored. Activity and fugacity coefficients were taken to be unity. Sulaiman et al. (1998) explains the model's applicability to amine blends, particularly MDEA+DEA blends. The model is complex and one of the first to consider activity coefficients in a reaction system consisting of six reactions. The model lacked accuracy when dealing with tertiary amines that did not form carbamates. The model's predictions were found to be inaccurate for mixed acid gases and amine blend systems (Weiland et al., 1993).

More complex models that could accommodate tertiary amines, mixed acid gases and amine blends, were the Electrolyte-Non-Random Two Liquid (Elec-NRTL) model, investigated by Chen and Evans (1968), and the Deshmukh-Mather Model (Deshmukh and Mather, 1981).

The use of the Elec-NRTL equation specifically for CO_2 absorption was investigated extensively in the work of Austgen et al. (1989) and Austgen et al. (1991). Austgen et al. (1989) studied the use of this model for systems involving single amines (MEA and DEA) and acid gas mixtures of H_2S and CO_2. The temperature range of the modelled data was 298.15 - 393.15 K. The model provided good agreement with experimental data.

The Elec-NRTL model was attempted by Manuel et al. (1998) for systems which included CO_2 and H_2S gas in MEA solvent. Alie (2004) also investigated the electrolyte NRTL model for MEA solvent at 30 wt%. Wappel et al. (2008) investigated the applicability of electrolyte NRTL in systems consisting of CO_2 and SO_2 gas.

The Elec- NRTL model rigorously includes solution chemistry, which allows for determination of all liquid-phase species, molecular or ionic. The model also accounts for interaction parameters. Austgen et al. (1991) shows a study of systems involving amine blends of MEA, DEA, and MDEA. The model provided satisfactory accuracy according to the study.

The benefit of trying to model data using the Elec-NRTL model, is that the model is well developed for use in other industries. It is built into simulation software such as Aspen and does not need to be entirely programmed, with the exception of initial parameters. The drawback when trying to model using Elec-NRTL is the computational complexity and resultant computing power and time needed for regression.

The lack of complexity of the Deshmukh-Mather model, compared to the Elec-NRTL model, has made its use increasingly popular. Like the Elec-NRTL model, the Deshmukh-Mather model is thermodynamically rigorous and provides broad generality with comparatively low computational requirements (Weiland et al., 1993). Long and short range species interactions are accounted for. It was also found to be highly applicable to amine blend systems. Weiland et al. (1993) investigated the model's use for systems involving CO_2 and H_2S gas, with amine blends of MEA, DEA, DGA, and MDEA. The model is also discussed in detail in Deshmukh and Mather (1981) where systems including H_2S and CO_2 gas and MEA solvent were studied.

A very simple model was introduced by Posey et al. (1996), assuming a single absorption reaction and a system using DEA solvent for H_2S and CO_2. Dicko et al. (2010) confirmed the model to be relatively accurate for systems involving MDEA at concentrations of up to 50 wt%, despite its simplicity.

2.11 Models used in this study

Three models were investigated in this study. The Posey-Tapperson-Rochelle model and the Deshmukh-Mather model were programmed in Matlab V. R2009b. The data measured in this study were regressed and parameters for these models were found. The Elec-NRTL model was available in Aspen Plus V.7.1 and its parameters were found by regressing the data measured in this study, in an Aspen regression routine.

The simple Posey-Tapperson-Rochelle model was investigated to determine its applicability and level of accuracy in prediction that can be achieved, when systems involving amine blends are considered.

The Deshmukh-Mather model was also investigated for its accuracy in comparison with the Posey-Tapperson-Rochelle model, as well as its overall performance when dealing with amine blends at high concentrations.

The associated Matlab® programmes for both the above models are described in Appendix E. The regressed parameters along with predicted data were tabulated and are available in Appendix D.

The Elec-NRTL model was already programmed in Aspen Plus V.7.1. This model was conveniently used to perform a simple preliminary Aspen simulation of the solvent absorption process, under dynamic conditions. The measured VLE data in this study were inputted into a regression routine to obtain accurate Elec-NRTL model parameter values to be used in this simulation. The parameters are presented in Table F1 of Appendix F. The simulation is discussed in Section 2.13 of Chapter 2and Section 4.3 of Chapter 4, with relevant data presented in Table F2 and F6 of Appendix F.

This section discusses the theoretical background of these models, including their assumptions and calculation procedure. Refer to the Nomenclature section of this thesis for a clarification of symbols that are used in this section.

2.11.1 Simple model: Posey-Tapperson-Rochelle

A simple model was developed by Posey et al. (1996), where the entire absorption reaction mechanism was assumed to contain a single reaction. The original study by Posey et al. (1996) involved a gas mixture of CO_2 and H_2S, with single amine solvents of MDEA: H_2O and DEA: H_2O at various concentrations.

The model was very easy to apply to the data in this study despite the differences in gas composition and the application of an amine blend. The model assumes the following reaction

for CO_2:

$$AmineH^+ + HCO_3^- \leftrightarrow Amine + CO_2(aq.) + H_2O \quad \text{(R2-29)}$$

Any presence of carbonate (CO_3^{2-}) and hydroxide (OH^-) ions are assumed to be small in concentration and hence neglected.

The equilibrium constant for the above reaction is calculated by the following equation (Posey et al., 1996, and Dicko et al., 2010):

$$\text{Ln}(K_{CO2}) = a + \frac{b}{T} + cL_T C^O{}_{AMINE} + d(L_T C^O{}_{AMINE})^{0.5} \quad \text{(2-1)}$$

With C^O_{AMINE} = Amine concentration neglecting the presence of acid gases.

$$= \frac{\text{Amine}}{\text{Amine} + H_2O}$$

Thereafter, P_{CO2} can be predicted using the following formula:

$$P_{CO2} = X_{CO2}K_{CO2}\frac{L_T}{(1-L_T)} \quad \text{(2-2)}$$

The programming of this model is found electronically. The programme is described in Appendix E, specifically in Sections E1 to E3. The programme regressed the VLE data presented in Appendix A, yielding appropriate values for a,b,c and d.

Figures E-1 and E-2 in Appendix E present a flowchart as the programme's description.

2.11.2 The Deshmukh-Mather model

The Deshmukh-Mather model is significantly more complex than the Posey-Tapperson-Rochelle model. For a system of 2 amines (MDEA+DEA) with CO_2 and N_2 gases, the Deshmukh-Mather model can accommodate a reaction mechanism including six key reactions (Benamor and Aroua, 2005). The original study of Deshmukh and Mather (1981) presented predictions of CO_2 and H_2S loading in MEA solvent. The study was expanded by Weiland et al. (1993) and thereafter Benamore and Aroua (2005) to accommodate amine blends. The following reactions are assumed:

Dissociation of protonated amine:

$$DEAH^+ \leftrightarrow DEA + H^+ \quad \text{(R2-30,DEA)}$$

$$MDEAH^+ \leftrightarrow MDEA + H^+ \quad \text{(R2-30,MDEA)}$$

Formation of carbamate (Only with DEA):

$$DEACOO^- + H_2O \leftrightarrow DEA + HCO_3^- \quad \text{(R2-31)}$$

Dissociation of carbon dioxide:

$$CO_2 + H_2O \leftrightarrow HCO_3^- + H^+ \quad \text{(R2-32)}$$

Dissociation of bicarbonate ion:

$$HCO_3^- \leftrightarrow CO_3^{2-} + H^+ \quad \text{(R2-33)}$$

Ionisation of water:

$$H_2O \leftrightarrow OH^- + H^+ \quad \text{(R2-34)}$$

The associated equilibrium constant equations for the above reactions are expressed as follows:

$$K_{2,DEA}[DEAH^+]_e \gamma_{DEAH^+} = [DEA]_t [H^+]_e \gamma_{DEA} \gamma_{H^+} \quad (2\text{-}3)$$

$$K_{2,MDEA}[MDEAH^+]_e \gamma_{MDEAH^+} = [MDEA]_t [H^+]_e \gamma_{MDEA} \gamma_{H^+} \quad (2\text{-}4)$$

$$K_3[DEA]_e[CO_2]\gamma_{DEA}\gamma_{CO_2} = [DEACOO^-][H^+](\gamma_{DEACOO^-} - \gamma_{H^+}) \quad (2\text{-}5)$$

$$K_4[CO_2]\gamma_{CO_2} = [HCO_3^-]_e[H^+]\gamma_{HCO_3^-}\gamma_{H^+} \quad (2\text{-}6)$$

$$K_5[HCO_3^-]_e \gamma_{HCO_3^-} = [CO_3^{2-}]_e[H^+]\gamma_{CO_3^{2-}}\gamma_{H^+} \quad (2\text{-}7)$$

$$K_6 a_{H_2O} = [OH^-]_e[H^+]\gamma_{OH^-}\gamma_{H^+} \quad (2\text{-}8)$$

Where "[]" indicate concentration of various species

The following set of balances must also be satisfied:

Amine balances:

$$[DEA]_t = [DEA]_e + [DEAH^+]_e + [DEACOO^-]_e \quad (2\text{-}9)$$

$$[MDEA]_t = [MDEA]_e + [MDEAH^+]_e \quad (2\text{-}10)$$

CO_2 balance:

$$\alpha[DEA + MDEA]_t = [HCO_3^-]_e + [DEACOO^-]_e + [CO_3^{2-}]_e + [CO_2] \quad (2\text{-}11)$$

Charge balance:

$$[DEAH^+]_e + [MDEAH^+]_e = [HCO_3^-]_e + [DEACOO^-]_e + 2[CO_3^{2-}]_e \quad (2\text{-}12)$$

CO_2 concentration is estimated using Henry's law:

$$P_{CO2} = H_{CO2}[CO_2] \quad (2\text{-}13)$$

The Deshmukh-Mather model uses the Guggenheim and Stokes equation as presented in Benamor and Aroua (2005) to calculate activity coefficients of each species:

$$\ln \gamma_i = -\frac{A^\gamma Z_i \sqrt{I}}{1 + B^\gamma \sqrt{I}} + 2\sum B_{i,j} C_j \quad (2\text{-}14)$$

Where $A^\gamma = \frac{F^3 (2000\rho_{solvent})^{1/2}}{2.303(\varepsilon_O D_S RT)^{3/2}.(8\pi N_A)}$ and $B^\gamma = \sqrt{\frac{2000.F^3}{\varepsilon_O D_S RT}}$ (Dicko et al., 2010)

$D_S = 78.54(1 - 4.579 \times 10^{-3} \times (T - 298.15) + 1.19 \times 10^{-5} \times (T - 298.15)^2 - 2.8 \times 10^{-7} \times (T - 298.15)^3)$ (Dicko et al., 2010).

$B_{i,j} = a_{ij} + b_{ij}T$ where a_{ij} and b_{ij} are parameters that need to be estimated. Interactions between solutes and solvents are not included.

I represents the ionic strength of the solution. $I = \frac{1}{2}\sum m_j Z_j^2$. The ions in solution for the system investigated here include H^+, OH^-, HCO_3^-, CO_3^{2-}, $DEACOO^-$, $DEAH^+$, and $MDEAH^+$.

The mathematical framework described above, that was used in the programming of this model, was taken from Benamor and Aroua (2005).

Equations (2-3) to (2-13) can be reduced to a single six order polynomial equation that can be used to first solve for $[H^+]$:

$$A[H^+]^6 + B[H^+]^5 + C[H^+]^4 + D[H^+]^3 + E[H^+]^2 + F[H^+] + G = 0 \quad (2\text{-}15)$$

Where

$$A = 1$$

$$B = [MDEA]_t + [DEA]_t + K_{1,DEA}K_{1,MDEA}$$

$$C = K_{1,MDEA}[DEA]_t + K_{1,DEA}[MDEA]_t - K_3\frac{P_{CO_2}}{H_{CO_2}} - K_5 + K_{1,DEA}K_{1,MDEA} + K_{1,DEA}K_2\frac{P_{CO_2}}{H_{CO_2}}$$

$$D = \frac{P_{CO_2}}{H_{CO_2}}(K_{1,DEA}K_2([MDEA]_t - [DEA]_t) - 2K_3K_4 + K_{1,DEA}K_2K_{1,MDEA}) - (K_{1,DEA} + K_{1,MDEA}) \times (K_3 \frac{P_{CO_2}}{H_{CO_2}} + K_5)$$

$$E = -K_{1,DEA}K_2K_{1,MDEA}[DEA]_t \frac{P_{CO_2}}{H_{CO_2}} + 2K_3K_4 \frac{P_{CO_2}}{H_{CO_2}}(K_{1,DEA} + K_{1,MDEA})$$

$$+ (K_{1,DEA}K_{1,MDEA} + K_{1,DEA}K_2 \frac{P_{CO_2}}{H_{CO_2}}) \times (K_3 \frac{P_{CO_2}}{H_{CO_2}} + K_5)$$

$$F = -\left[2K_3K_4 \frac{P_{CO_2}}{H_{CO_2}} \left(K_{1,DEA}K_{1,MDEA} + K_{1,DEA}K_2 \frac{P_{CO_2}}{H_{CO_2}} \right) + K_{1,DEA}K_{1,MDEA}K_2 \frac{P_{CO_2}}{H_{CO_2}} \left(K_3 \frac{P_{CO_2}}{H_{CO_2}} + K_5 \right) \right]$$

$$G = -2K_1K_2K_3K_4K_{1,DEA} \left(\frac{P_{CO_2}}{H_{CO_2}} \right)^2$$

The CO_2 loading is given by:

$$\alpha = \frac{P_{CO_2}}{[H^+]H_{CO_2}} \frac{K_2[DEA]_t / (1 + ([H^+]/K_{1,DEA}) + K_2(P_{CO_2}/[H^+]H_{CO_2})) + K_3 + K_3K_4/[H^+] + [H^+]}{[MDEA]_t + [DEA]_t} \quad (2\text{-}16)$$

The carbamate concentration can be found as follows:

[Carbamate]=

$$\frac{(P_{CO_2}/[H^+]H_{CO_2}).(K_2[MDEA]]_t / (1 + ([H^+]/K_{1,DEA}) + K_2(P_{CO_2}/[H^+]H_{CO_2})))}{[DEA]_t + [MDEA]_t} \quad (2\text{-}17)$$

The programming of the Deshmukh-Mather model is described in Appendix E in Sections E1, E4, E5 and E6. Figures E-3 and E-4 provide a flow sheet description of the programme principle. The programme is available electronically as Matlab mfiles, titled as in Appendix E.

2.11.3 The Electrolyte-Non-Random Two Liquid (Elec-NRTL) model

The Elec-NRTL model is a comprehensive model used for modelling amine absorption. The model has gained popularity with increasing computer processor speeds. The advantage of this model is that it is highly developed and already in use for simulations of other absorption processes and processes involving ionic compounds. It is comprehensively available in simulation packages such as Aspen.

There have been many attempts at using the Elec-NRTL model for amine absorption. Austgen et al. (1989) obtained VLE data for DEA and MEA solvents absorbing CO_2 and H_2S at

temperatures of 25 - 393.15 K. A similar study was done on MDEA and DEA at 313.15 - 353.15 K by Austgen et al. (1991), on CO_2 partial pressures of 0.001 – 2.6 bar.

In Elec-NRTL modelling, binary interaction parameters are expressed as follows (Aspen, 2008):

Molecule-Molecule Interaction Parameters:

$$B_{i,j} = a_{i,j} + \frac{b_{i,j}}{T} + f_{i,j}\ln(T) + g_{i,j}T \tag{2-18}$$

Electrolyte-Molecule and Electrolyte-Electrolyte Parameters:

$$B_{ca,j} = c_{ca,j} + \frac{d_{ca,j}}{T} + e_{ca,j}\left[\frac{(T^{ref} - T)}{T} + \ln\left(\frac{T}{T^{ref}}\right)\right] \tag{2-19}$$

$$B_{j,ca} = c_{j,ca} + \frac{d_{j,ca}}{T} + e_{j,ca}\left[\frac{(T^{ref} - T)}{T} + \ln\left(\frac{T}{T^{ref}}\right)\right] \tag{2-20}$$

For the electrolyte-electrolyte pair parameters, the two electrolytes must share either one common cation or one common anion.

$$B_{c'a,c''a} = c_{c'a,c''a} + \frac{d_{c'a,c''a}}{T} + e_{c'a,c''a}\left[\frac{(T^{ref} - T)}{T} + \ln\left(\frac{T}{T^{ref}}\right)\right] \tag{2-21}$$

$$B_{ca',ca''} = c_{ca',ca''} + \frac{d_{ca',ca''}}{T} + e_{ca',ca''}\left[\frac{(T^{ref} - T)}{T} + \ln\left(\frac{T}{T^{ref}}\right)\right] \tag{2-22}$$

a-f = parameters for finding binary interaction parameters.

For the Elec-NRTL model, the Gibbs excess energy is expressed using the following equation (Aroua et al., 2002):

$$\frac{g^{ex,local}}{RT} = \sum_m X_m \frac{\sum_j X_j G_{j,m} B_{j,m}}{\sum_k X_k G_{k,m}} + \sum_c X_c \sum_{a'}\left(\frac{X_{a'}}{\sum_{a''} X_{a''}}\right)\frac{\sum_j X_j G_{jc,a'c,jc,a'c}}{\sum_k X_k G_{kc,a'c}}$$
$$+ \sum_a X_a \sum_{c'}\left(\frac{X_{c'}}{\sum_{c''} X_{c''}}\right)\frac{\sum_j X_j G_{ja,c'a,ja,c'a}}{\sum_k X_k G_{ka,c'a}} \tag{2-23}$$

The activity coefficient is then expressed as:

$$\ln \gamma_i = \frac{1}{RT}\left[\frac{\partial(n_t g^{ex})}{\partial n_j}\right]_{T,P,n_{j\neq i}} \tag{2-24}$$

It is important to note that the expressions for the binary interaction parameters differ for the Elec-NRTL model depending on whether each species is an electrolyte (cation or anion), or a molecule. This is a feature that the Deshmukh-Mather model does not possess.

The Elec-NRTL was used in this study in an Aspen absorption simulation. The measured data obtained in this study were entered into an Aspen regression routine to obtain accurate interaction parameters for the systems measured. The regressed parameters are available in Table F1 of Appendix F. Thereafter, an absorption simulation was conducted using these interaction parameters. The details of such are described in Section 2.12 of Chapter 2 and Section 4.3 of Chapter 4.

2.12 Aspen simulations for CO_2 capture by solvent absorption

Among the many developments surrounding solvent absorption for use in CO_2 capture, are absorption simulations conducted in various simulation software.

Numerous sources investigated attempts to simulate amine solvent absorption for CO_2 capture in simulation packages such as Aspen Plus Engineering Suite, using the Elec-NRTL model. Manuel et al. (1998) performed a rate-based Aspen absorption and stripping simulation based on the Elec-NRTL model. Various techniques were implemented to minimise energy consumption and optimise solvent loadings, which include size alterations, column packing, and tray changes. A MDEA + AMP + CO_2 system was studied by Aroua et al. (2002). In this case Aspen was used to predict VLE data and thereafter CO_2 loading data with the absence of any rigid absorption process.

Alie (2004) presents a detailed description of simulation attempts using Aspen. Different flow processes were considered, including recycling loops and other separations units between absorption and stripping. Effects on energy consumption and CO_2 loading such as absorber and stripper temperature and pressure, as well as number of stages and reflux ratios were investigated. Although the Elec-NRTL model was used, other modified versions of the model were also investigated, such as the ENRTL-HG (Electrolyte-Non-Random Two Liquid-Helgeson) and ENRTL-HF (Electrolyte-Non-Random Two Liquid-Heilig Franck) models.

Simulations of absorption processes are made in an attempt to facilitate a transition from laboratory scale experiments to industrial testing. They are a stepping stone towards pilot plant development and ultimately industrial scale absorption. Important results of Aspen simulations

are preliminary process design and design estimates, capital investment estimates, energy penalty of CO_2 capture (GJ/tonne CO_2), and CO_2 capture costs ($/tonne CO_2). Refer to Table 2-2 for some of these estimates, which were made by various other literature sources.

2.13 Aspen simulations conducted in this study

A preliminary Aspen simulation was conducted in this study to check if CO_2 loading results similar to that obtained in the VLE measurements, could be obtained in a simulation of industrial amine absorption coupled with stripping. Another objective was to determine the energy consumption and capital expenditure required for such an operation.

In this study, a simple absorption and stripping process has been developed in Aspen, based on the Elec-NRTL model. Flue gas and solvent flow rates have been chosen to mimic an industrial scale CTL plant (Kawesha, 2009). The design is very basic, as it is done based on many assumptions and without any clear constraints.

The first step in the simulating of CO_2 capture by absorption was to input the measured data into Aspen to obtain, by regression, accurate interaction parameters for the Elec-NRTL model. Total system pressure, system temperature, vapour mole fraction, and liquid mole fraction were entered into the Aspen regression routine. The results of this regression are available in Table F1 of Appendix F. The Aspen file is available electronically as "ElecNRTL Regression.apw"

Thereafter, simulations of the absorption process were developed. The relevant data for these simulations are available in Tables F2 to F6 of Appendix F. The Aspen files are available electronically as "CO_2 Absorption Simulation No Recycle.apw", "CO_2 Absorption Simulation With Recycle.apw", and "CO_2 Absorption Simulation Modified.apw",

The results of these simulation attempts are discussed in detail in Section 4.3 of Chapter 4, including the process design, all design choices, flow rate choices, unit modifications, stream results and CO_2 loading results.

3. APPARATUS AND EXPERIMENTAL PROCEDURE

In order to investigate the use of amine solvents for CO_2 capture, a programme of vapour-liquid equilibrium (VLE) measurements was planned, in particular to expand on the effectiveness of amine solvent blends (combinations of two or more amines). The use of amine solvent blends was chosen not only because of the gaps found in the literature, in comparison to single amine solvents, but also because their use, as effective CO_2 capture solvents, shows much promise theoretically and in the few literature sources that chose to investigate them experimentally.

Measurements were grouped into four systems as described in Table 2-3 in Section 2.8. This chapter describes the apparatus and compounds that were used and the experimental procedure that was followed in measuring these systems. Also included in this chapter are gas chromatograph (GC) and pressure transducer calibration procedures, solvent preparation techniques, the equilibrium cell loading procedure, measurement techniques, and the cell discharge procedure.

3.1 Apparatus used

A static-analytic apparatus was used to determine the solubility of CO_2 and N_2 for the systems mentioned. The apparatus was made available by CEP/TEP Laboratories of Mines-Paristech. Experimentation was done at Mines-Paristech in Fontainebleau, France. This apparatus was used for other measurements described in Dicko et al. (2010). The work done using this apparatus is also described in Osman et al. (2010) which contains measurements done as part of the completion of this work.

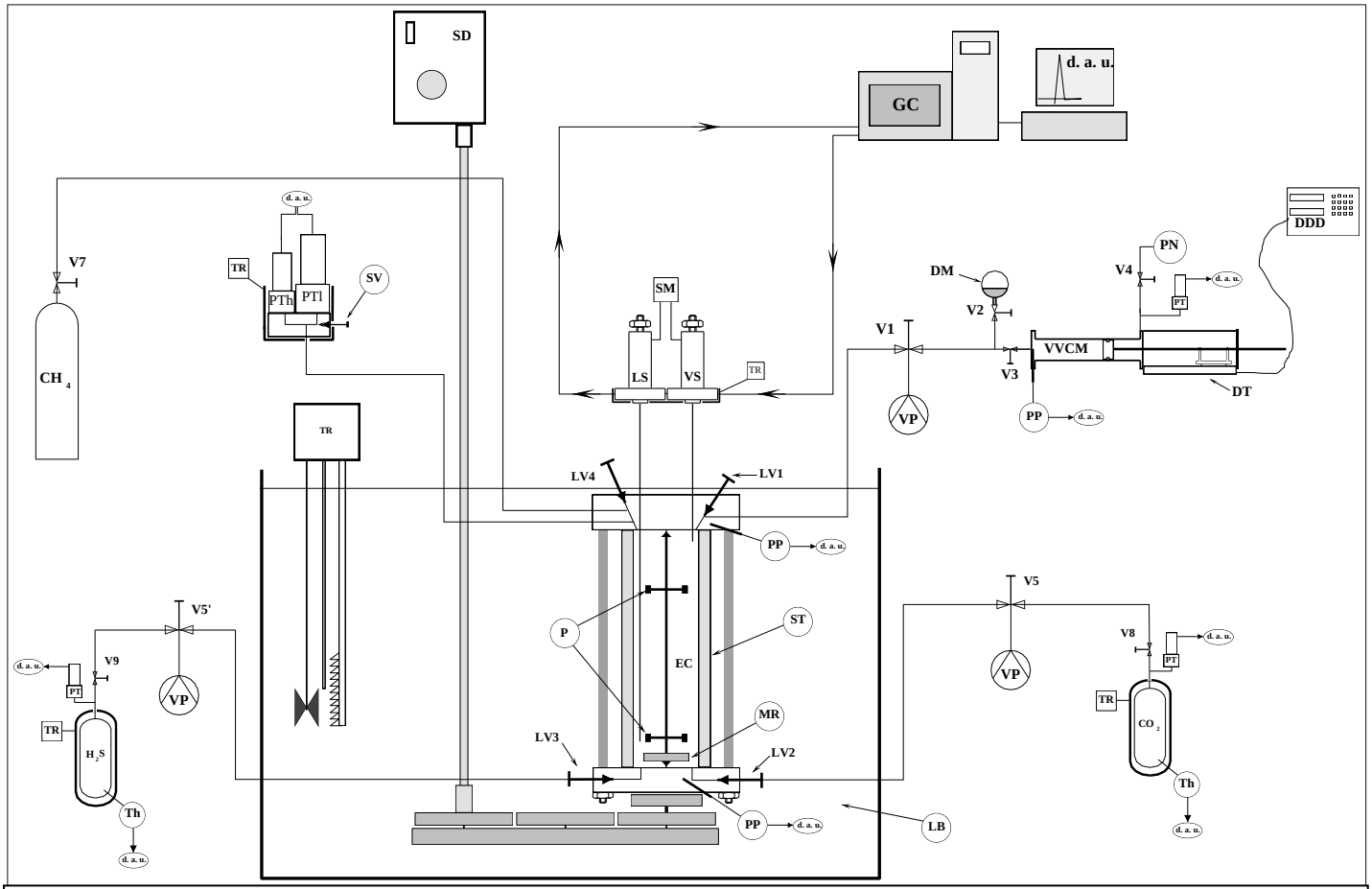

d. a. u. : Data Acquisition Unit ; DDD : Displacement Digital Display ; DM : Degassed Mixture ; DT : Displacement Transducer ; EC : Equilibrium Cell ; GC : Gas Chromatograph ; LB: Liquid Bath; LS : Liquid Sampler ; LVi : Loading Valve ; MR; Magnetic Rod; P: Propeller; PP : Platinum Probe ; PN : Pressurized Nitrogen ; PT: Pressure transducer; PTh: Pressure transducer for high pressure values; PTl: Pressure transducer for low pressure values; SD : Stirring Device ; SM: Sample Monitoring; ST : Sapphire Tube ; TR: Thermal Regulator; Th: Thermocouple Vi: Valve; VP: Vacuum Pump; VS: Vapor Sampler; VVCM: Variable Volume Cell for Mixture

Figure 3-1: Static Analytic Apparatus used in VLE measurements (Dicko et al. (2010))

Figure 3-1 shows a diagram of the apparatus. The equilibrium cell (EC) is composed of a sapphire tube (ST) between two hastelloy flanges. The design and construction allows system pressures of up to 100 bar and operating temperatures up to 473.15 K. The total volume of the cell is 34 cm^3 ($\pm 1x10^{-6}$ cm^3) and the internal diameter is 25 mm (±0.01 mm). Two non-rotating stem valves (LV1 and LV4) were installed on the top flange for gas or liquid loading. For this project, one valve was closed and inactive, while the other was used for N_2 pressurisation. For liquid solvent and CO_2 loading, the bottom flange has two non-rotating stem valves (LV2 and LV3). A rotating axis holding a magnetic rod (MR) is contained inside the equilibrium cell, which has two propellers (P) (one for liquid stirring and one for gas stirring). A stirring motor (SD) with a stirring assembly rotates the magnetic rod (MR) together with its propellers (P).

The cell was immersed in a Ultra-Kryomat Lauda constant temperature liquid bath (LB) to control and maintain system temperature. Silicone oil was used as the heating medium. This oil can be used as a heating medium for up to 553.15 K. Pt100 thermometer devices connected to an HP Data Acquisition unit (HP34970A), monitor temperature. Temperature is controlled to within 0.01 K. Liquid and vapour phase temperature in the cell are each measured by two thermometers, to check for thermal gradients and determine thermal equilibrium. To ensure constant temperature while loading, the temperature of CO_2 gas is also monitored at its cylinder. Calibration of the Pt100 thermometers is done periodically against a 25 Ω reference platinum resistance thermometer (Tinsley Precision Instruments). A second order calibration was achieved by *Laboratoire National d'Essais* (Paris) based on the 1990 International Temperature Scale. The uncertainty is ±0.01 K in the range of 278.15 to 402.81 K.

N_2 gas is used merely to achieve the desired total system pressure. Druck pressure transducers monitor pressure. All transducers are connected to an HP data acquisition unit (HP34970A). The equilibrium cell has two pressure transducers: One for accurate pressure measurement of pressures of 0 - 10 bar; and one for 0 - 100 bar. Pressure in the CO_2 cylinder is also measured using pressure transducers. Transducers were calibrated using a Dead Weight Pressure Balance. (Desgranges & Huot 5202S, CP 3 to 400 bar, Aubervilliers, France). The uncertainty was found to be ±0.001 bar. Table B8 of Appendix B contains calibration data for pressure.

ROLSI^{TM} samplers (LS and VS) are used for vapour and liquid sampling. Sampling is controlled and monitored using a sample monitoring device (SM) and are analysed by a Gas Chromatograph (GC) (PERICHROM model PR-2100). A "Porapak R80/100 mesh" (1.2 m x 2 mm ID Silicosteel) column was used in the GC. The thermal conductivity detector is sufficient for the purpose of this project.

The HP data acquisition unit is connected to a personal computer through one RS-232 interface. The sample monitoring device and gas chromatograph (GC) is also connected to the personal computer. WINILAB III software version 4 was used as the interface. Uncertainty in area determination and resultant composition measurement occurred due to manual integration of areas using the WINILAB III software. The uncertainty on molar composition is estimated to be ±2 % for both vapour and liquid samples. Refer to Tables B1to B4 of Appendix B for molar composition calibration.

An Anton Paar DMA 5000 density meter was used to measure the density of solvents. Densities were measured over a range of 278.15 – 343.15 K (the upper and lower bounds of good performance of the measuring instrument). Thereafter, densities were extrapolated to 363.15 K and 413.15 K (the temperature of the systems studied). Measurements for each solvent were

done twice to ensure repeatability of measurements. The uncertainty in density was found to be ±0.5 % (relative). The density calibration data are available in Tables B5 - B7 of Appendix B.

3.2 Gases and chemicals used

MDEA at 99 % purity was available from ATOFINA Chemicals Inc., ALDRICH. DEA at 99 % was supplied by SIGMA ALDRICH©. A Millipore Direct-Q™ 5 water filter was used to obtain distilled H_2O. Ethanol, used for cleaning the apparatus was available at 99 % purity from Vitlab.

The N_2 gas used was purchased from *Air Liquide*. Impurities included CO_2 < 1ppm v; CO < 1 ppm v; H_2O < 3 ppm v; NO_x < 0.1 ppm v and CN_{HM} < 0.2 ppm v. CO_2 was available at 99 % purity.

The amount of CO_2 charged was measured by pressure and density difference of the CO_2 tank under constant temperature conditions. The uncertainty is ±0.001 bar or ±0.001 mol CO_2.

The solvents were prepared by combining weighted amounts of DEA, MDEA and H_2O in a round bottom flask under vacuum. A Trivac D2-5E vacuum pump was used. 400 g solvent mixtures were prepared each time.

Three solvents were prepared. Their exact composition in wt% is given in Table 3-1, along with uncertainties in its synthesis:

Table 3-1: Solvent Compositions and Uncertainties

	MDEA (wt%)	Relative Uncertainty	DEA (wt%)	Relative Uncertainty	Water (wt%)	Relative Uncertainty
Mixture 1	24.90	0.39 %	25.00	0.07 %	50.10	0.02 %
Mixture 2	30.00	0.29 %	19.90	0.01 %	50.10	0.03 %
Mixture 3	-	-	50.00	0.03 %	50.00	0.02 %

Solvent was charged into the cell for each system run using a Variable Volume Cell (VVCM) attached to a displacement meter with an uncertainty of ±0.001mm. The volumes charged had an uncertainty of ±0.01 cm^3.

3.3 GC calibration

Before VLE measurements were taken, the Gas Chromatograph (GC) needed to be calibrated to correlate its response with the actual composition of the gas it is measuring. The GC was calibrated for N_2 and CO_2 gases, as well as liquid water. A 1000 µl syringe was initially used. The GC was calibrated for quantities of N_2 and CO_2 gas of 100 to 1000 µl. The following procedure was applied.

Procedure:

1. N_2 gas was obtained in a gas cylinder and supplied at 10 bar. The temperature was monitored.
2. A 1000 µl syringe was cleaned with compressed air and N_2 gas.
3. The GC with Winilab III V.5 software was prepared. The thermal conductivity detector TCD was prepared for GC calibration. This detector was sufficient for this purpose as the system contained no hydrocarbons. The flame ionisation detector (FID) was not used.
4. Calibration for N_2 began by drawing 100 µl of N_2 from the cylinder, using the syringe. The atmospheric pressure at time of drawing the N_2, was noted.
5. Data acquisition commenced and N_2 was promptly injected into the GC. The retention time was noted.
6. Once the first sample was noted in the software, another N_2 sample of the same volume was drawn and injected as in steps 4 and 5. Samples in Winilab are noted graphically as peaks of N_2 recorded by the TCD. The completed peak was integrated to obtain the area under it.
7. Steps 4 to 6 were repeated five to ten times until the areas of the peaks were found to be of similar magnitude, indicating good reproducibility. These areas were recorded in a spreadsheet, along with atmospheric temperature and pressure.
8. Steps 4 to 7 were repeated for volumes of 1000, 200, 800, 400 and 600 µl. The volumes were drawn specifically in this order to eliminate any hysteresis doubts and reduce the tendency to form any particular pattern as the sampling progresses.
9. All samples were regressed to 1^{st} order and 2^{nd} order equations.

The same calibration procedure was done for CO_2 gas. For both gases, the 2^{nd} order fit proved to have the lowest error. The 1^{st} order fit produced errors far greater than 3 % particularly for low volumes such as 100µl.

At the end of the entire measurement programme, it was found that the range of calibration of the gases and liquid H_2O was too great. A more accurate calibration was done over a smaller range of volumes. The data for the calibration of CO_2, H_2O and N_2 are shown in Tables B1 to B4, and Figures B1 to B3, of Appendix B.

3.4 Pressure transducer calibration

The inaccuracy of the pressure transducer that measures the pressure in the equilibrium cell, is due to manufacturing limitations. To correct this inaccuracy, the pressure transducer was calibrated using a Dead Weight Pressure balance (Desgranges and Hout 5202S, Aubervilliers, France). The calibration was done using N_2 gas from a cylinder.

Procedure:

1. A N_2 cylinder was attached to the pressure balance, along with the pressure transducer.
2. The pressure balance was switched on.
3. The pressure balance used in this study had a 200 g mass fixed onto it, which enabled pressure measurements above 3 bar.
4. The first calibration point commenced by noting the atmospheric pressure on the barometer and calculating the real pressure read by the pressure balance due to the 200 g weight.
5. Pressure equilibrium on the balance had to be achieved before recording data.
6. Pressure readings from the pressure balance were recorded at the equilibrium point. The real pressure given by the pressure balance and the pressure read from the pressure transducer were found to be notably different.
7. Steps 4 to 6 were repeated for different pressures by loading 100 g masses on the pressure balance. The greater the number of masses taken into account, the smoother and more precise the calibration curve was. The pressure transducer in this case was calibrated for a pressure range of 3 - 121 bar. This was sufficient for the study presented in this thesis.

3.5 Preparation of solvent mixture

Before any measurements could be done, the solvent under investigation needed to be prepared. Two solvent blends were used. One contained 25 wt% MDEA, 25 wt% DEA, and 50 wt% Water. The other contained 30 wt% MDEA, 20 wt% DEA, and 50 wt% Water. Solvents were made in batches in a 500 ml round bottom Pyrex vacuum flask. Other necessary equipment needed were:

1. Beakers. 250 ml and 150 ml
2. Deionized Water
3. MDEA 99 % purity
4. DEA 99 % purity
5. Mettler Balance
6. Compressed air supply
7. Evacuator apparatus
8. Thermal gun
9. Gloves
10. Ethanol
11. Paper towel

Procedure:

1. All beakers and round bottom flasks were cleaned using a paper towel, ethanol and compressed air.
2. 200 g of deionized water was measured precisely and added into an empty round bottom flask.
3. Vacuum was then established in the round bottom flask. A vacuum pump pressure of about 5 Pa was sufficient.
4. 100 g of MDEA was precisely measured and carefully added to the round bottom flask without compromising the vacuum.
5. The mixture shaken manually to facilitate good mixture. The outlet of the flask was cleaned using ethanol, a paper towel and compressed air to prevent contamination.
6. DEA exists as a solid at room temperature. It had to be heated to convert it to the liquid phase. Thereafter, 100 g of DEA was then measured precisely and added to the flask, following steps 4 and 5.

The mixture is then ready for loading into the Variable Volume Cell.

3.6 Preparing and loading the press (Variable Volume Cell)

The press is a cylindrical container made of rust resistant, inert metal alloy. The press in use for this apparatus had a diameter of 30.03 mm. The press stored the liquid solvent that was loaded in the equilibrium cell. There is a piston inside that acts against the liquid. This piston is moved using nitrogen gas under 5 bar pressure. A procedure for preparing the press is as follows.

Procedure:

1. The press, including the piston and all associated equipment, was cleaned using ethanol and compressed air.
2. The press was then evacuated using an evacuator with a vacuum pump. The round bottom flask which contained the solvent was attached to the evacuator to establish vacuum between the flask and the press.
3. Once vacuum was complete, the flask valve and associated connections were opened and solvent was allowed to flow by gravity into the press.
4. Once full, the press was closed and disconnected from the evacuator, together with the flask.
5. Relevant equipment was then cleaned using a paper towel, water, ethanol, and compressed air.

6. The press was then attached to the apparatus for use in VLE measurement of absorption. A displacement meter was attached to the press to measure the amount of solvent to be discharged into the equilibrium cell.

3.7 Loading the equilibrium cell

The loading of the equilibrium cell involves the introduction of CO_2 and N_2 gases, and liquid solvent into the cell. In practice the procedure is laborious and intricate. Much care was taken to ensure that precise quantities of the above compounds were introduced.

Procedure:

1. The equilibrium cell temperature was controlled by submerging the cell in an oil bath which was connected to a thermostat. Before any other step was done, the oil bath was brought to the desired system temperature.
2. Upon making sure that all necessary valves to the equilibrium cell were closed, the cell, along with relevant vapour and liquid lines, was then evacuated using a vacuum pump. 0.08 – 0.09 bar vacuum was achieved.
3. Pressure from the N_2 cylinder outlet was set to 5 bar and connected to the variable volume cell, which contained the solvent. The solvent was then charged into the equilibrium cell, taking special note of the piston displacement in order to establish the volume of solvent introduced. Approximately 14.17 cm^3 of solvent was used for each run in this study.
4. After ensuring necessary lines remained connected, the equilibrium cell was then submerged in the oil bath to achieve the desired system temperature. The solvent agitator in the cell was switched on.
5. The desired amount of CO_2 gas was then introduced into the equilibrium cell. The amount of CO_2 was calculated by noting the pressure change in the CO_2 cylinder, as well as the density of CO_2 at the CO_2 cylinder temperature.
6. N_2 was finally added into the cell until the desired system pressure was achieved.
7. CO_2 was being absorbed into the solvent as expected, reducing the system pressure slightly. If the system pressure changed significantly, N_2 gas was introduced with special caution.
8. Once system conditions reached equilibrium in terms of pressure and temperature, it became possible to take measurements. Depending on system conditions (temperature, pressure, vapour, and liquid mole fractions), it took 3 to 14 hours for equilibrium to be achieved.

3.9 Taking measurements

Once the cell was loaded and equilibrium was achieved, measurements were taken. Vapour and

liquid samples were drawn using ROLSI^{TM} samplers. Vapour sampling was typically done first. Liquid sampling was done thereafter. Temperature and pressure readings were taken by transducers.

Procedure:

1. The thermal conductivity detector in the GC was switched on. Carrier gas was set to 119. Carrierref was set to 189.
2. Winilab III software was initiated.
3. A probe acquisition programme was used to record temperature and pressure on the computer every 15 seconds, to ensure equilibrium was not severely affected during sampling.
4. Open the probe acquisition program and set it to take measurements of pressure and temperature every 15 seconds.
5. Vapour sampling was conducted first. The ROLSI^{TM} samplers were first used to take 3 quick samples in order to purge the GC column of any impurities.
6. Thereafter the ROLSI^{TM} samplers were set to take measurements every 26 minutes. 19 minutes to take the sample and 7 minutes to establish normal GC operating temperature.
7. Five samples were taken to ensure good repeatability of results.
8. Once measurements are done, integration of peaks commenced using Winilab III software. The peak areas, along with system temperature and pressure, was recorded in a spreadsheet.
9. Steps 5 to 8 were repeated for liquid sampling.

3.8 Unloading the equilibrium cell

The procedure of unloading the cell involves the removal of all species from the cell. Much caution needs to be taken in terms of liquids handling, waste removal and prevention or minimising of spillage.

Procedure:

1. The thermostat and agitator was switched off
2. The cell was removed from the oil bath and the oil bath was covered using a metal lid.
3. A waste line was attached to the equilibrium cell, the solvent valve at the cell was opened and the solvent was drained into a waste container.
4. The N_2 valve was then opened. Distilled water was added to the cell through the entrance of N_2 valve.
5. The agitator was switched on and water was used to clean the interior of the cell.
6. Compressed air was used to force out all the water into the waste container.

7. Steps 4 to 6 were repeated using ethanol instead of water.
8. The solvent line was cleaned using water, compressed air and ethanol. The exterior of the cell was cleaned using compressed air.
9. Once all equipment was thoroughly cleaned, relevant lines were reconnected and the equilibrium cell was prepared for solvent loading for the next run.

4. RESULTS AND DISCUSSION

The objective of this study was to first identify the CO_2 capture technique that was best suited for CO_2 capture in South African industries. As mentioned before, solvent absorption using amine blends was identified to be the most promising CO_2 capture solution.

Further investigation into the effectiveness of solvent absorption was conducted to ensure that this technique provides great potential for industrial applications. VLE measurements were first undertaken, which were explained in Section 2.8 and Chapter 3. Thereafter, the measurements obtained were modelled using the Posey-Tapperson-Rochelle model and the Deshmukh-Mather model, as explained in Section 2.11. Finally an Aspen simulation of the solvent absorption process, using the Elec-NRTL model, was conducted as discussed in Section 2.13.

This chapter discusses the results that were obtained from the endeavours mentioned above. CO_2 loading values obtained during VLE measurements, are first presented and discussed, followed by the modelling results. The details of the Aspen simulation, including the approach and process design decisions that were made, as well as key results were discussed thereafter. The chapter concludes with design and cost estimates and a discussion on the feasibility of the process obtained in Aspen, including the identification of limitations of the design and recommendations on its improvement.

4.1 Discussion of experimental VLE measurements and CO_2 loading results

The programme of measurement conducted in this study was discussed in Section 2.8. The measurements were categorised into four main systems, based on solvent composition and system temperature. The conditions of these systems are found in Table 2-3 of Section 2.8. As an added study, a fifth system consisting of three data points was developed. The conditions and results of this system are presented in Tables A5-1 and A5-2 of Appendix A.

This section analyses and discusses the results obtained from VLE measurements. The systems are compared to each other and to literature sources, in terms of CO_2 solvent loading at corresponding CO_2 partial pressures. CO_2 loading, as the results and figures in this chapter suggest, is the amount of CO_2 absorbed into the amine solvent blend (mol CO_2/mol amine (DEA + MDEA). The effect of system pressure, system temperature, CO_2 partial pressure, and solvent composition on CO_2 loading is discussed.

For the purpose of this thesis, the performance of a solvent shall refer to the magnitude of CO_2 liquid loading of the solvent in relation to its system conditions (ie. system temperature, system pressure and CO_2 partial pressure). Results for each run are found in Appendix A in tabulated form and are presented in this chapter in graphical form. Figures 4-1 to 4-8 and the associated

discussion below can also be found in Osman et al. (2010) which was developed during the progress of this thesis. The data and discussion in Osman et al. (2010) were developed by the author, and supervised and corrected by co-authors.

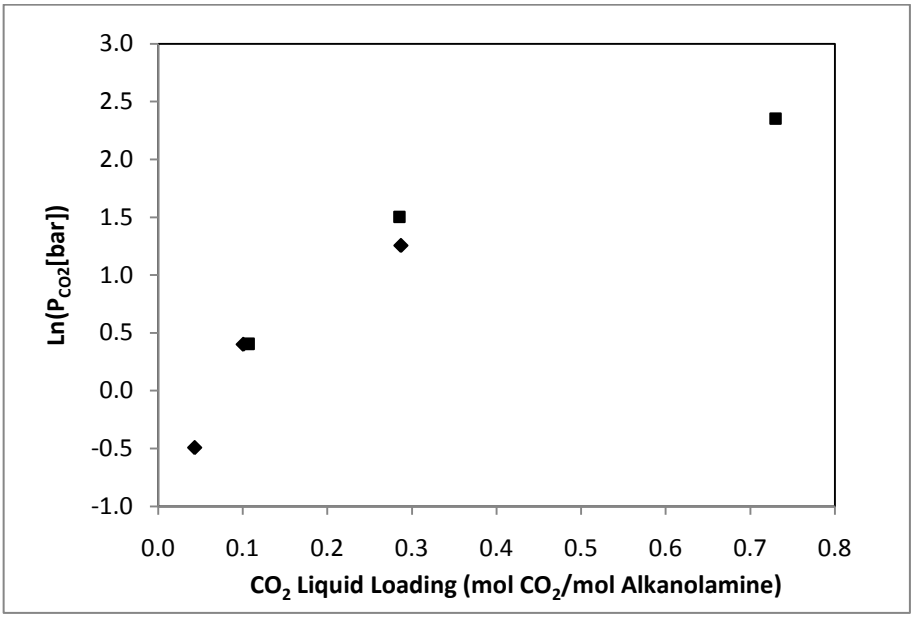

Figure 4-1: Ln(P_{CO2}) vs CO_2 loading for System 1: 25 wt% MDEA + 25 wt% DEA + 50 wt% H_2O, at 363.15 K. Comparison of 5 bar and 15 bar system pressure. ♦ - 5 bar system pressure; ■ – 15 bar system pressure

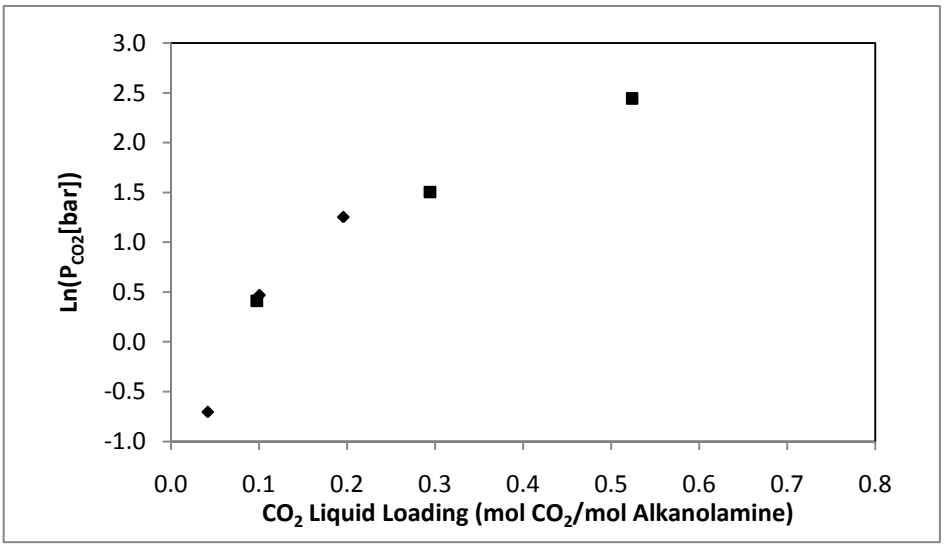

Figure 4-2: Ln(P_{CO2}) vs CO_2 loading for System 2: 25 wt% MDEA + 25 wt% DEA + 50 wt% H_2O, at 413.15 K. Comparison of 5 bar and 15 bar system pressure. ♦ - 5 bar system pressure; ■ – 15 bar system pressure

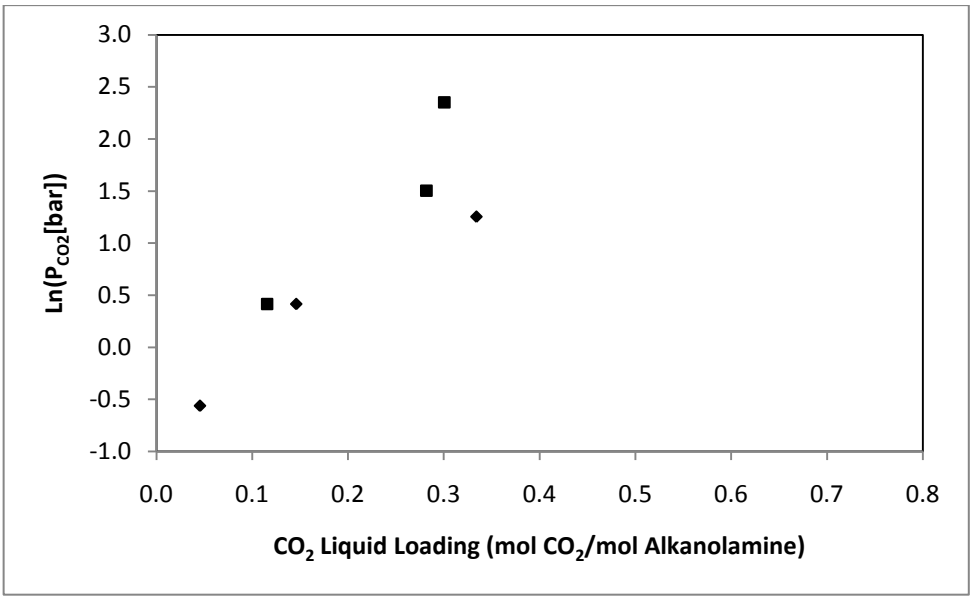

Figure 4-3: Ln(P_{CO2}) vs CO_2 loading for System 3: 30 wt% MDEA + 20 wt% DEA + 50 wt% H_2O, at 363.15 K. Comparison of 5 bar and 15 bar system pressure. ♦ - 5 bar system pressure; ■ – 15 bar system pressure

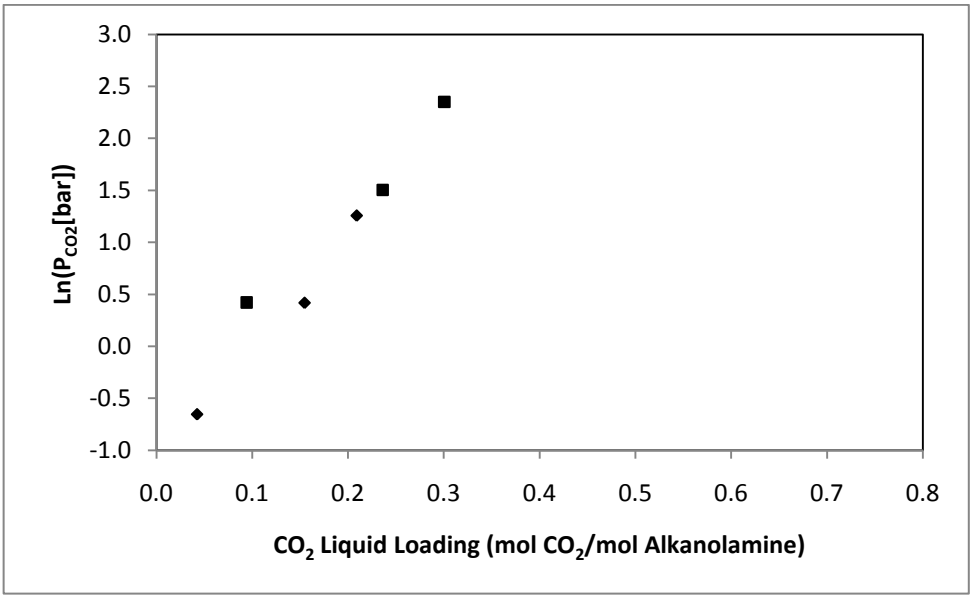

Figure 4-4: Ln(P_{CO2}) vs CO_2 loading for System 4: 30 wt% MDEA + 20 wt% DEA + 50 wt% H_2O, at 413.15 K. Comparison of 5 bar and 15 bar system pressure. ♦ - 5 bar system pressure; ■ – 15 bar system pressure

Figures 4-1 to 4-4 immediately suggest that the total system pressure has a substantial effect on the CO_2 loading in the solvent. An exponential (in this case log) pattern of CO_2 loading in the solvent was observed for both system pressures (5 bar and 15 bar). However the CO_2 loading was found to be more limited in the case of 5 bar system pressure. This is evident in the trends

of the data shown in Figures 4-1 to 4-4. The difference is not as significant as expected however. Tripling the system pressure produced only minor variations in the data obtained.

This observation however provides no conclusions on the operation of this process on an industrial scale, since this lack of effect of system pressure can be attributed to the fact that N_2 gas was used as the pressurising gas. N_2 gas is practically insoluble in the solvents used in this study. The relatively high rate of CO_2 absorption and the high absorption capacity of the solvent could be another reason for the lack of difference in results due to total pressure.

Another consequence of low system pressure is shown in Tables A1-1 to A4-1 of Appendix A. At total pressures of 5 bar, there is increased H_2O composition in the vapour phase. This indicates evaporation losses of H_2O to the gaseous phase. Industrially, this would be absolutely undesirable.

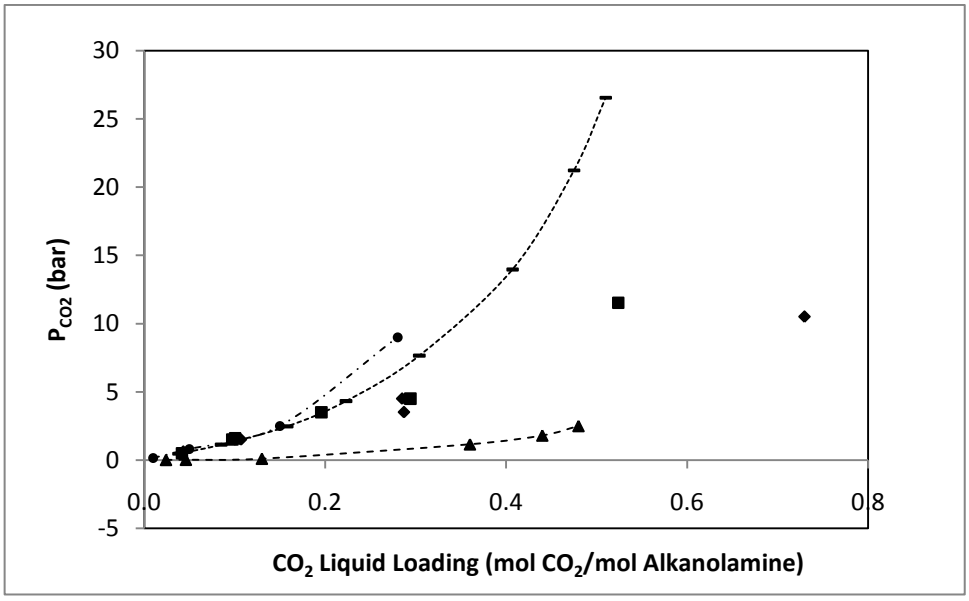

Figure 4-5: Comparison of System 1 (363.15 K) and System 2 (413.15 K), using 25 wt% MDEA+ 25 wt% DEA + 50 wt% H_2O, with other closely related literature data. ♦ - System 1; ■ – System 2; "-" - Murrieta-Guevara et al. (1998), 393.15 K, 20 wt% MDEA+10 wt% DEA; ▲- Sulaiman et al. (1998), 353.15 K, 23 wt% MDEA+20 wt% DEA; ●- Gabrielson et al. (2005), 393.15 K, 50 wt% MDEA.

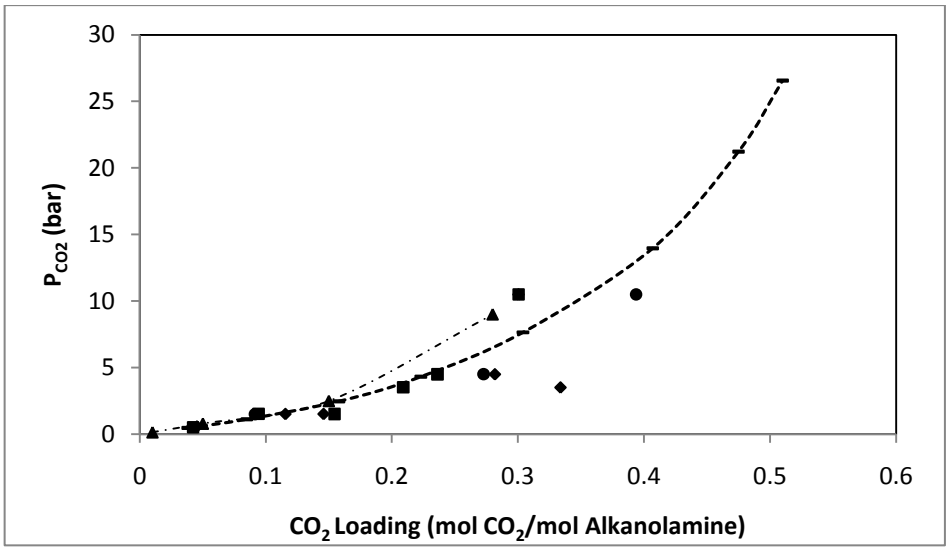

Figure 4-6: Comparison of System 3 (363.15 K) and System 4 (413.15 K), using 30 wt% MDEA + 20 wt% DEA + 50 wt% H_2O, with other closely related literature data. System 5 (50 wt% DEA + 50 wt% H_2O at 393.15 K) also shown. . ♦ - System 3; ■ – System 4; ● - System 5; "-" - Murrieta-Guevara et al. (1998), 393.15 K, 20 wt% MDEA+10 wt% DEA; ▲- Gabrielson et al. (2005), 393.15 K, 50 wt% MDEA.

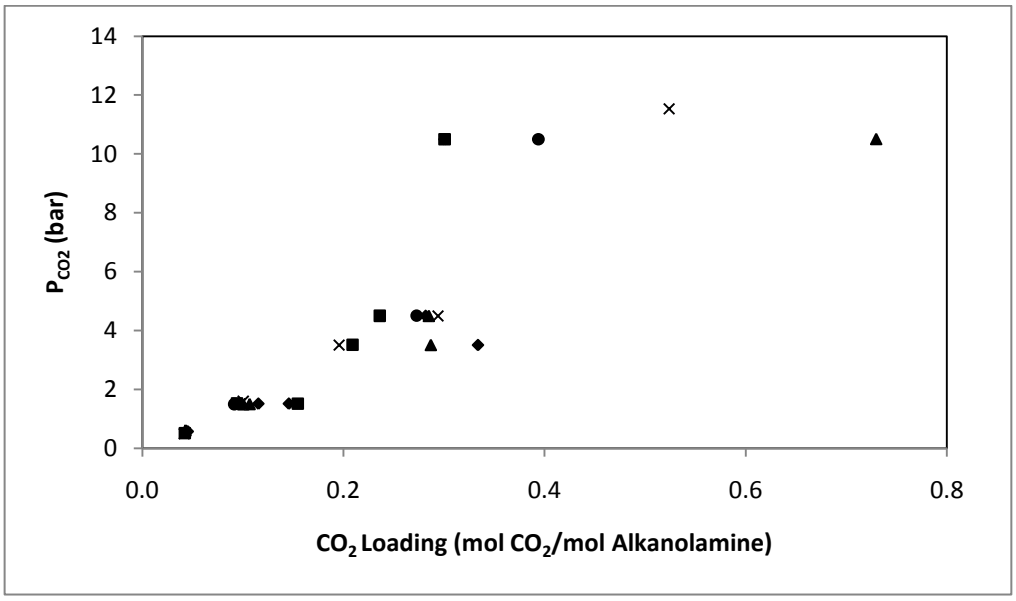

Figure 4-7: Comparison of all measured systems in this study. ▲- System 1 (25 wt% MDEA+ 25 wt% DEA + 50 wt% H_2O, 363.15 K); x – System 2 (25 wt% MDEA+ 25 wt% DEA + 50 wt% H_2O, 413.15 K); ♦ - System 3 (30 wt% MDEA+ 20 wt% DEA + 50 wt% H_2O,363.15 K); ■ – System 4 (30 wt% MDEA+ 20 wt% DEA + 50 wt% H_2O,413.15 K); ● - System 5 (50 wt% DEA + 50 wt% H_2O,393.15 K)

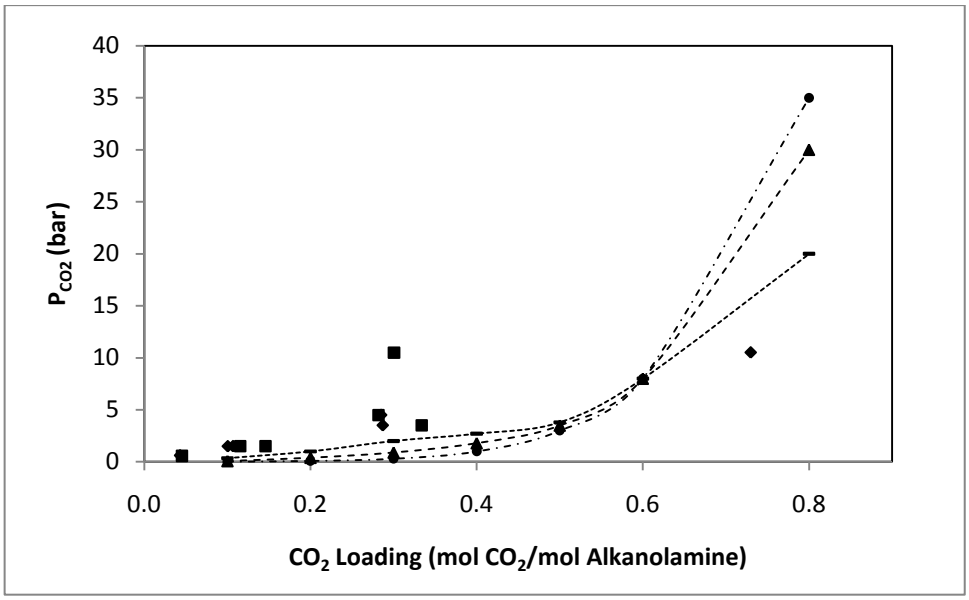

Figure 4-8: Comparison of System 1 (25 wt% MDEA+ 25 wt% DEA + 50 wt% H_2O) and System 3 (30 wt% MDEA+ 20 wt% DEA + 50 wt% H_2O), at 363.15 K, with other closely related literature data. ♦ - System 1; ■ – System 3; "-" - Austgen et al. (1991), 353.15 K, 45.2 wt% MDEA ; ▲- Austgen et al. (1991), 353.15 K, 22.6 wt% MDEA+19.9 wt% DEA; ●- Austgen et al. (1991), 353.15 K, 39.8 wt% DEA.

Refer for Figure 4-7. A sharp decrease in equilibrium CO_2 loading prevails for systems of high temperature (Systems 2 and 4) as compared with Systems 1 and 3. This is consistent with the reaction mechanism described by (R2-20) to (R2-28) as reactive absorption occurs and the absorption reaction is exothermic, for both secondary and tertiary reaction mechanisms. Higher desorption is favoured at increased in temperature. There is a wide difference in results between systems operating at 363.15 K and 413.15 K. Even with literature comparison, as shown in Figures 4-5 and 4-6, solvents with lower concentration achieved better loading performance, because they were used at lower system temperatures. It is evidently imperative that in industrial applications, flue gases with temperatures exceeding 393.15 K, need to be cooled before undergoing CO_2 capture by solvent absorption, in order to achieve greater efficiency. Knudsen et al. (2008) shows a pilot plant in Austria operating with a flue gas at 320.15 K, a low temperature which is expected to provide good efficiency and solvent performance.

Tables A1-1 to A4-1 of Appendix A also shows that with higher temperature, the H_2O in the solvent mixture gets evaporated into the vapour phase. Industrially H_2O may even be lost by entrainment once in the vapour phase. This provides more reason to limit absorption temperature.

Another observation of Figure 4-7 is that a solvent having 25 wt% MDEA and 25 wt% DEA (system 1 and 2) yielded higher CO_2 loading than the solvent with 30 wt% MDEA and 20 wt%

DEA (system 3 and 4). This is true when the experiment was done at system temperatures of 363.15 K and 413.15 K. This result is somewhat unexpected since a higher amount of MDEA, a tertiary amine, is expected to provide a relatively higher absorption capacity (GPA, 2004) than a solvent having high secondary and primary amine composition.

The low absorption rate of tertiary amines, including MDEA, is suspected to have produced the above mentioned result. Each system that was measured took typically 12 hours to reach equilibrium, during which time small changes in system pressure were observed. Thereafter only minuscule changes of system pressure are observed, indicating a very low rate of CO_2 absorption.

The reaction mechanism explains the reason for the low absorption rate of CO_2 in MDEA. With secondary amines such as DEA, CO_2 reacts directly with the amine (reaction R2-24 as described in Section 2.9 of Chapter 2), but with tertiary amines CO_2 undergoes a hydroxide reaction before reacting with the amine (reaction R2-26 and R2-27).

Three measurements were done using 50 wt% DEA (System 5). This was done as a secondary study for comparing such a solvent with similar solvents studied in the literature. The data of Figure 4-6 show that system 5 has better performance than the literature data of 50 wt% MDEA and 20 wt% MDEA + 10 wt% DEA. However, Figure 4-7 shows that the performance is not as good as the amine blends of System 1 to 4 measured in this work. This proves that while high quantities of MDEA are not to be recommended, a balanced or low amount of MDEA increases CO_2 liquid loading capacity of the solvent significantly.

Figure 4-6 shows that better performance was achieved with 50wt% DEA solvent when compared to the data of Murrieta-Guivara et al. (1998) and Gabrielsen et al. (2005) at the temperature of 393.15 K. By experimentation, it has been successfully proven that under the same temperature, a solvent of 50 wt% DEA produces better performance than 50 wt% MDEA. A broader study using different P_{CO2} would be required to confirm overall benefits and drawbacks of using DEA over MDEA. The superior performance recorded by Sulaiman et al. (1998) were probably due to the decreased temperature.

All systems measured show either similar or better performance than that recorded by Murrieta-Guivara et al. (1998) and Gabrielsen et al. (2005). This is true even though some systems were measured at 413.15 K, higher than the temperature of literature measurements. This confirms that higher amine concentrations in the solvent provide a significant increase in performance, in terms of absorption capacity and rate. It also further emphasises the benefit of blending tertiary amines such as MDEA to produce a solvent that is high in concentration and has low corrosiveness. While MDEA provides lower absorption rates, its inclusion facilitates higher

amine concentrations and hence higher absorption capacity.

System 2 showed better performance than the literature data despite the higher temperature of 413.15 K. Figure 4-6 clearly indicates the superiority of the solvent used in system 2 (25 wt% MDEA + 25 wt% DEA + 50 wt% H_2O) over the solvents studied by Murrieta-Guivara et al. (1998) and Gabrielsen et al. (2005).

A valuable conclusion from Figure 4-7 is that the solvent used in Systems 1 and 2 are a success in performance, surpassing those of other measured amine blends and also blends used in other literature sources such as those shown in Figures 4-5 and 4-6.

However, literature data in Figure 4-8 seems to show better results than the results of the solvents studied in this work. The data by Austgen et al. (1991) were however recorded at a lower system temperature of 353.15 K. This further stresses another equally valuable conclusion, that decreasing the system temperature of solvent absorption is highly imperative, in order to obtain higher CO_2 loading.

A final observation worth noting is that shown in Figures A-1 to A-4 of Appendix A. The partition coefficients do not show much consistency with changes in system pressure, system temperature and solvent composition. The complex reaction mechanism involved between CO_2 and both secondary and tertiary amines could be the reason for this. Sidi-Boumedine et al. (2004) provided liquid and vapour mole fraction results for their study of 25.73 wt% MDEA solvent at 313.13 K, with system pressures ranging from 5 to 43 bar. According to the study, partition coefficient decreases with CO_2 liquid loading. While this trend is followed in Figures A-2 and A-3, Figures A-1 and A-4 do not possess the same trend. A possible reason for this discrepancy could be related to the fact that this study concerns MDEA and DEA blends at conditions that are very dissimilar to Sidi-Boumedine et al. (2004). The presence of nitrogen in this study could also be a contributing factor. The total pressure in the study of Sidi-Boumedine et al. (2004) was not stated.

4.2 Modelling results and discussion

After experimentation was conducted, CO_2 loading data were modelled using the Posey-Tapperson-Rochelle model and the Deshmukh-Mather model, using Matlab Version R2009b.

The importance of data modelling was discussed in Section 2.10 of Chapter 2, while the models applied in this study were explained in detail in Section 2.11.

This section presents the results of the modelling that was done in Matlab for this work. The results are discussed and compared in terms of model accuracy. Dependence of model accuracy

on system conditions was also investigated. The Posey-Tapperson-Rochelle modelling results and discussion are presented first, followed by Deshmukh-Mather modelling results and discussion.

4.2.1 Posey-Tapperson-Rochelle model

As mentioned before, the Posey et al. Model (1996) was programmed in Matlab R2009b. The programme code is available electronically, and decribed in Section E1, E2 and E3 of Appendix E. Figures E1 and E2 of Appendix E give a graphical description of the code.

Figure E1 shows the description of the programme "Posey_model.m" (Programme E3). The programme first prompts the user to select the desired system (system 1 to 4, as in Table 2-3 of Section 2.8). Thereafter, experimental data stored in the programme "Data_Bank.m" (Section E1) are used to calculate the experimental CO_2 liquid loading. Parameters a to d are then initialised for equation 2-1 (as shown in Section 2.11.1). The programme "Amine_Var.m" (Figure E2 and Section E2) is then used to regress these parameters until good estimates of CO_2 partial pressure, for the required CO_2 liquid loading, are found.

This section discusses the results of the above-mentioned modelling. Results for the modelling of each system (1 to 4) are presented graphically and discussed here, while associated data are found in Tables D1 and D2 of Appendix D.

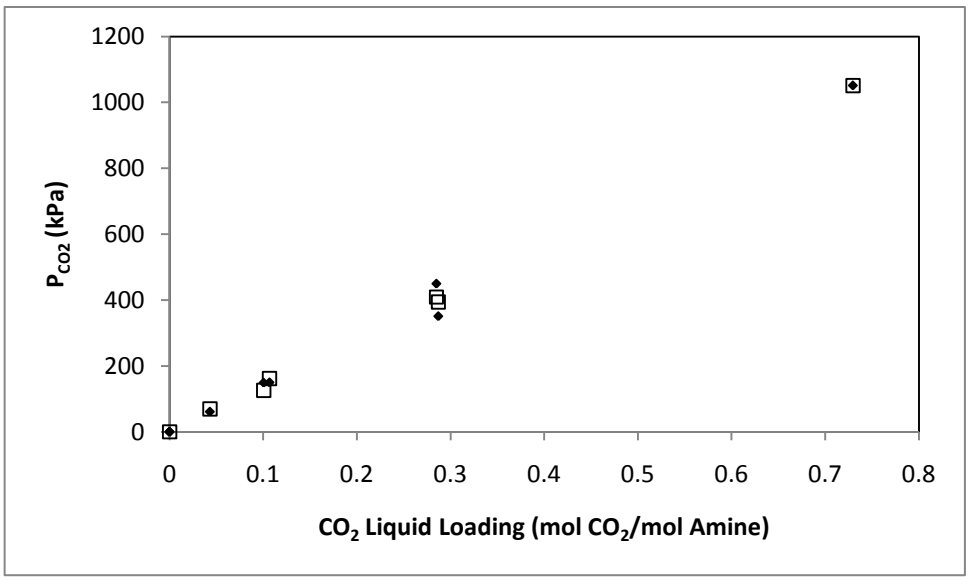

Figure 4-9: Comparison of experimental data with Posey-Tapperson-Rochelle model estimates for System 1 (25 wt% MDEA + 25 wt% DEA + 50 wt% H_2O, 363.15 K) ♦ - Experimental data; -□- – Posey model estimates

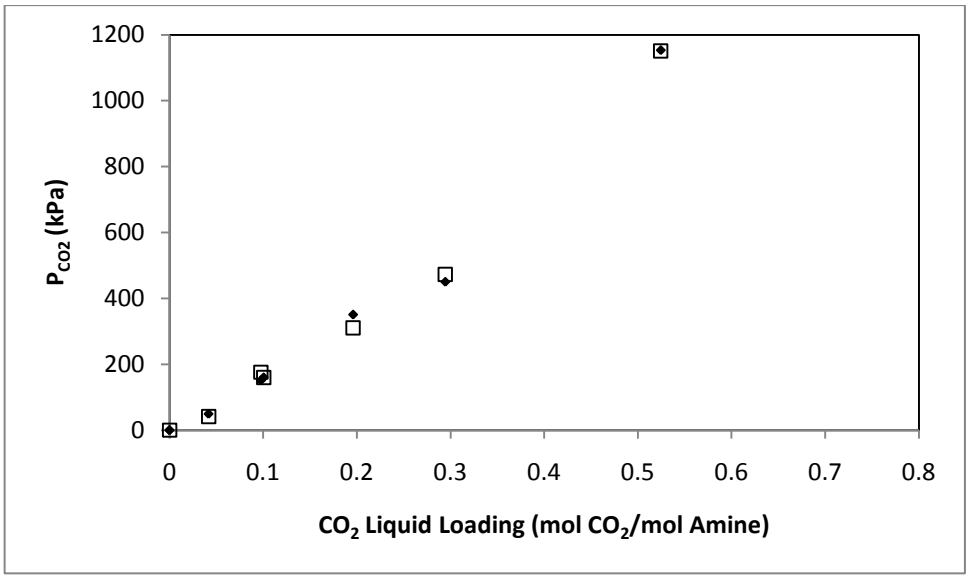

Figure 4-10: Comparison of experimental data with Posey-Tapperson-Rochelle model estimates for System 2 (25 wt% MDEA + 25 wt% DEA + 50 wt% H_2O, 413.15 K) ♦ - Experimental data; -□- – Posey model estimates

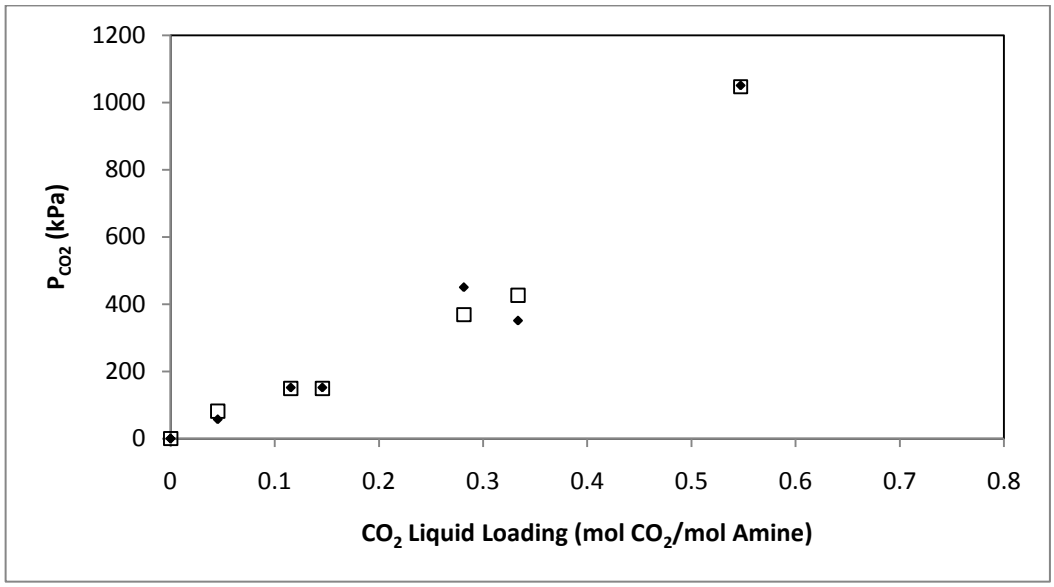

Figure 4-11: Comparison of experimental data with Posey-Tapperson-Rochelle model estimates for System 3 (30 wt% MDEA + 20 wt% DEA + 50 wt% H_2O, 363.15 K) ♦ - Experimental data; -□- – Posey model estimates

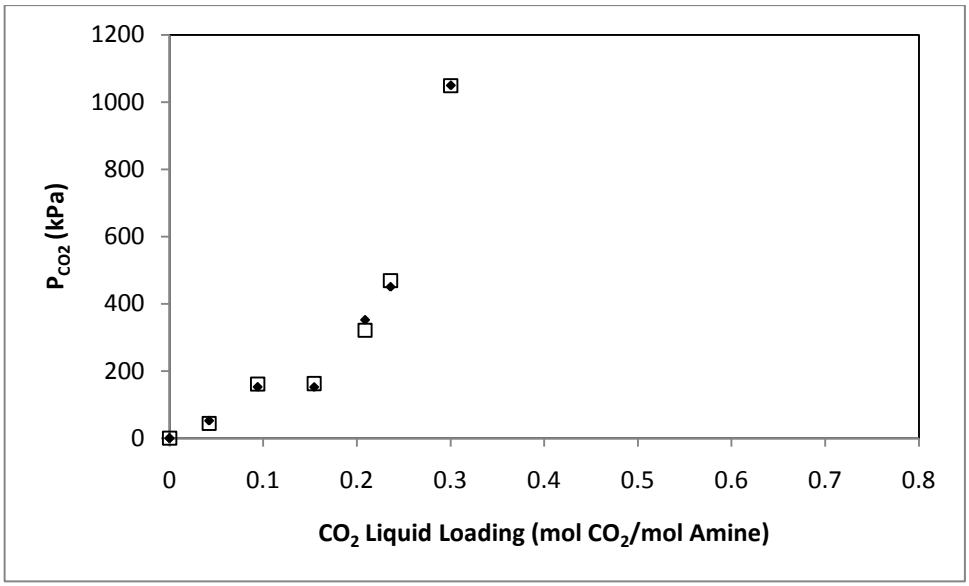

Figure 4-12: Comparison of experimental data with Posey-Tapperson-Rochelle model estimates for System 4 (30 wt% MDEA + 20 wt% DEA + 50 wt% H_2O, 413.15 K) ♦ - Experimental data; -□- – Posey model estimates

Figures 4-9 to 4-12 are a graphical analysis of the accuracy of the Posey-Tapperson-Rochelle model predictions. Numerical results for these figures, including error calculation, are presented in Table D1 of Appendix D. Error was calculated by taking the difference between experimental P_{CO2} data and calculated P_{CO2} values and converting to a percentage.

$$\text{Error (\%)} = \frac{P_{CO_2}(\text{exp } erimental) - P_{CO_2}(calculated)}{P_{CO_2}(\text{exp } erimental)} \times 100 \quad \text{.....(4-1)}$$

All P_{CO2} values were recorded in bar.

The relatively significant error of the model predictions is due to the model's simplicity. It does not account for the different characteristics of various amines. The differences in reaction mechanism and other characteristics between primary, secondary and tertiary amines is not recognised or accounted for in the model. The presence on N_2 gas in the system is also not accounted for.

One particular observation was that the model provided better predictions for systems at higher temperature. Data points for systems at 363.15 K were predicted fairly inaccurately in comparison to points measured at 413.15 K. Tables D1 and D2 of Appendix D indicate this. The reason for this is uncertain but is consistent with the measurements done by Posey et al. (1996) which show better fits for systems operating at 393.15 K than at those operating at 313.15 and 353.15 K.

Refer to Table D2 of Appendix D. The parameters A, B, C and D were obtained by regression using Matlab. These parameters are to be used in equation 2-1, as shown in Section 2.11.1. The first parameter estimates were as follows: A = 32; B = -7440; C = 33; D = -18.5 (taken from Dicko et al., 2010). These estimates were chosen as they were regressed in the study of Posey et al. (1996) and suffice for a system using 50 wt% MDEA. However, the parameter estimates obtained in this study were very different to the regressed parameters reported in Dicko et al. (2010) and Posey et al. (1996).

Parameters A and B accounted for an overall correction factor and a temperature factor respectively. Values for parameters A and B in this study were particularly different from the above stated values, as shown in Table D2. This is possibly due to the difference in temperature between the systems analysed in this study and the system analysed in Posey et al. (1996) And Dicko et al. (2010). The temperature studied in the literature was 323.15 K, which is much lower than the temperatures investigated in this study.

Parameters C and D were of similar magnitude to the literature sources mentioned above. The minor difference is possibly due to the fact that an amine blend of MDEA and DEA was used in this study, instead of a single amine as presented in the literature.

Regardless of the difference in parameters, the error obtained was very low, considering the simplicity of the model. Errors for individual data points are shown in Table D1 of Appendix D while a collective error for each of the four systems is shown in Table D2. The numerical errors clearly show that the model provides a better fit for Systems 2 and 4, which ran at temperatures of 413.15 K.

When comparing parameters for each system, it is also found that the parameters are vastly different even in magnitude amongst the four systems. It is concluded that a single set of parameters cannot be used for all amine blends and temperatures. Nevertheless, the parameter sets are very useful as they can be used to predict the CO_2 Loading for a wide range of CO_2 partial pressures, for a particular system temperature and solvent composition.

One advantage of the Posey-Tapperson-Rochelle model is its simplicity. Computations are simple, quick and easy to set up, producing results immediately when using an Intel Core 2 Duo, 2 GHz processor with 2GB RAM. The model is ideal for cases involving low processor speed and capability. Is must be noted however that this advantage has become redundant with the relatively high availability of high speed processors that can accommodate more complex and more accurate models.

A disadvantage of the Posey-Tapperson-Rochelle model, is that the model links CO_2 partial pressure to CO_2 loading by first inputting the CO_2 loading and then calculating the partial

pressure. This is a problem in the more common cases where CO_2 partial pressure is given and CO_2 loading needs to be predicted.

It is recommended that the model be used only for preliminary analysis. More complex models are needed to provide more accurate predictions.

4.2.2 Deshmukh-Mather model

The programming of the Deshmukh-Mather model is available electronically and described specifically in Sections E1, E4, E5 and E6 of Appendix E..

A description of these programmes is presented in the flowcharts in Figures E3 and E4. The programme "Deshmukh12.m" (Section E6) first requires that the desired system be chosen for calculation. Experimental data are then obtained from Data_bank.m and experimental CO_2 loading is calculated. Equilibrium constants K_i are then calculated using parameters available in Table D5. γ_i is calculated using equation 2-14 as shown in Section 2.11.2. Binary interaction parameters (B_{ij}) are initialised using data obtained from Benamor and Aroua (2005). Parameters for equation 2-15 are then calculated using the procedure as described in Section 2.11.2.

The programme "NewtonRaphson.m" (Section E4) is used thereafter to calculate $[H^+]$ concentration in order to obtain an initial estimate of predicted CO_2 loading.

The programme "Amine_Var_Deshmukh7.m" (Section E5 and Figure E4) is finally used to regress B_{ij} values to provide optimised CO_2 loading predictions using equation 2-16 of Section 2.11.2. This is done by re-estimating B_{ij} values, and recalculating γ_i and K_i simultaneously using equations 2-3 to 2-12. Carbamate concentration is also found using equation 2-17.

This section discusses the CO_2 loading estimates obtained using the Deshmukh-Mather model. Associated data are available in Table D3 of Appendix D. Regressed B_{ij} values are found in Table D4.

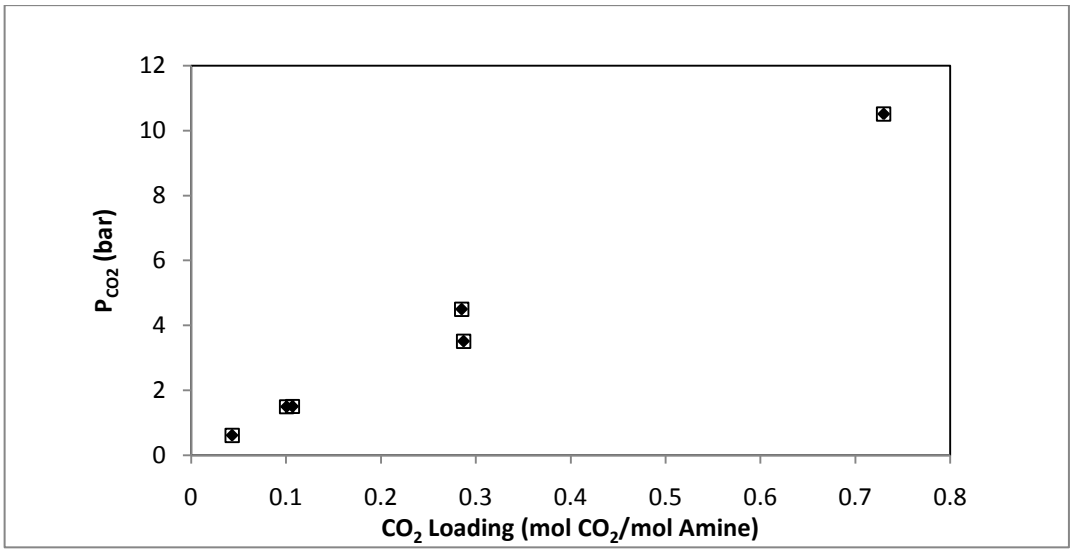

Figure 4-13: Comparison of experimental CO_2 loading data with Deshmukh-Mather model estimates, for System 1 (25 wt% MDEA + 25 wt% DEA + 50 wt% H_2O, 363.15 K) ♦ - Experimental CO_2 loading data; -□- – Model estimate of CO_2 loading

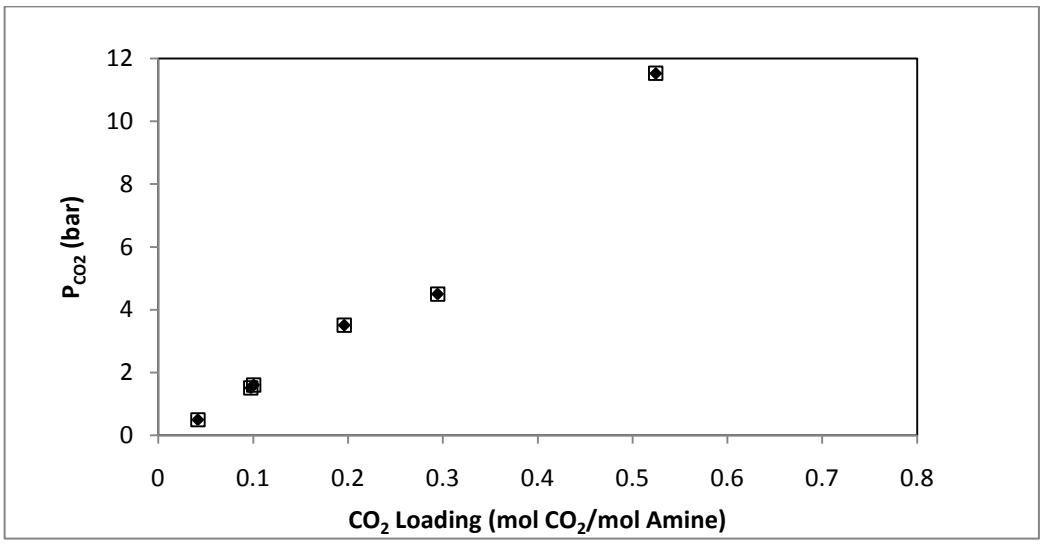

Figure 4-14: Comparison of experimental CO_2 loading data with Deshmukh-Mather model estimates, for System 2 (25 wt% MDEA + 25 wt% DEA + 50 wt% H_2O, 413.15 K) ♦ - Experimental CO_2 loading data; -□- – Model estimate of CO_2 loading

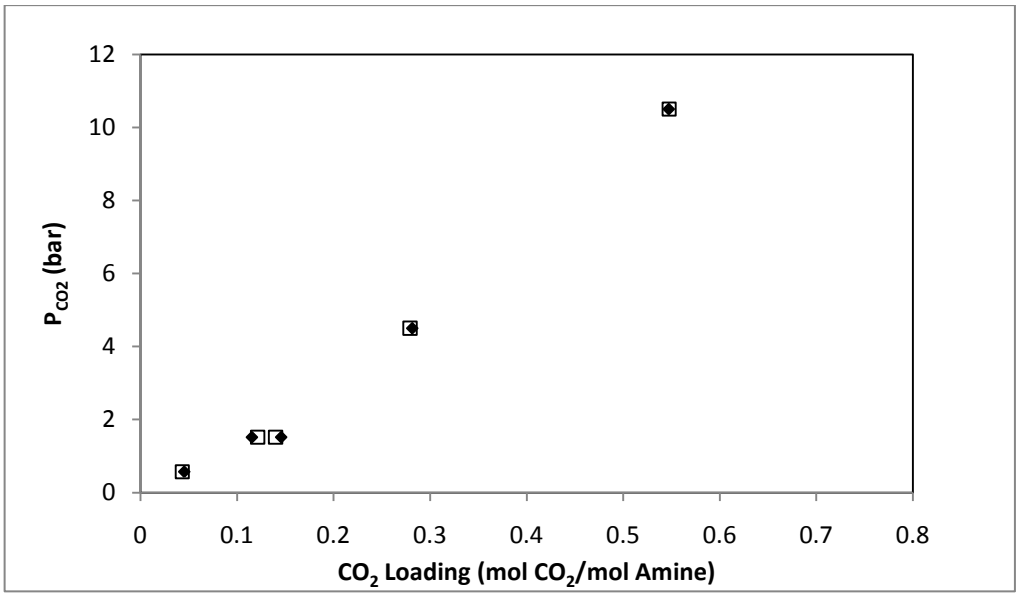

Figure 4-15: Comparison of experimental CO_2 loading data with Deshmukh-Mather model estimates, for System 3 (30 wt% MDEA + 20 wt% DEA + 50 wt% H_2O, 363.15 K) ♦ - Experimental CO_2 loading data; -□- – Model estimate of CO_2 loading

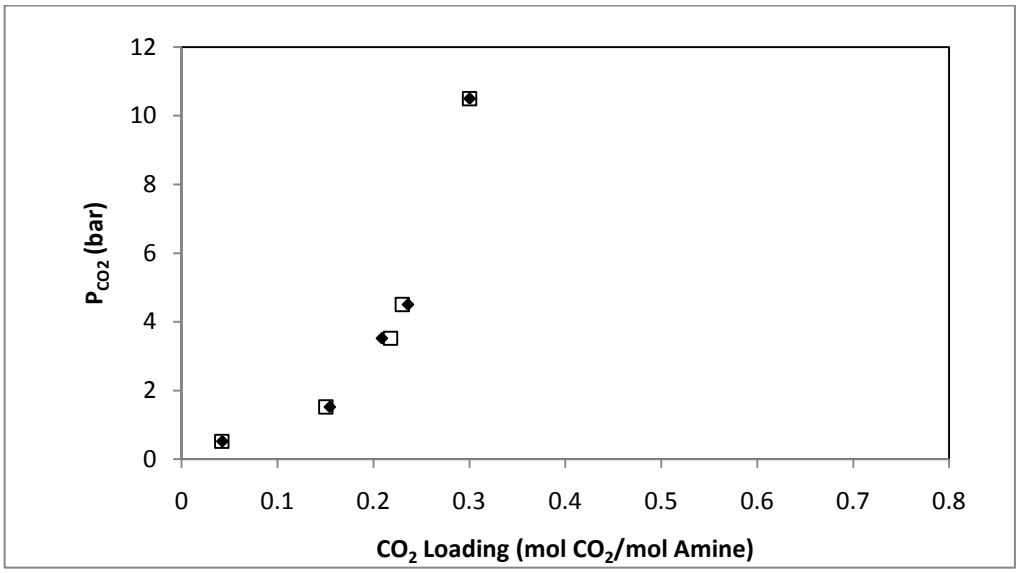

Figure 4-16: Comparison of experimental CO_2 loading data with Deshmukh-Mather model estimates, for System 4 (30 wt% MDEA + 20 wt% DEA + 50 wt% H_2O, 413.15 K) ♦ - Experimental CO_2 loading data; -□- – Model estimate of CO_2 loading

Figures 4-13 to 4-16 present data predicted by the Deshmukh-Mather model, in comparison with experimental data obtained during VLE measurement. Table D3 of Appendix D contains the numerical values as presented in the figures above.

It is clearly evident that the predictions of the Deshmukh-Mather model are much more accurate in comparison to the Posey-Tapperson-Rochelle model. In all four systems shown in Figures 4-

13 to 4-16, the prediction has far less error than the predictions shown in Figures 4-9 to 4-12. A more definite result can be found when comparing the error data of Table D1 of Appendix D for the Posey-Tapperson-Rochelle model to that of the Deshmukh-Mather error evaluations shown in Table D3. Errors in Deshmukh-Mather predictions are of the magnitude of 0.05 % at the most, while errors in Posey-Tapperson-Rochelle predictions are of a magnitude of up to 0.4 %. For all systems studied, the Deshmukh-Mather model certainly provided better predictions.

The performance of the Deshmukh-Mather model is not uniform for all systems however. The model has performed exceptionally well when predicting CO_2 Loading for Systems 1 and 2, producing upper-bound errors on the magnitude of $1x10^{-13}$ %. This holds true for both System temperatures (90 and 413.15 K). But for systems 3 and 4, error is as high as 0.04 %. This may suggest a limited ability of the model to accommodate tertiary amines which undergo an alternative reaction mechanism to that of primary and secondary amines, as explained in Section 2.9. The more MDEA added to the solvent blend, the less accurate the model predictions are.

For all practical purposes however, the predictions for systems 3 and 4 are of very high accuracy. Regardless of the complications posed by tertiary amines, the Deshmukh-Mather model still provides remarkably accurate CO_2 loading predictions.

Table D4 of Appendix D presents the binary interaction parameters which were estimated by the modelling in Matlab. There are very little consistently identifiable similarities in the parameter estimates with each system and the values reported by Benamor and Aroua (2005). There are some vague similarities however. Interaction parameter (B_{ij}) values for DEA-DEA, DEA-CO_3^{2-}, CO_2-$DEACOO^-$, CO_2-HCO_3^-, MDEAH-CO_3^{2-}, MDEA-CO_3^{2-}, MDEA-HCO_3^-, MDEAH-$DEACOO^-$, and DEA-HCO_3^- were estimated to be of low magnitude, indicating a relatively low influence in the loaded solvent. The magnitude themselves often differ even by a few decimal places for each system.

No single set of interaction parameters can be indentified to suffice for the accurate prediction of CO_2 loading for all systems. The Parameters are dependent on temperature and solvent composition. Provided that temperature and solvent composition remain constant, the parameters and model can be used to accurately predict CO_2 loading for a relatively wide range of CO_2 partial pressures (0.5 to 10.5 bar).

Benefits of the Deshmukh-Mather model over the Posey-Tapperson-Rochelle model include accuracy in predictions, accommodation of amine blends and its associated interaction parameters and the prediction of CO_2 loading using input P_{CO2} values. The model can also be used to find other quantities such as different electrolyte and other species concentrations as well as activity coefficient values.

Although the model is quite accurate in its predictions, the drawback is its complexity. The model took extremely long to develop in Matlab.

Computations however, were reasonably quick, producing results in 1.5 to 3 minutes (depending on the System studied), using an Intel Core 2 Duo, 2 GHz processor with 2GB RAM. With high processor speeds already being widely available, the Deshmukh-Mather model is significantly more useful that the Posey-Tapperson-Rochelle model.

4.3 Discussion and results of Aspen simulation using the Electrolyte-NRTL model

Aspen simulations were conducted in this study to observe, through predictive methods, the results that CO_2 capture by amine solvent absorption would yield in an industrial application. A further objective was to obtain energy penalty and investment cost estimates.

The Elec-NRTL model was used in the simulation for all necessary predictions. This model was used because it was the most popularly recommended model in literature for amine solvent absorption (see Section 2.12), and because the model was already programmed into Aspen for convenient use, whereas the other models investigated in this study were not built into Aspen.

Results of the regression of binary interaction parameters using the Elec-NRTL model, are presented in Table F1 in Appendix F. The data are also found electronically in an Aspen file titled "ElecNRTL_Regression.apw".

The simulation investigated in this study is a basic preliminary design, which was sufficient to conduct certain sensitivity analysis, observe vapour and liquid stream properties, and to investigate energy penalty and certain physical design specifications of the CO_2 capture process.

Attempts were made to optimise the design but to a very limited extent. A fully optimised design was not within the scope of this study, because it was not possible due to the lack of specified constraints on the simulation. A fully optimised design would only be possible if budget, space, energy and product specifications were formally stated, as in an actual industrial CO_2 capture initiative.

The simulation of solvent absorption included an absorber for CO_2 absorption, and a stripper to release CO_2 and recycle the solvent. The basic process flow diagram is shown in Section 2.5.1 in Figure 2-6. This idea was expressed in Alie (2004) and Figueroa et al. (2007). This process was built upon in this study.

The simulation was conducted for all data points that were measured in the VLE experimentation. The solvent composition, flue gas composition, system temperature, and system pressure were accommodated into the simulation. Flue gas flow rates were set to a

magnitude which mimics that of industrial coal-to-liquids (CTL) plants (Kawesha, 2010). Solvent flow rates were adjusted proportionally according to the amount of solvent used to treat CO_2 gas in the VLE measurements.

Initially, the simulation contained no recycle of solvent back to the absorber. This basic simulation was performed to compare the magnitude of CO_2 loading that would be achieved in the simulation, to that of the CO_2 loading results obtained experimentally. This also provides an indication of the magnitude of CO_2 loading that occurs in the absorber for a single pass of liquid and gas at specified absorber stages. Refer to Figure 4-17 for the process flow diagram.

Thereafter, a solvent -recycle stream was installed between the stripper and absorber and the simulation underwent many modifications, including changes to the number of stages in the absorber and stripper, the introduction of pump-arounds, and modifications on reflux ratios. Figure 4-29 provides an illustration of some of these modifications.

This section discusses, in detail, the above mentioned Aspen simulations that were performed, as well as the results of these simulations. Further limitations on the process were identified and recommendations were noted. Finally a cost analysis was conducted using basic design assumptions in order to get a general indication of the overall capital costs of an industrial CO_2 capture process using amine solvent absorption. The energy efficiency and industrial feasibility of the process is also discussed in this section

4.3.1 Results of Aspen CO_2 absorption simulation (without recycle)

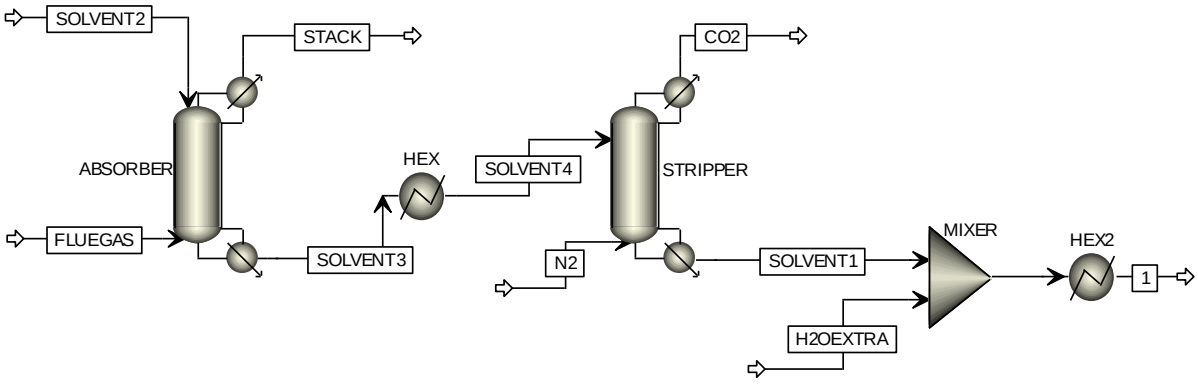

Figure 4-17: Aspen Flow sheet of CO_2 Capture Process (Without Recycle)

Figure 4-17 shows the CO_2 capture process including an absorber, a heater and stripper. A mixer and additional heat exchanger is installed to prepare the solvent from the stripper for recycle.

Feed flow rates needed to be specified. The flue gas flow rate was set at 10.38 kmol/s, which was a recommended flow rate from a typical CTL process in South Africa (Kawesha, 2009).

The solvent flow rate to the absorber was set to 211.05 kmol/s based on the solvent: gas proportionality ratio obtained during the amine absorption measurements done, as explained in Chapter 3 and Section 2.8. While the flue gas in this study contains only N_2 and CO_2 gas, industrial flue gases particularly for coal processes usually comprise many different gases such as H_2S, SO_2, O_2, Ar and even Ash. This was neglected in the simulation.

Contrary to the Aspen flow sheet display, the absorber and stripper did not have a reboiler or condenser as they are used purely as absorption and stripping columns. As a preliminary design, the absorber was set to possess 10 stages while the stripper possessed 6 stages. Guidelines for the number of stages were taken from Alie (2004) and Manuel et al. (1998). This was beneficial in lowering investment costs.

Once absorption occurs, N_2 gas is intended to leave through the "Stack" stream, while the solvent, now loaded with CO_2, leaves through the "Solvent 3" stream.

The heat exchanger labelled "HEX" heats the loaded solvent from the absorber, to 428.15 K for the CO_2 to be released in the stripper. The stripper temperature was chosen to maximise CO_2 stripping without resulting in substantial H_2O evaporation at the specified operating pressure. The stripper was used without a condenser and reboiler and served purely as a column for stripping.

An "N_2" stream is introduced into the stripper and serves as a sweep gas. Initially, the simulations were run without this stream. It was found that the separation of CO_2 from the solvent was practically impossible, as the CO_2 would continuously re-dissolve into the solvent along the column, and leave some stages dry. The N_2 sweep stream provides enough sweep to entrain the CO_2 and keep it separated from the solvent. CO_2, along with N_2 sweep gas left the stripper via the stream labelled "CO_2", while the solvent left the stripper via the "Solvent 1" stream.

The Mixer, H_2O stream and HEX2 restore solvent composition and system temperature.

Relevant data from the simulation are tabulated and shown in Table F2 and F3 of Appendix F. The simulation is available electronically as an Aspen file titled: "CO_2 Absorption Simulation No Recycle.apw"

4.3.2 Discussion of the Aspen CO_2 absorption simulation results (no recycle)

This section discusses the stream and unit results of the simulation, including CO_2 loading, recovery, and purity results.

Refer to Table F2 and F3. A few observations have been made from these results. A desirable

result shown in Table F3 is that amine losses to the stack are negligible, as shown in their flow rates of the "Stack" stream. This was true for all data points, at all temperatures and pressures observed. Amines losses to the CO_2 stream from the Stripper were also found to be negligible.

A highly undesirable effect is the loss of H_2O to the stack and to the CO_2 stream. For a given operating temperature, the losses were far greater at system pressures of 5 bar. System pressures of 15 bar resulted in much lower H_2O losses.

An interesting result occurred when comparing H_2O losses for different absorption temperatures, as shown in Table F3. Note that in Figure 4-17, H_2O losses occur primarily through the "Stack" and "CO_2" streams. The stripping temperature was set to a constant 428.15 K for all data points mentioned in Table F3, to ensure stripping of CO_2. At absorber temperatures of 413.15 K, increased amounts of H_2O was lost in the absorption process through the "Stack" stream, whereas reduced amounts of H_2O was lost to the "CO_2" stream during stripping. At absorber temperatures of 363.15 K however, H_2O losses to the "Stack" were low but very high H_2O losses occurred during stripping. Increased amounts of H_2O was lost to the CO_2 stream, as more H_2O was subjected to temperatures of 428.15 K. Overall, more H_2O was lost when the absorber temperature was 363.15 K.

However, the simulation data in Table F2 also show that low absorption temperatures provide for better CO_2 loading results. This is qualitatively consistent with experimental findings. It is hence clearly evident that it is better to run absorption at low temperatures.

While the results of the H_2O losses during absorption were qualitatively consistent with those obtained during actual experimentation, stripping creates a new issue for H_2O losses, which suggests that while low absorption temperatures yield better loading results, it causes more H_2O losses during stripping. More investigation is needed to establish an ideal temperature which provides high CO_2 loading and low H_2O losses. Alternatively, further downstream separation and H_2O replenishment would be necessary to ensure the correct solvent concentration is maintained and no corrosion occurs.

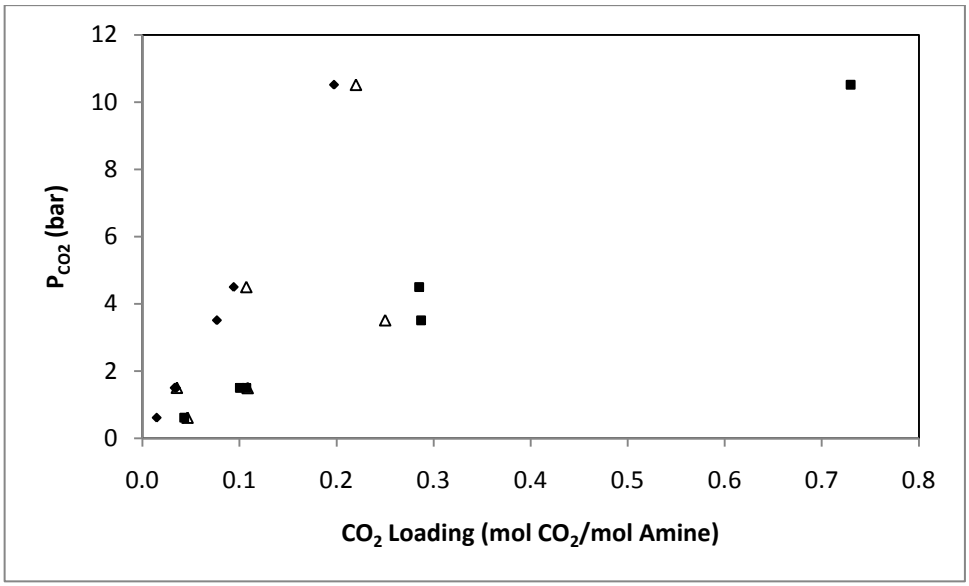

Figure 4-18: Comparison of Aspen simulation (without recycle) CO_2 loading estimates to experimental results: System 1 (25 wt% MDEA + 25 wt% DEA + 50 wt% H_2O, 363.15 K). - ♦ - Simulated actual CO_2 loading; ■ – System 1 experimental loading results; Δ - Simulated maximum potential CO_2 loading

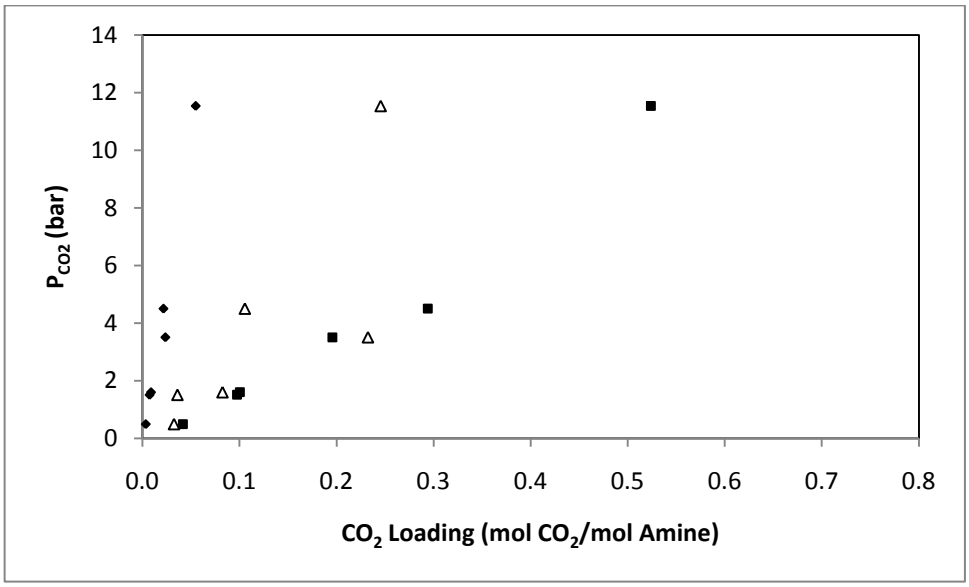

Figure 4-19: Comparison of Aspen simulation (without recycle) CO_2 loading estimates to experimental results: System 2 (25 wt% MDEA + 25 wt% DEA + 50 wt% H_2O, 413.15 K). - ♦ - Simulated actual CO_2 loading; ■ – System 2 experimental loading results; Δ - Simulated maximum potential CO_2 loading

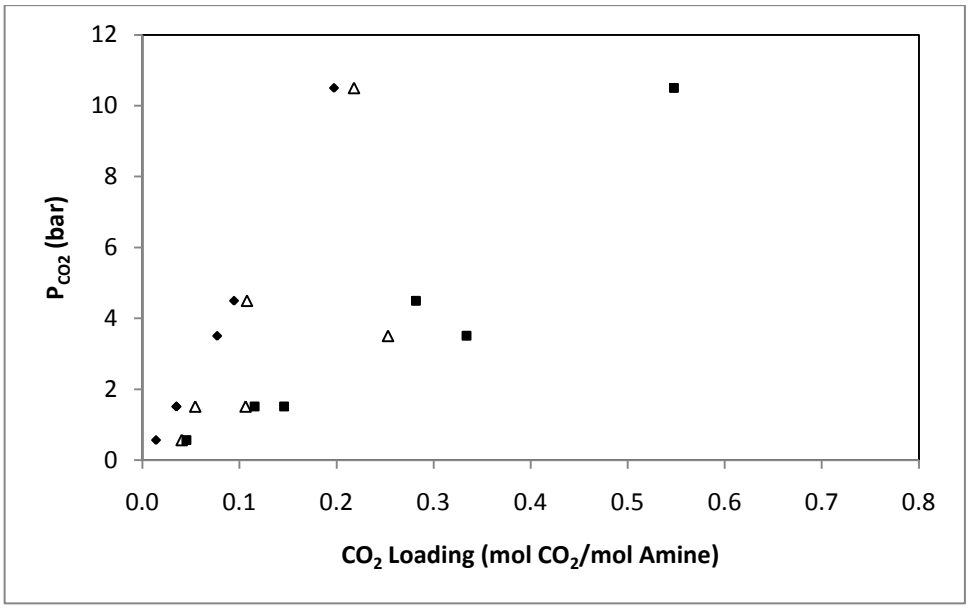

Figure 4-20: Comparison of Aspen simulation (without recycle) CO_2 loading estimates to experimental results: System 3 (30 wt% MDEA + 20 wt% DEA + 50 wt% H_2O, 363.15 K). - ♦ - Simulated actual CO_2 loading; ■ – System 3 experimental loading results; Δ - Simulated maximum potential CO_2 loading

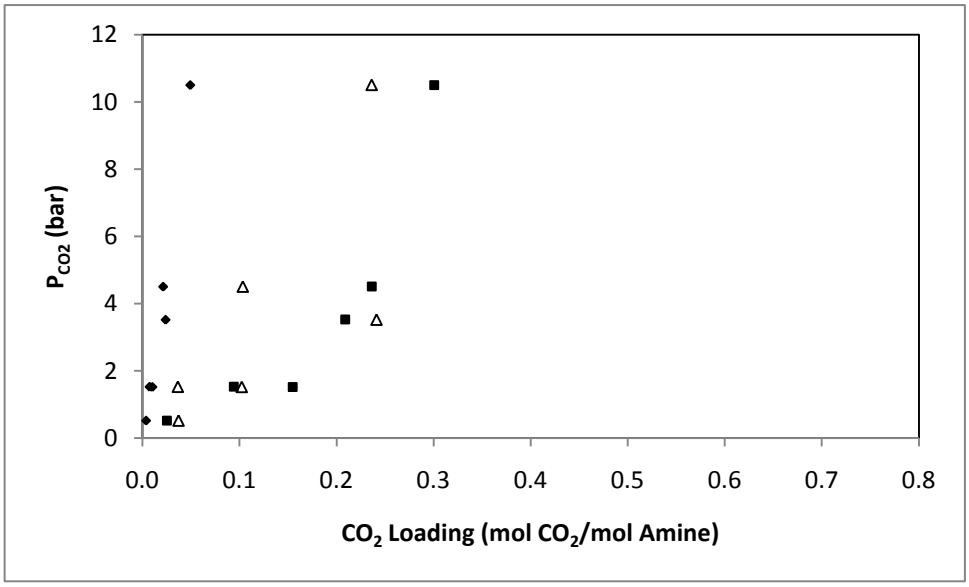

Figure 4-21: Comparison of Aspen simulation (without recycle) CO_2 loading estimates to experimental results: System 4 (30 wt% MDEA + 20 wt% DEA + 50 wt% H_2O, 413.15 K). - ♦ - Simulated actual CO_2 loading; ■ – System 4 experimental loading results; Δ - Simulated maximum potential CO_2 loading

Figure 4-18 to 4-21 shows the difference in CO_2 loading between the experimental and simulated results. The difference is expected, as the experimental measurements were done using a static analytic apparatus, where much time was given (typically 12 hours) for the system

to reach equilibrium. The Aspen simulation done here mimics a dynamic system. And in the absence of recycle streams, the flue gas only contacted the solvent in the absorber once.

This difference further illustrates the low rate of absorption of CO_2 in amines by reactive absorption. Figures 4-18 to 4-21 all show an increasing difference in loading results for increasing CO_2 partial pressures. This shows an increasing difference in performance for high CO_2 concentrations in the flue gas.

Numerical data for maximum potential and actual CO_2 loading in the absorber are tabulated in Table F3 of Appendix F. The potential CO_2 loading was calculated merely by considering the total amount of CO_2 gas and the total solvent entering the absorber. When comparing the potential CO_2 loading that can be achieved in the absorber, to the actual CO_2 loading achieved by the simulation, it is quite evident that there is much room for improvement in the absorption process. For many data points particularly for Systems 1 and 3 (shown in Figures 4-18 and 4-20), the actual CO_2 loading very closely achieves its potential value. This indicates that temperature is highly important in the absorption process achieving its desired purpose to the fullest extent. Low temperatures of System 2 and 4 resulted in great differences between actual and potential CO_2 loading, as shown in Figures 4-19 and 4-21.

The divergence in actual CO_2 loading results are more apparent for System 3 and 4 simulations than Systems 1 and 2 simulations. This is qualitatively consistent with experimental results. Systems 1 and 2 have less MDEA and more DEA than Systems 3 and 4. Absorption rates were much higher when the solvent had more DEA, a secondary amine, than MDEA, a tertiary mine. The higher MDEA content in the solvent used for Systems 3 and 4 resulted in these systems achieving lower CO_2 loading for a single pass CO_2 capture process. This is true even at constant temperature and system pressure.

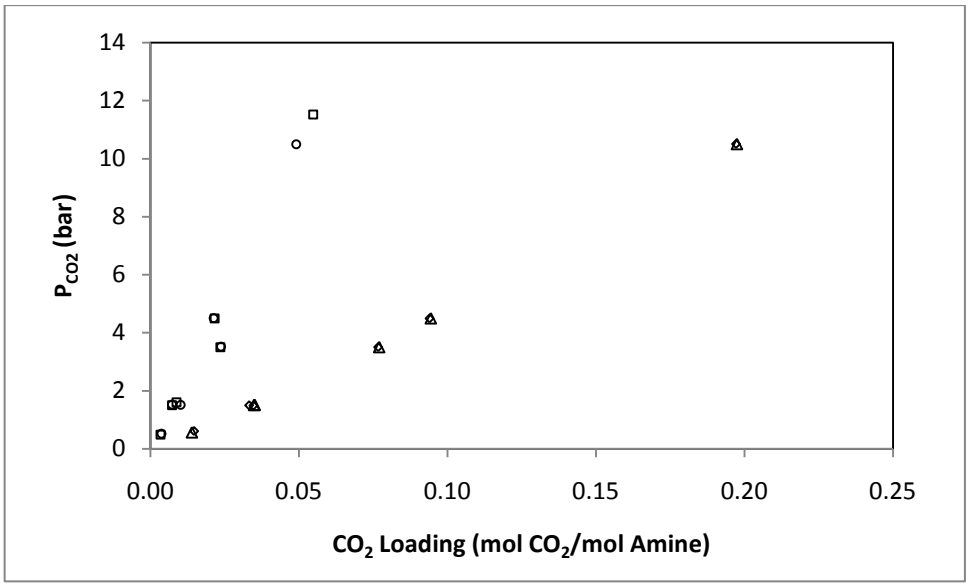

Figure 4-22: Comparison of Aspen simulation (without recycle) actual CO_2 loading estimates for all systems: ◊-System 1 (25 wt% MDEA + 25 wt% DEA + 50 wt% H_2O, 363.15 K); □ – System 2 (25 wt% MDEA + 25 wt% DEA + 50 wt% H_2O, 413.15 K); Δ - System 3 (30 wt% MDEA + 20 wt% DEA + 50 wt% H_2O, 363.15 K); ○ – System 4 (30 wt% MDEA + 20 wt% DEA + 50 wt% H_2O, 413.15 K)

Figure 4-22 compares the actual CO_2 loading achieved for different simulations at measured CO_2 partial pressures. Systems 2 and 4 produce lower CO_2 loadings than systems 1 and 3. Qualitatively this is consistent with experimental results as shown in Figure 4-7, as higher operating temperatures produce lower CO_2 loadings because the reaction mechanism of amine absorption is exothermic.

Overall, the Aspen simulation results, using the Elec-NRTL model, are qualitatively consistent with experimental results. However, Table F2 of Appendix F also shows disappointing results in terms of CO_2 recovery in cases of low system pressure and high system temperature. It is expected that the CO_2 loading would be lower at low pressures of 5 bar and high temperatures of 413.15 K, but the difference in magnitude is very high when the absorption process is observed in an industrial simulation. At system pressures of 15 bar and system temperatures of 363.15 K, percentage CO_2 recovery from the absorber is as high as 90 %. But at 363.15 K, the percentage CO_2 recovery from the absorber drops to as little as 30 % when the system pressure is at 5 bar.

At a system temperature of 413.15 K, percentage CO_2 recovery from the absorber ranges from 10 to 30 %, regardless of system pressure. This result clearly indicates the importance of system conditions to the efficiency of the absorption process, especially when developing the process for industrial use.

No distinguishable correlation could be made between the partial pressure of CO_2 in the flue gas and the percentage CO_2 recovered from absorption. From the data recorded, percentage CO_2 recovery from absorption on a dynamic industrial scale is dependent mainly on system pressure and temperature, and not the concentration of CO_2 in the flue gas.

The results for the percentage CO_2 recovered from the total process show that stripping is highly efficient. In all systems studied, the CO_2 recovered in the solvent in the absorber was released in the stripper and recovered in the "CO_2" stream. Minimal DEA, MDEA and H_2O losses to the CO_2 stream occurred.

A crucial flaw in the stripper process in this investigation is the use of N_2 gas as a carrier to remove CO_2 efficiently. The process design ensured that all CO_2 will leave the stripper as a distillate product while all solvent, including H_2O left as bottoms product. It achieves this purpose. But this also results in a low percentage purity of CO_2 in the distillate, since N_2 is recovered at the distillate as well. In some cases CO_2 mass fraction is even lower than that in the flue gas. In practice, this would mean that the process separates CO_2 gas from O_2, Ar, SO_2 and H_2S, but is combined with N_2 to create a CO_2-N_2 stream of low CO_2 purity. The CO_2 capture from the flue gas would've been somewhat achieved, but further processing would be needed to obtain a purer stream of CO_2 for sequestration. This is indeed not a desirable result.

In order to investigate modifications of the process to obtain higher CO_2 recovery and purity, a solvent recycle stream was installed. This is discussed in the next section.

4.3.3 Aspen CO_2 capture absorption simulation (containing recycle)

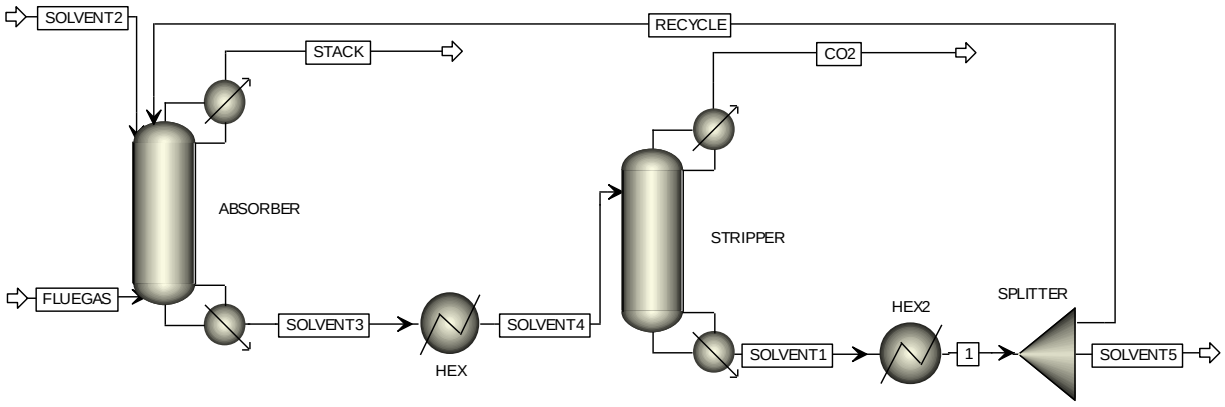

Figure 4-23: Aspen Absorption Simulation (With Recycle)

As explained earlier, the Aspen simulation was repeated with the instalment of a recycle stream for the amine solvent, as shown in Figure 4-23.

The absorber was set to contain 20 stages, which became possible due to the added solvent

present in the absorber from the recycle stream, which facilitated absorption without resulting in any stages drying up. To increase contact time and absorption, a pump-around was introduced with the draw stage at 10 and return stage at 1. The flow rate of the pump-around stream was set to 200 kmol/s, as it was found to give the highest CO_2 absorption without drying any stages.

The splitter was used to draw out a recycle stream. The split ratio was set to 1:1, as it facilitated good percentage CO_2 removal results while maintaining amine solvent purity. The recycle stream entered the absorber at the top stage.

Other changes include the removal of the N_2 stream into the stripper in order to reduce heat duty and N_2 content in the CO_2 stream, as well as the omission of extra H_2O to the mixer. The stripper was converted to a distillation column, complete with a reboiler and condenser to facilitate separation without any use of a N_2 carrier gas. These changes were done to simplify the process for easy integration of a recycle loop.

A kettle reboiler and a partial-vapour condenser were used as a preliminary setup. A reflux ratio of 0.9 and a boilup ratio of 3 were qualitatively identified to be the optimum configuration for separating the CO_2 from the solvent without facing problems of drying stages in the stripper.

The stripper contained 6 stages as before to keep costs low. A pump-around was installed to pump solvent from stage 5 up to stage 2, in order to facilitate more efficient stripping by increasing stripping time.

This simulation is also available electronically as "CO_2 Absorption Simulation With Recycle.apw"

4.3.4 Discussion of results of the Aspen CO_2 absorption simulation (with recycle)

The results of this modified simulation are discussed in this section, in terms of CO_2 loading, recovery, and purity. Tables F4 and F5 of Appendix F contains relevant data for all systems accommodated in the Aspen simulation, for simulations with solvent recycle, while Table F6 contains information pertaining to the energy requirements of the process.

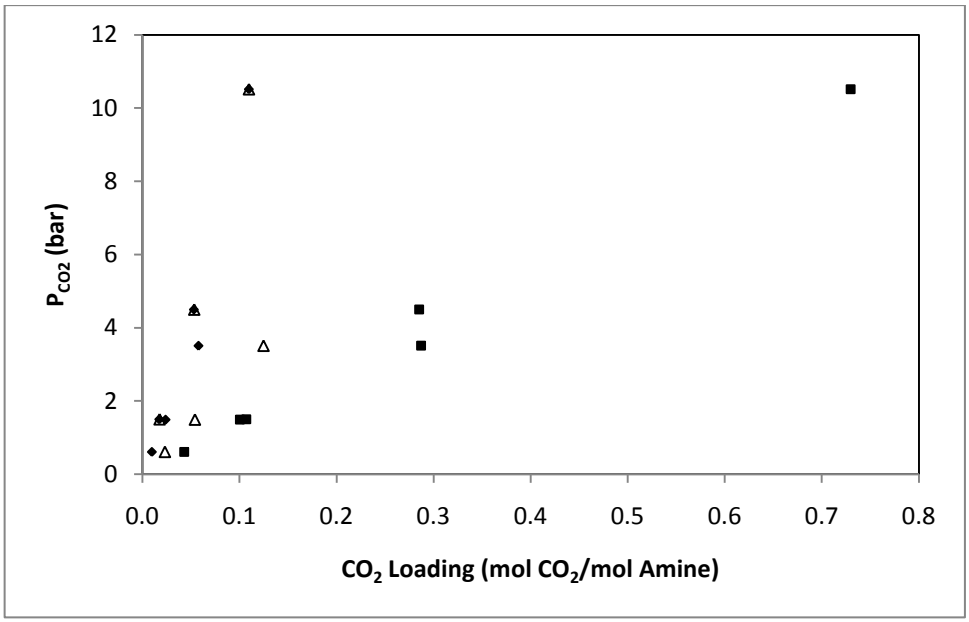

Figure 4-24: Comparison of Aspen simulation (with recycle) CO_2 loading estimates to experimental results: System 1 (25 wt% MDEA + 25 wt% DEA + 50 wt% H_2O, 363.15 K). - ♦ - Simulated actual CO_2 loading; ■ – System 1 experimental loading results; Δ - Simulated maximum potential CO_2 loading

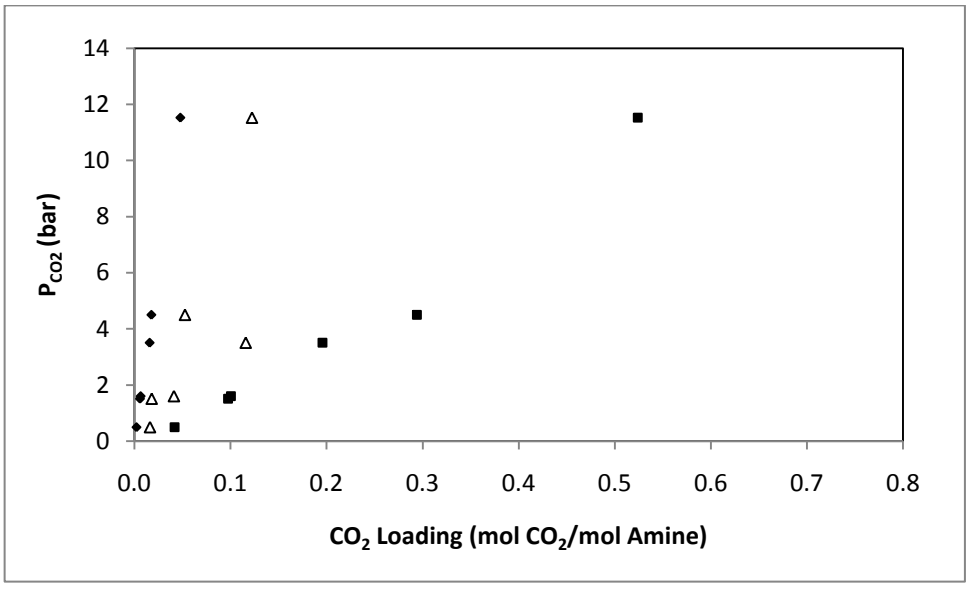

Figure 4-25: Comparison of Aspen simulation (with recycle) CO_2 loading estimates to experimental results: System 2 (25 wt% MDEA + 25 wt% DEA + 50 wt% H_2O, 413.15 K). - ♦ - Simulated actual CO_2 loading; ■ – System 2 experimental loading results; Δ - Simulated maximum potential CO_2 loading

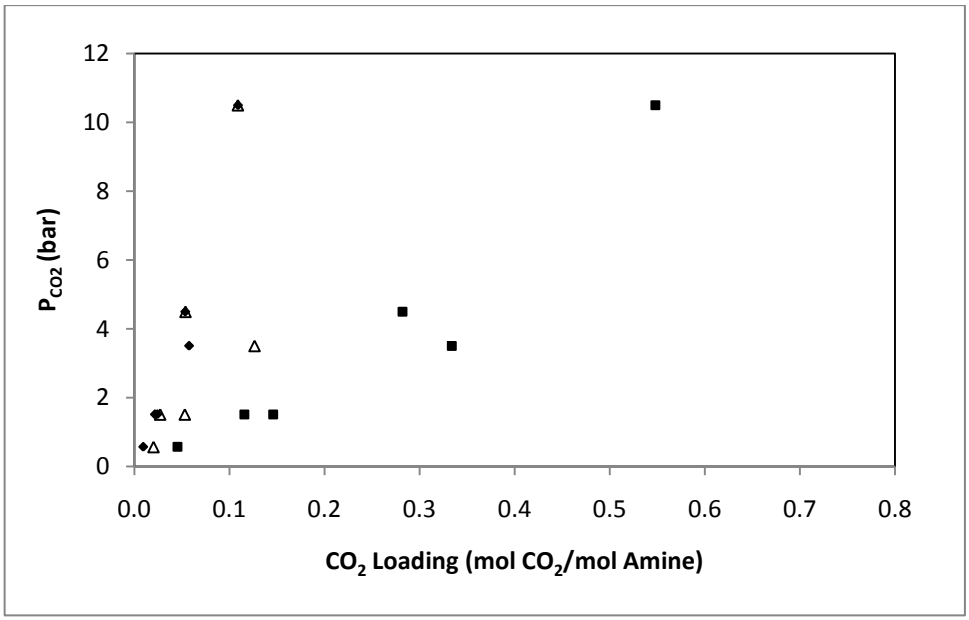

Figure 4-26: Comparison of Aspen simulation (with recycle) CO_2 loading estimates to experimental results: System 3 (30 wt% MDEA + 20 wt% DEA + 50 wt% H_2O, 363.15 K). - ♦ - Simulated actual CO_2 loading; ■ – System 3 experimental loading results; Δ - Simulated maximum potential CO_2 loading

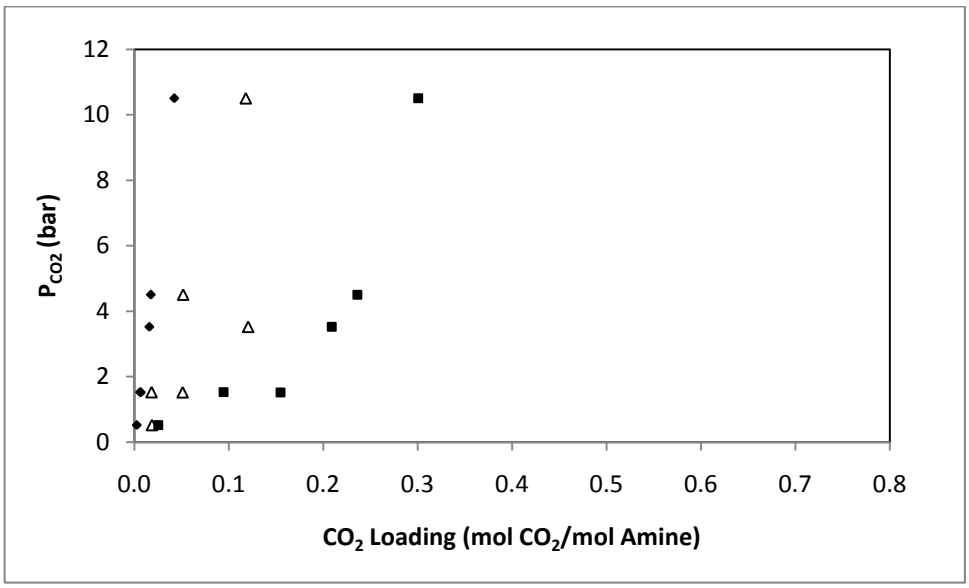

Figure 4-27: Comparison of Aspen simulation (with recycle) CO_2 loading estimates to experimental results: System 4 (30 wt% MDEA + 20 wt% DEA + 50 wt% H_2O, 413.15 K). - ♦ - Simulated actual CO_2 loading; ■ – System 4 experimental loading results; Δ - Simulated maximum potential CO_2 loading

Figures 4-24 to 4-27 display CO_2 loading results obtained from the simulation. It is immediately apparent that the CO_2 loading values are small in comparison to the CO_2 loading results of the simulation without recycle. This is due to the fact that more solvent enters the absorber due to the recycle stream, whereas the amount of CO_2 in the flue gas in unchanged.

When comparing Figures 4-24 to 4-27 with Figures 4-18 to 4-21, it is observed that the actual CO_2 loading compares more closely to the maximum potential CO_2 loading in the simulations involving recycle rather than simulations without a recycle stream. This is a marked improvement and identifies the addition of a recycle stream to be of high importance towards achieving greater absorption efficiency. From studying the data between Tables F2 and F4, it was found that on average, actual simulation CO_2 loadings are 9.97 % closer to maximum potential CO_2 loadings when recycle is used, than in simulations containing no recycle stream to the absorber.

As in the cases of simulation without recycle, the actual CO_2 loading in the simulations with recycle, resembled the maximum potential CO_2 loading the closest in the cases of lower temperature and low MDEA content. This is evident when comparing Figure 4-24 with Figures 4-25, 4-26 and 4-27.

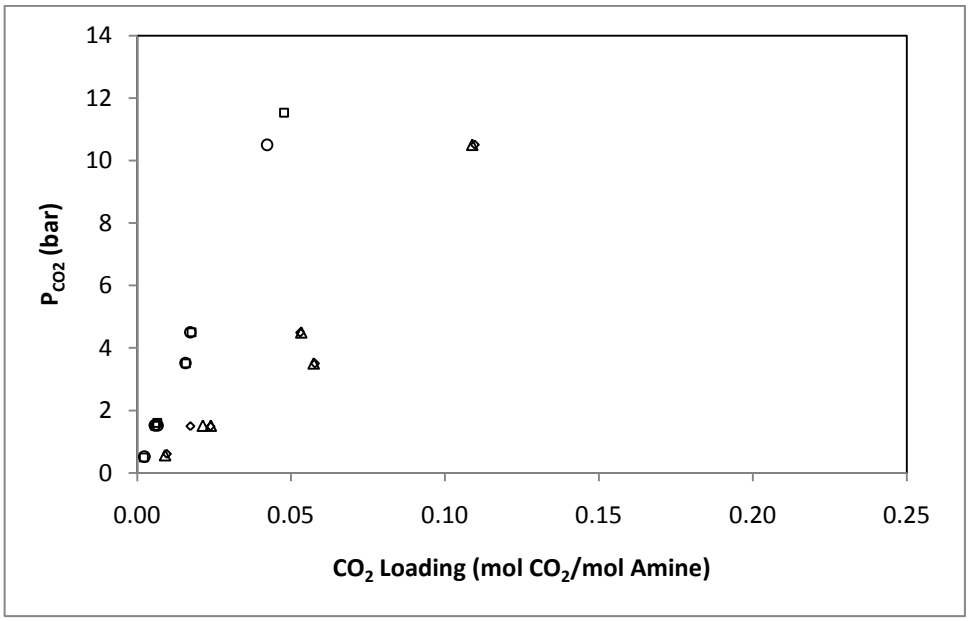

Figure 4-28: Comparison of Aspen simulation (with recycle) actual CO_2 loading estimates for all systems: ◊-System 1 (25 wt% MDEA + 25 wt% DEA + 50 wt% H_2O, 363.15 K); □ – System 2 (25 wt% MDEA + 25 wt% DEA + 50 wt% H_2O, 413.15 K); Δ - System 3 (30 wt% MDEA + 20 wt% DEA + 50 wt% H_2O, 363.15 K); ○ – System 4 (30 wt% MDEA + 20 wt% DEA + 50 wt% H_2O, 413.15 K)

Figure 4-28 shows a comparison of all measured systems using the Aspen simulation. The results are qualitatively consistent with the experimental results as shown in Figure 4-7, and with CO_2 loading results using no recycle, shown in Figure 4-22. A high temperature of 413.15 K produced low CO_2 loading in comparison with a low system temperature of 363.15 K. A solvent consisting of 25: 25: 50 wt% of MDEA: DEA: H_2O produced better loading results than

a solvent possessing higher MDEA and lower DEA compositions. This is evident in the comparison of System 1 and 3 of Figure 4-28.

Refer to Tables F2 - F5 of Appendix F. A crucial confirmation of the CO_2 loading results is that the amine solvents do not provide a high enough absorption rate. Even with increased solvent present in the absorber, due to recycled solvent, the percentage CO_2 recovery from the absorption process into the solvent only increased by 10 % in all data points. This is evident when comparing the percentage CO_2 Recovery from the Absorber in Table F2 with no recycle, to that of the percentage CO_2 recovery from the Absorber in Table F4 with recycle.

An important benefit of the recycle stream is that less amine solvent is lost to the stack during the absorption process. This is a combination of recycle and pump-around effect in the absorber, as well as the higher amount of stages in the absorber. MDEA, DEA and H_2O quantities in the stack were much lower in Tables F4 and F5, as opposed to Table F2 and F3. A drawback however, is that 5 % less N_2 gas is recovered at the stack stream. It is possible that entrainment occurs due to the greater quantity of solvent present in the absorber.

Less DEA and MDEA is lost to the CO_2 stream during stripping, than if no recycle was used. This is evident in comparing the data on Tables F3 and F5 for MDEA and DEA lost during stripping. A major drawback however, is that much H_2O is lost to the CO_2 stream in the case where recycle is employed. This is due to the fact that the N_2 carrier stream was omitted and a condenser and reboiler were installed in the stripper. This result however is better than in the case of no recycle, as is it easier to separate H_2O from CO_2 by using a condenser. N_2 lost to the CO_2 stream from stripping is also much lower than in the case of no recycle, providing a average CO_2 vapour purity in the CO_2 stream of 57 %, as opposed to the 25.7 % purity achieved in the case of no recycle.

Another drawback of the high H_2O losses during stripping is that the solvent composition is not maintained. The result is that the amine concentration is higher than it should be. This is undesirable as high amine concentrations can be corrosive to the units and piping. An imperative recommendation is to condense the CO_2 stream and recover the H_2O, and combine it into the recycle stream. A further benefit of this is that energy is recovered and can be reused in other units such as the stripper reboiler or HEX1 and hence the overall required heat duty of the process is lowered.

Overall it is evident that a system which utilises the recycle of solvent is much more efficient at CO_2 separation and recovery than a system without recycle of solvent.

The final conclusion of the CO_2 separation and recovery results presented in Appendix F however, is that the simulation provided overall disappointing results, due to the simulations

simplicity. The great improvements made with the instalment of a recycle stream do however provide much optimism that the simulation has much room for improvement.

It is recommended that a detailed project be undertaken in terms of the simulation of CO_2 capture by the absorption process. This simulation would include all binary interaction parameters available for a flue gas containing all gas components that industries typically emit, as mentioned above. A detailed study into different absorber components such as different packing and tray types, splitter sensitivity analysis for recycle streams, as well as optimum reflux and boil up ratios in the stripper, needs to be conducted.

Table F6 presents data pertaining to the energy requirements for the process. It was found that the heat duty for all units was less for system temperatures of 413.15 K, as opposed to 363.15 K. This was due to the fact that lower H_2O losses occurred when the temperature was 363.15 K, which resulted in more H_2O in circulation in the process. Higher solvent volume was present that needed to be heated before stripping and cooled thereafter.

For any particular system temperature, condenser duty was less for higher system pressures of 15 bar, due to the fact that latent heat requirements are less at higher pressure. The same observation was made upon heating the solvent in the heat exchanger HEX1, which produced a stream of liquid and vapour for stripping. Stripper reboiler duties and HEX2 duties were higher in the case of higher pressure, since higher solvent volumes occurred due to lower H_2O losses to the distillate.

No distinguishable difference in heat duty was observed when studying the effect of the change in solvent composition. This is probably because, although the mass-fraction of the two solvents studied was significantly different, the effective change in molar composition was not very large.

In all cases however, it is evident that the heat duty results are not promising using the current process flow diagram as shown in Figure 4-23. Table F6 presents total heat duties required for each process, as well as the Energy Penalty in GJ/tonne CO_2, to capture the CO_2 from the flue gas, assuming efficient heat transfer and recovery. The energy penalty (GJ/tonne CO_2) required is significantly high, in comparison with literature (see Table 2-2 and Section 2.12).

Oexmann et al. (2008) provided energy penalty values of 2.44 to 3.07 GJ/tonne CO_2 for carbonate solvent blends containing potassium carbonate and piperazine at various compositions. Kanniche and Bouallou (2007) provide energy penalty estimates of 2.4 to 3.14 GJ/tonne CO_2 for solvents containing single amines of MDEA and DEA at various concentrations. Other sources of energy penalty values include Knuutila et al. (2008) which

presents energy penalties of 3.2 to 7.4 GJ/tonne CO_2 for sodium carbonate solvents, Knudsen et al. (2008) which contains MEA and Castor solvent energy penalties of 3.5 to 3.7 GJ/tonne CO_2, and France (2007) with estimates of 4 GJ/tonne CO_2 for MEA solvents.

A common limitation of these literature sources however, is that the energy penalty values cited often only include the energy penalty for the absorption process. The stripping process is often neglected. Be that as it may, the energy penalty values obtained from the Aspen simulation in this study are still unrealistically high.

The reason for the above issue is that much energy is wasted on heating H_2O in the stripper. As Table G5 of Appendix G shows, the CO_2 stream contains a high temperature product (470.4 K) consisting primarily of H_2O. Such results are undesirable not only from an energy point of view, but also from a CO_2 purity point of view. A solution to recovering this lost energy and gaining CO_2 purity in this stream, is to condense the stream. This idea was briefly investigated using Aspen.

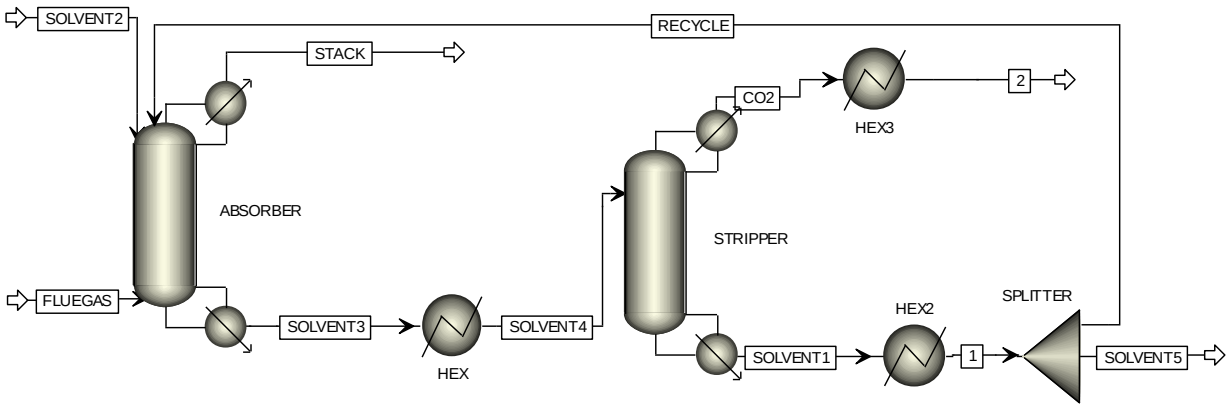

Figure 4-29: Modified CO_2 Capture Process

Refer to Figure 4-29. A condensing unit HEX3 was added to recover lost energy by cooling the CO_2 stream from 470.4 K to the Recycle stream temperature of 412.13 K. 6126.86 MW of heat energy was recovered. Overall, this recovery results in a 77.3 % decrease in energy penalty. For the system described in Table G5, this results in an energy penalty of 39 GJ/tonne CO_2, as opposed to 173.47 GJ/tonne CO_2 as shown in Table F6 of Appendix F.

This modified process was done under the conditions expressed as data point 4 (as shown in Table 2-3 of Section 2.8). The simulation is available electronically as "CO_2 Absorption Simulation Modified.apw".

The primary conclusion of this is that there is much room for improvement in the process design. Such improvements would have to be made based on additional information unique to

various industrial conditions.

4.3.5 Preliminary costing of CO_2 capture by absorption

A preliminary cost analysis was briefly conducted using Aspen's costing routines. This was done through a simple preliminary design of the simulation depicted in Figure 4-23. The design and costing was done on the basis of Data Point 4 conditions (refer to Experimental Results A1-1 and A1-2 of Appendix A or Table 2-3 of Section 2.8) as these conditions have proven experimentally and in simulations to provide the best CO_2 loading results. Table G5 of Appendix G provided stream and unit results for the simulation.

The absorber and stripper were assumed to be constructed of carbon steel, and possessing sieve trays. The low corrosiveness of the solvent enables the use of this material. Both units were designed for a system pressure of 15.65 bar. Trays were spaced 0.61m apart. Further specifications were recorded in Tables G1 and G2 of Appendix G. The stripper design temperature was made higher than the absorber design temperature, due to the higher temperature necessary during stripping. While the simulation investigated a 20 stage absorber, Aspen design routines yielded a recommendation of 29 trays to accommodate these stages. The above specifications accommodated safe operation.

Column diameters were quite high: 14.63m for the absorber and 20m for the stripper. In practice this would mean that much area is required to accommodate the CO_2 capture process, unless many more stages are added to the design.

Tables G3 and G4 provide specifications on the two heat exchangers HEX1 and HEX2. Very basic and generalised specifications were considered by Aspen. Both heat exchangers were assumed to be U Tube type exchangers, with 2 tube passes and 1 shell pass. HEX1 required much higher surface area due to the fact that Stream Solvent3 (refer to Figure 37 and Table G5) possessed a far higher flow rate than stream Solvent 1. Design temperatures were higher for HEX2 due to the higher temperature of the Stripper bottoms stream. Design pressures however, were equal. The HEX material of construction was unspecified by Aspen.

Table H1 of Appendix H contains estimated capital costs of the equipment to be used for the process. The primary unit in terms of cost is the absorber, due to the large number of stages required to ensure effective CO_2 absorption. Increased costs are incurred with the inclusion of a pump-around between stages in order to increase contact time for absorption.

The stripper is significantly cheaper due to the much smaller size of the column. However, increased costs are incurred due to the stripper being operated as a standard distillation column. A reboiler and condenser need to be installed, as well as a reflux pump from the condenser.

HEX1 costs were significantly higher than HEX2 costs, due to the higher heat transfer required for HEX1 to accommodate the significantly larger flow rate.

Costs estimated by Aspen Version 7.1 were presented as 2008 cost estimates. General cost indices were used to provide an estimate of 2010 figures. Cost indices were obtained from Statistics South Africa (2010).

Cost Index 2008: 100 ; Cost Index 2010: 112

The total capital investment cost is contained Table H1, at R203 042 821. This includes all equipment discussed, as well general correction mark-ups for piping for streams, assuming piping is constructed of Carbon Steel (Aspen, 2008). There is no mention of solvent costs, safety costs, pumping costs, heater and cooler costs as well as costs for circulating heat transfer fluid. The cost of these additions is subject to the construction of the process.

The operating cost of the process is also not known, due to the lack of information. Such costs can only be accurately estimated upon a detailed actual design of a real process, which would involve the liaison of national electricity utilities. Moreover, meaningful estimates can only be made once the design itself is optimised to meet the requirements of the enterprise.

5. CONCLUSIONS

- The literature review of CO_2 capture techniques shows clearly that solvent absorption is the best developed and likely to be the most promising of all capture techniques.
- Blended amine solvents in particular showed comparatively better performance in key feasibility measurements such as energy penalty, absorption rate, CO_2 loading and heat of absorption. It is for this reason that experimentation has been done to further investigate this technique.
- It was found that CO_2 loading decreases substantially with increasing temperature. Industrially, flue gas will have to be cooled to at least below 393.15 K for efficient CO_2 capture to occur. System temperature is a very great influence on solvent performance, sometimes enabling lower amine concentrations to achieve higher CO_2 loading performance.
- Between the two amine blends studied, 25 wt% MDEA: 25 wt% DEA resulted in higher CO_2 loadings for each CO_2 partial pressure. This was true for both temperatures: 363.15 K and 413.15 K. This solvent also produced higher CO_2 liquid loadings than those studied in the literature. This solvent is hence proven to be a good candidate for use in pilot plant testing and a likely solvent to be used in industry.
- Comparison with other literature sources studied in this paper however, confirms that lower system temperature can certainly allow for lower amine concentrations in the solvent without compromising CO_2 loading.
- The complex Deshmukh-Mather model provided significantly more accurate CO_2 loading predictions than the simple Posey-Tapperson-Rochelle model. Results were achieved in a very reasonable computational time. This model is hence recommended for use in all amine absorption systems.
- The Deshmukh-Mather model provided better predictions for the solvent of 25:25:50 wt% MDEA: DEA: H_2O, indicating that the model's accuracy is sensitive towards solvent composition and chemical reaction.
- The Aspen simulation of CO_2 capture by amine absorption possessed qualitatively consistent results with experimental and modelled data. This is true for the simulations with and without recycle.
- CO_2 loading was calculated to be significantly lower in the Aspen simulations, due to the high amount of solvent present in the absorber (in the case of recycle present) and due to the much lower contact time achieved (especially in the case of recycle absent).
- CO_2 was recovered more efficiently and with higher purity in cases of lower system temperatures of 363.15 K and high system pressures of 15 bar. This is consistent with

experimental results. The effect of system pressure and temperature was more pronounced in the simulation than with experimental measurements.

- The simulation that included recycle recovered CO_2 much more efficiently than the simulation without recycle. This was achieved due to higher solvent quantities in the absorber due to recycle as well as design modifications.
- Overall, the simulations provided disappointing CO_2 loading results, due to the low absorption rate of the solvent blend that was studied. However, much room for process optimisation was identified and recommendations were noted.
- An attempt to provide general design specifications and costing was made, using Aspen costing routines. The costs were found to be within reason and were justifiable.
- The primary flaw of the simulation was the high energy penalty incurred, in comparison with literature estimates. However, much room for optimisation was identified and recommendations were made.

6. REFERENCES

Alie C., Backham L., Croiset E., Douglas P.L., 2005, "Simulation of CO_2 capture using MEA scrubbing: a flow sheet decomposition method", Energy Conversion and Management, vol. 46, page 475-487.

Alie C.F., 2004, "CO_2 capture with MEA: Integrating the absorption process and steam cycle of an existing coal-fired power plant", University of Waterloo, Ontario, Canada. Accessed 1 April 2009. http://etd.uwaterloo.ca/etd/calie2004.pdf

Altona Energy, 2008. "The CTL process", published by Altona Energy Ltd. Accessed 21 April 2009. http://www.altonaenergy.com/Coal_to_liquid.html

Aroua M.K., Haji-Sulaiman M.Z. and Ramasamy K., 2002, "Modelling of carbon dioxide absorption in aqueous solutions of AMP and MDEA and their blends using Aspenplus", Separation and Purification Technology, Vol. 29, Page 153-162.

Aspen Version 7.1. (32.0.4507), 2008, Aspen Technology Inc., Copyright 1998-2008.

Austgen D.M., Rochelle G.T., Peng X., Chen C.C., 1989, "Model of vapor-liquid equilibria for aqueous acid gas-alkanolamine systems using the electrolyte-NRTL equation". Ind. Eng. Chem. Res, vol 28, pg. 1060-1073

Austgen D.M., Rochelle G.T., Chen C.C., 1991, "Model of vapour-liquid equilibria for aqueous acid gas-alkanolamine systems. 2. Representation of H_2S and CO_2 solubility in aqueous MDEA and CO_2 solubility in aqueous mixtures of MDEA with MEA or DEA", Industrial and Engineering Chemistry Research, 30, pg 543-555

Benamor A., and Aroua M.K., 2005, "Modelling of CO_2 solubility and carbamate concentration in DEA, MDEA and their mixtures using the Deshmukh–Mather model", Fluid Phase Equilibria 231, pg 150-162.

Coal Ash Research Centre (CARC), 2008, "Pulverised coal combustion", Energy and Environment Research Centre, University of North Dakota, U.S.. Accessed 8/4/2009. http://www.undeerc.org/carrc/html/CoalCombustion.html

Carbon Dioxide Information Analysis Centre (CDIAC), 2008, "Recent greenhouse gas concentration", Published by Department of Energy (DOE), U.S. http://cdiac.ornl.gov/pns/current_ghg.html, accessed 23 March 2009.

Chakravarti S., Gupta A., Hunek B., 2001, "Advanced technology for the capture of carbon dioxide from flue gases", Praxair, Inc. Process & Systems R&D, CO_2 Technology, USA.

Chatti I., Delahaye A., Fournaison L., Petitet J.P., 2005, "Benefits and drawbacks of clathrate hydrates: a review of the areas of interest", Energy Conversion and Management Vol. 46, pg. 1333–1343

Chen, C.-C.; Evans, L. B., 1986, "A local composition model for the excess gibbs energy of aqueous electrolyte system". AIChE Journal, Vol. 32, 444−454

Clodic D., Hitti R., Younes M., Bill A. and Casier F., 2005, "CO_2 capture by anti-sublimation: thermo-economic process evaluation", 4th Annual Conference on Carbon Capture and Sequestration, U.S.A.

Coquelet C., Richon D., 2007, "Chapter 14: Solubility of BTEX and Acid Gases in Alkanolamine Solutions in Relation to the Environment", from the book: "Developments and applications of solubility", RSC, Cambridge, UK.

Davison J., 2006, "Performance and costs of power plants with capture and storage of CO_2", Energy Vol. 32, pg 1163–1176

Descamps C., Coquelet C., Bouallou C. and Richon D., 2005, "Solubility of hydrogen in methanol at temperatures from 248.41 to 308.20K", Thermochimica Acta Vol. 430, pg. 1-7.

Descamps C, Bouallou C, Kanniche M, 2008, "efficiency of an integrated gasification combined cycle (IGCC) power plant including CO_2 removal.", Energy 33, pg 874-881.

Deshmukh R.D., Mather A.E., 1981, "A mathematical model for equilibrium solubility of hydrogen sulphide and carbon dioxide in aqueous alkanolamine solutions". Chemical Engineering Science, vol. 36, pg 355-362

Dicko M., Coquelet C., Jarne C., Northrop S., Richon D., 2010, "Acid gases partial pressures above a 50 wt% aqueous methyldiethanolamine solution experimental work and modelling", Fluid Phase Equilibria 289, pg. 87-97.

Dry M.E., 2002, "The Fischer–Tropsch process: 1950–2000", Catalysis Today, 71, pg. 227-241.

Duc N.H., Chauvy F and Herri J.M., 2007, "CO_2 capture by hydrate crystallization – a potential solution for gas emission of steelmaking industry", Energy Conversion and Management, Vol 48, pg 1313-1322.

Enhanced Capture of CO_2, 2008, "Pre-combustion decarbonisation technologies", http://www.encapco2.org/sp2.htm. Accessed 25 August 2010.

Eon Technology, 2007, "Oxyfuel: using pure oxygen to produce pure CO_2", Published by EON, Germany. Accessed 24 April 2009 http://www.eon.com/en/unternehmen/26502.jsp .

Figueroa J.D., Fout T, Plasynski S., McIlvried H. and Srivastava R.D., 2008, "Advances in CO_2 capture technology—The U.S. department of energy's carbon sequestration program", International Journal of Greenhouse Gas Control, Vo. 2, pg 9—20

France L., 2007, "Development of new amine absorbents in new COCS project", 10th International CO_2 Capture Network, Research Institute of Innovative Technology for the Earth, Kyoto, Japan. Accessed 1 April 2009. http://www.rite.or.jp

Gabrielsen J., Michelsen M.L., Stenby E.H., and Kontogeorgis G.M., 2005 "A model for estimating CO_2 solubility in aqueous alkanolamines", Ind. Eng. Chem. Res., Vol 44, pg 3348-3354

GibbinsJ. and Chalmers H, 2008, "Preparing for global rollout: a 'developed country first' demonstration programme for rapid CCS deployment." Energy Policy Vol. 36, pg 501-507

Gielen D., 2003, "The energy policy consequences of future CO_2 capture and sequestration technologies", International Energy Agency, France. Accessed 19 February 2009. http://www.resourcemodels.org/pap060503.pdf

Gas Processors Association (GPA), 2004. "GPSA Engineering Data Book: Section 21 – Hydrocarbon Treating", 12th Edition, published by GPA. Accessed 12 April 2009. http://www.gasprocessors.com/gpsa_book.html#About.

Green D.A., Turk B.S., Portzer J.W., Gupta R.P., McMichael W.J, Nelson T., Gangwal S., Liang Y, Moore T., Williams M., Harrison D.P., 2004, "Carbon dioxide capture from flue gas using dry regenerable sorbents", Topical report for the U.S. Department of Energy, NETL, Pittsburgh.

Griffiths J., 2008, "Lose the carbon, not the capacity.", TCE Magazine, issue 810. December 2008/January 2009, Pg. 43. www.tcetoday.com.

Hansen J., Sato M, Ruedy R., Lo K, Lea D.W. and Elizade M.M., 2006, "Global temperature change", NASA Goddard Institute for Space Studies, USA. Accessed 8 April 2009. http://www.pnas.org/content/103/39/14288.full.pdf+html

Hook R.J., 1997, "An investigation of some sterically hindered amines as potential carbon dioxide scrubbing compounds", Ind. Eng. Chem. Res., Vol 36, Pg. 1779-1790

International Energy Agency (IEA), 2004, "Prospects for CO_2 Capture and Storage – 2004 IEA report", Paris Cedex, France. Accessed 5 March 2009.
http://www.iea.org/textbase/nppdf/free/2004/prospects.pdf

International Energy Agency (IEA), 2007, "CO_2 Capture Ready Plants", United Kingdom: Organisation for Economic Cooperation and Development, Greenhouse Gas R&D Programme. Accessed 22 January 2009
http://www.iea.org/Textbase/Papers/2007/CO2_Capture_Ready_ Plants.pdf

International Energy Agency (IEA), 2007, "Capturing CO_2", IEA Greenhouse Gas R&D Programme, Accessed 29 January 2009
http://www.ieagreen.org.uk/glossies/co2capture.pdf

International Energy Agency (IEA), 2010, "Key World Energy Statistics – 2010", International Energy Agency, Paris Cedex, France.

Intergovernmental Panel on Climate Change (IPCC), 2004, "Carbon Dioxide Capture and Storage: Summary for Policy Makers and Technical Summary". IPCC, Nairobi, Kenya. Accessed 21 January 2009 http://www.climnet.org/EUenergy/IPCC_CCS_0905.pdf

Jadhawar P., Mohammadi A.H., Yang J., Tohidi B., 2006, "Subsurface carbon dioxide storage through clathrate hydrate formation", Institute of Petroleum Engineering, Heriot-Watt University, Edinburgh, United Kingdom.

Kaewsichan L., Al-Bofersen O., Yesavage V.F. and Selim M.S., 2001, "Predictions of the solubility of acid gases in monoethanolamine (MEA) and methyldiethanolamine (MDEA) solutions using the electrolyte-UNIQUAC model", Fluid Phase Equilibria, Vol. 183-184, pg, 159-171

Kanniche M., Bouallou C., 2007, "CO_2 capture study in advanced integrated gasification combined cycle", Applied Thermal Engineering Vol. 27, pg. 2693-2702.

Kawesha D., 2009. Personal correspondence with Mr. D. Kawesha, a process engineer at SASOL Ltd, Sasolburg.

Kim I., and Svendsen H.F., 2007, "Heat of absorption of carbon dioxide (CO_2) in monoethanolamine (MEA) and 2 (aminoethyl)ethanolamine (AEEA) solutions", *Ind. Eng. Chem. Res.*, Vol. 46, pg. 5803-5809

Klyamer, S. D.; Kolesnikova, T. L.; Rodin, Y. A., 1973 “Equilibrium in aqueous solutions of ethanolamines during the simultaneous absorption of hydrogen sulphide and carbon dioxide from gases.” Gazov. Promst. Vol. 18, pg. 44-48

Knudsen J.N., Vilhelmsin P.J., Jensen J.N and Biede O., 2008, “Performance review of Castor pilot plant at Esbjerg”. Published by Dong Energy, Austria.

Knuutila H., Hallvard F. Svendsen, and Mikko Anttila, 2008, “CO_2 capture from coal-fired power plants based on sodium carbonate slurry; a systems feasibility and sensitivity study”, International Journal of Greenhouse Gas Control, Vol 3, pg 143-151.

Kundu M. and Bandyopadhyay S.S., 2006, “Solubility of CO_2 in water + diethanolamine + *N*-methyldiethanolamine”, Fluid Phase Equilibria, Volume 248, pg 158-167.

Leci C.L., 1997, “Development requirements for absorption processes for effective CO_2 capture from power plants”, Energy Conversion and Management, Vol. 38, pg. S45-S50.

Lee J.B., Ryu C.K., Baek J., Lee J.H., Eom T.H., Kim S.H., 2008, “Sodium based dry regenerable sorbent for carbon dioxide capture from power plant flue gas”, Ind. Eng. Chem Vol. 47, pg. 4465-4472.

Linga P., Kumar R., Englezos P., 2007, “The clathrate hydrate process for post and pre combustion capture of carbon dioxide”, Journal of Hazardous Materials 149, pg. 625–629.

Linga P., Kumar R., Englezos P., 2007, “Gas hydrate formation from hydrogen/carbon dioxide and nitrogen/carbon dioxide gas mixtures”, Chemical Engineering Science, Vol. 62, pg 4268-4276.

Ma’mun S, Svendsen HF, Hoff K.A. and Juliussen O, 2006, “Selection of new absorbents for carbon dioxide capture”, Energy Conversion and Management, Vol. 48, pg 251-258.

Ma’mun S., 2005, “Selection and characterisation of new absorbents for carbon dioxide capture”, Faculty of Natural Science and Technology, Department of Chemical Engineering, NTNU, Norway.

Ma’mun S., Nilsen R. and Svendsen H.F., 2005, “Solubility of carbon dioxide in 30 mass % monoethanolamine and 50 mass % methyldiethanol amine solutions”, Journal of Chemical Engineering Data, vol. 50, page 630-634

Manuel A., Pacheco T. and Rochelle G.T., 1998, "Rate-based modelling of reactive absorption of CO_2 and H_2S into aqueous methyldiethanolamine", Ind. Eng. Chem. Res. Vol. 37, pg. 4107-4117

Meisen A, Shuai X., 1997, "Research and development issues in CO_2 capture", Energy Conversion and Management Vol. 38, pg. S37-S42.

Miller B.G., 2005, "Coal Energy Systems", Academic Press Sustainable World Series, Elsevier Inc., London.

Mongabay, 2008, "CO_2 emissions could doom fishing industry", Mongabay San Francisco, USA. accessed 23 March 2009 http://news.mongabay.com/2008/0703-oceans.html,

Murrieta-Guevara F., Rebolledo-Libreros M.E., Romero-Martínez A. and Trejo A., 1998, "Solubility of CO_2 in aqueous mixtures of diethanolamine with methyldiethanolamine and 2-amino-2-methyl-1-propanol", Fluid Phase Equilibria, Vol. 150-151, pg 721-729

Nerula S.C. and Ashraf M., 1987, "Carbon dioxide separation", Process Economics Program, S.R.I International, California, USA.

National Energy Technology Laboratory (NETL), 2007, "Chemical looping process in a coal to liquids configuration", published by Department of Energy, accessed 29 January 2009, http://www.netl.doe.gov/energy-analyses/pubs/DOE%20Report%20on%20OSU%20Looping%20final.pdf

Oexmann J, Hensel C., Kather A., 2008, "Post-combustion CO_2-capture from coal-fired power plants: Preliminary evaluation of an integrated chemical absorption process with piperazine-promoted potassium carbonate", International Journal of greenhouse gas control, Vol 2, pg 538-552.

Osman K., Coquelet C., Ramjugernath D., 2010, "Absorption of CO_2 in aqueous blends of methyl-diethanolamine (MDEA) and diethanol amine (DEA): 25wt% MDEA-25wt% DEA and 30wt% MDEA-20wt% DEA concentrations", manuscript submitted for review to Journal of Chemical Engineering Data.

Park J., Seo Y.T, Lee J.W., Lee H., 2006, "Spectroscopic analysis of carbon dioxide and nitrogen mixed gas hydrates in silica gel for CO_2 separation", Catalysis Today Vol. 115, pg. 279-282.

Posey M.L., Tapperson K.G. and Rochelle G.T., 1996, "A simple model for prediction of acid gas solubilities in alkanolamines", Gas Sep. Purif. Vol 10, pg 181-186

Ritter J.A. and Armin D.E., and Reynolds S.P. and Du H., 2006, “New adsorption cycles for carbon dioxide capture and concentration”, Department of Chemical Engineering, University of South Carolina, Columbia.

Rogers W.J., Bullin J.A. and Davison R.R., 1998, “FTIR measurements of acid-gas-methyldiethanolamine systems”, AICHe Journal Vol. 44, pg 2423-2430.

Science Daily, 2009, “Artificial photosynthesis: turning sunlight into liquid fuels moves a step closer”, Published by Science Daily LLC, USA. Accessed 7/04/2009. http://www.sciencedaily.com/releases/2009/03/

Sidi-Boumedine R, Horstmann S., Fisher K., Provost E., Fürst W. and Gmehling J., 2004, "Experimental determination of carbon dioxide solubility data in aqueous alkanolamine solutions", Fluid Phase Equilibria, Vol., pg. 218, 85-94

Singh D., Croiset E., Douglas P.L., Douglas M.A., 2003, “Techno-economic study of CO_2 capture from an existing coal-fired power plant: MEA scrubbing vs O_2/CO_2 recycle combustion.” Energy Conversion and Management 44, 3073-3091.

Statistics South Africa, 2010, "Statistical Release: Consumer Price Index 2010", Statistics South Africa, Pretoria, http://www.statssa.gov.za/publications/P0141 /P0141September2010.pdf

Steeneveldt R., Berger B. and Torp. T.A., 2006, “CO_2 capture and storage. closing the knowing-doing gap”, Chemical Engineering Research and Design Vol. 84, pg 739-763.

Sulaiman M.Z., Aroua M.K., Benamor A., 1998, “Analysis of equilibrium data of CO_2 in Aqueous Solutions of Diethanolamine (DEA), Methyldiethanolamine (MDEA) and their mixtures using the modified Kent Eisenberg model”, Chemical Engineering Research and Design, Vol 76, pg 961-968

Surridge T., 2005, “South African activities related to carbon capture and storage – September 2005”, Department of Minerals and Energy, South Africa, Carbon Sequestration Leadership Forum, accessed 28 January 2009
http://www.cslforum.org/documents/pg_RomeMinutespublic.pdf,

Teng F. and Tondeur D., 2006, “Efficiency of carbon storage with leakage: physical and economical approaches”, Energy Vol. 32, pg. 540-548.

Trachtenberg M.C., Tu C.K., Landers R.A., Willson R.C., McGregor M.L., Laipis P.J., Kennedy J.F., Paterson M., Silverman D.N., Thomas D., Smith R.L., Rudolph F.B., 1999,

"Carbon dioxide transport by proteic and facilitated transport membranes", International Journal of Earth Space, Vol. 6, pg. 293-302.

Van Bibber L., Thomas C., Chaney R., 2007, "Alaska coal gasification feasibility studies–Healy coal-to-liquids plant", published by NETL. Accessed 29 January 2009. http://www.netl.doe.gov/technologies/coalpower/gasification/pubs/pdf/FINALHealy%20FT%201251%200706 2007.pdf

Vierde Nationaal Symposium (VNS) CCS, 2007, "CATO CO_2 Catcher, A CO_2 Capture Plant Treating Real Flue Gas", Published by EON Ltd. Accessed 12 February 2009. http://www.co2-cato.nl/modules.php?name= CATO&page =79& symposium=true.

Wappel D., Khan A., Shallcross D., Joswig S, Kentish S., Stevens G, 2008, "The effect of SO_2 on CO_2 absorption in an aqueous potassium carbonate solvent", Energy Procedia Vol. 1, pg 1-7.

Weiland R.H., Chakravarty T, and Mather A.E., 1993, "Solubility of carbon dioxide and hydrogen sulphide in aqueous alkanolamines", *Ind. Eng. Chem. Res.* 1993,32, 1419-1430.

Zhao C., Chen X., Zhao Ch., Liu Y., 2008, "Carbonation and hydration characteristics of dry potassium-based sorbents for CO_2 capture", Energy and Fuels Journal 2008, Thermoenergy Engineering Research Institute, China.

7. BIBLIOGRAPHY

Amann J.M.G., Bouallou C., 2009, "A new aqueous solvent based on a blend of nmethyldiethanolamine and triethylene tetramine for CO_2 recovery in post-combustion: kinetics study", Energy Procedia, Vol. 1, pg. 901-908

Amann J.M., Kanniche M., Bouallou C., 2008, "Reforming natural gas for CO_2 pre-combustion capture in combined cycle power plant", Clean Techn Environ Policy, Vol. 11, pg. 67–76.

Asthary R., 2008, "IGCC Technology Overview", published by Majari Magazine Ltd., Accessed 26 May 2009, http://majarimagazine.com/2008/06/igcc-technology-overview-part-1/

Awan J.A., Valtz A., Coquelet C. And Richon D., 2008, "Effect of acid gases on the solubility of *n* propylmercaptan in 50wt% methyl-diethanolamine aqueous solution", Chemical Engineering Research and Design Vol. 86, pg. 600-605

Bahadori A., Vuthaluru H.B., Mokhatab S., 2008, "Rapid prediction of CO_2 solubility in aqueous solutions of diethanolamine and methyldiethanolamine", Chemical Engineering Technology, 31, No. 2, pg 245-248.

British Geological Survey (BGS), 2006, "Trapped in ice", published by BGS Ltd., Kingsley, Dunham Centre, Keyworth, Nottinghamshire. Accessed 26 January 2009. http://www.nerc.ac.uk/publications/planetearth/2006/autumn/aut06-ice.pdf

Cesar enhanced Separation and Recovery, 2008, "CESAR project objectives", Published by TNO Industry and Science, Netherlands. http://www.co2cesar.eu/, accessed 23 March 2009.

Chalmers H. and Gibbins J., 2007, "Initial evaluation of the impact of post-combustion capture of carbon dioxide on supercritical pulverised coal power plant part load performance", Fuel, Vol. 86, pg 2109-2123

Clean Synthetic Fuel Research Unit (CFRU), 2008, "Clean synthetic fuel research unit", Department of Chemical Technology, Faculty of Science, Chulalongkorn University, Thailand. Accessed 21 April 2009 http://www.cgfru.research.chula.ac.th/

Clement D., Moisan F., Bonijoly D., Fabriol H., Gastine M., Coussy P., Thiez P.L., Rojey A., 2007, "CO_2 capture and storage in the subsurface – A technological pathway for combating climate change", BRGM Communication and Publications Division, France.

Edali M., Aboudheir A. and Idem R., 2009, "Kinetics of carbon dioxide absorption into mixed aqueous solutions of MDEA and MEA using a laminar jet apparatus and a numerically solved

2D absorption rate/kinetics model", International Journal of Greenhouse Gas Control, vol. 3, pg. 550-560

Freguia S., Rochelle G.T., 2003, "Modeling of CO_2 capture by aqueous monoethanolamine", AICHE Journal, Vol. 49, pg 1676-1686

Ghawas H, Hagewlesche D.P., Rulz-Ibanez G., and Sandall O.C., 1989, "Physicochemical properties important for carbon dioxide absorption in aqueous methyldiethanolamine" J. Chem. Eng. Data, Vol. 34, pg 385-391.

Global Warming, 2007, "Industry CO_2 emissions", Published by Global Greenhouse Warming. Accessed 23 March 2009. http://www.global-greenhouse-warming.com/ industry-CO_2-emissions.html

Hong S.Y. and Li M.H., 2002, "Kinetics of absorption of carbon dioxide into aqueous solutions of monoethanolamine + triethanolamine", Ind. Eng. Chem. Res. 2002, 41, 257-266.

Hsu C.H, Li M.H., 1997, "Densities of aqueous blended amines", Journal of Chemical Engineering Data, vol. 42, pg 502-507

International Emissions Trading Association (IETA), 2008, "What is the science behind climate change?", IETA, Geneva, Switzerland. Accessed 27 January 2009. http://www.ieta.org/ ieta/www/pages/index.php?IdSitePage=121.

Kohl A., Nielson R., 1997, "Gas Purification", 5th Edition, published by Gulf Publishing Company, Houston, Texas, U.S.

Litynski J.T., Plasynski S., McIlvried H.G., Mahoney C. and Srivastava R.D., 2008, "The United States department of energy's regional carbon sequestration partnerships program validation phase", Environment International, Vol. 34, pg. 127-138.

Mohammadi A.H., Tohidi B., Anderson R., 2005, "Carbon monoxide clathrate hydrates: equilibrium data and thermodynamic modelling", Centre for gas Hydrate Research, Institute of Petroleum Engineering, Herit-Watt University, United Kingdom.

O'Rear D.J. and Goede F., 2007, "Concepts for reduction in CO_2 emissions in GTL facilities", Studies in Surface Science and Catalysis, Vol. 163, pg. 401-409.

Pérez-Alonso F.J., Ojeda M., Herranz T., Rojas S., González-Carballo J.M., Terreros P., Fierro J.L.G., 2008, "Carbon dioxide hydrogenation over Fe-Ce catalysts", Catalysis Communications Vol. 9, pg 1945-1948.

Plaza J.M., Van Wagner D., Rochelle G.T., 2009, "Modeling CO_2 capture with aqueous monoethanolamine", Energy Procedia vol.1, pg. 1171-1178.

Ravikrishna C., Amit K. B., Thote A. J, Kumar V., Jadhav P., Lokhande S.K., Biniwale R.B., Labhsetwar N.K., Rayalu S.S., 2009, "Amine loaded zeolites for carbon dioxide capture: amine loading and adsorption studies", Microporous and Mesoporous Materials Vol. 121, pg. 84-89.

Rubin E.S., Chen C., Rao A.B., 2007, "Cost and performance of fossil fuel power plants with CO_2 capture and storage", Energy Policy Vol. 35, pg. 4444-4454.

Steynberg A and Dry M., 2004, "Introduction to Fischer-Tropsch technology", Studies in Surface Science and Catalysis Vol. 152, Elsevier Inc.

Surridge A.D., 2007, "Carbon capture and storage – South African activities and plans", South African National Energy Research Institute, South Africa, accessed 27 January 2009 http://www.un.org/esa/sustdev/sdissues/energy/op/ccs_egm/ccs_egmdraftprogramme.pdf

Van der Merwe C., 2007, "South Africa years away from being 'country ready'" published by Mining Weekly. Accessed 28 January 2009.
http://www.miningweekly.com/article.php?a_id=109338

Wang R., Li D.F. and Liang D.T., 2004, "Modeling of CO_2 capture by three typical amine solutions in hollow fiber membrane contactors", Chemical Engineering and Processing, 43, pg. 849-856

Yagi T., Mimura T., Yonekawa T., Yoshiyama R., 2008, "Development and improvement of CO_2-capture system" Environmental Research Centre, Japan.

Appendix A: Data obtained

Table A1-1: System 1 Experimental Data – 25 wt% MDEA + 25 wt% DEA + 50 wt% H_2O - 363.15 K									
Measurement	P_{CO2} (bar)	y_{N2}	y_{CO2}	y_{H2O}	x_{N2} ($x10^8$)	x_{CO2}	x_{H2O}	x_{DEA}	x_{MDEA}
1	0	0.979	0.000	0.021	1.149	0.000	0.861	0.074	0.065
2	0	0.936	0.000	0.064	1.285	0.000	0.861	0.074	0.065
3	0	0.924	0.000	0.076	1.344	0.000	0.861	0.074	0.065
4	1.500	0.951	0.008	0.041	2.342	0.009	0.853	0.073	0.065
5	0.611	0.881	0.006	0.114	1.444	0.003	0.858	0.074	0.065
6	1.492	0.923	0.026	0.051	1.562	0.005	0.856	0.074	0.065
7	4.496	0.901	0.079	0.020	0.988	0.028	0.837	0.072	0.063
8	3.508	0.704	0.233	0.063	0.996	0.025	0.839	0.072	0.064
9	10.510	0.175	0.760	0.065	1.485	0.054	0.815	0.070	0.062

Table A1-2 :System 1 Experimental data (contd.) 25 wt% MDEA + 25 wt% DEA + 50 wt% H_2O - 363.15 K							
Measurement	Average Temperature (K)	Average Pressure (bar)	Density of Solvent ρ_m (g/cm^3) at 363.15 K	Measured Volume of Solvent (cm^3)	Amount of CO_2 Charged (mol)	CO_2 Liquid Loading (mol CO_2/mol DEA+MDEA)	Partition coefficient
1	361.69	14.970	1.042	14.137	0.000	0	0
2	362.17	9.845	1.042	14.165	0.000	0	0
3	362.19	4.913	1.042	14.173	0.000	0	0
4	362.17	14.995	1.042	14.173	0.007	0.107	0.976
5	362.14	4.649	1.042	14.165	0.003	0.043	1.988
6	362.22	4.883	1.042	14.165	0.007	0.101	4.995
7	362.15	14.898	1.042	14.165	0.020	0.285	2.875
8	362.16	4.966	1.042	15.596	0.022	0.287	9.256
9	362.14	16.919	1.042	14.173	0.058	0.730	14.064

Table A2-1: System 2 Experimental Data - 25 wt% MDEA + 25 wt% DEA + 50 wt% H_2O - 413.15 K									
Measurement	P_{CO2} (bar)	y_{N2}	y_{CO2}	y_{H2O}	x_{N2} ($x10^8$)	x_{CO2}	x_{H2O}	x_{DEA}	x_{MDEA}
10	0	0.725	0.000	0.275	1.000	0.000	0.861	0.074	0.065
11	0.494	0.365	0.045	0.591	1.197	0.001	0.860	0.074	0.065
12	1.509	0.644	0.097	0.259	1.058	0.007	0.855	0.073	0.065
13	4.500	0.813	0.187	0.000	1.288	0.020	0.844	0.072	0.064
14	1.600	0.268	0.172	0.559	1.750	0.010	0.853	0.073	0.065
15	0.000	0.004	0.000	0.996	1.337	0.000	0.861	0.074	0.065
16	11.529	0.186	0.076	0.737	1.732	0.025	0.839	0.072	0.064
17	3.506	0.004	0.368	0.628	1.960	0.014	0.849	0.073	0.064

Table A2-2: System 2 Experimental Data (contd.) 25 wt% MDEA + 25 wt% DEA + 50 wt% H_2O - 413.15 K							
Measurement	Average Temperature (K)	Average Pressure (bar)	Density of Solvent ρ_m (g/cm^3) at 413.15 K	Measured Volume of Solvent (cm^3)	Amount of CO_2 Charged (mol)	CO_2 Loading (mol CO_2/mol DEA+MDEA)	Partition coefficient
10	412.13	15.241	1.039	14.180	0.000	0	0
11	412.18	5.391	1.039	14.165	0.003	0.042	36.481
12	412.15	14.824	1.039	14.173	0.007	0.097	13.690
13	412.17	15.120	1.039	14.173	0.021	0.294	9.558
14	412.16	6.866	1.039	14.173	0.007	0.100	18.136
15	411.01	5.018	1.039	14.173	0.000	0	0
16	412.13	16.644	1.039	14.173	0.036	0.524	3.009
17	412.17	5.343	1.039	14.173	0.014	0.196	26.043

Table A3-1: System 3 Experimental Data – 30 wt% MDEA + 20 wt% DEA + 50 wt% H_2O - 363.15 K									
Measurement	P_{CO2} (bar)	y_{N2}	y_{CO2}	y_{H2O}	x_{N2} (x10^8)	x_{CO2}	x_{H2O}	x_{DEA}	x_{MDEA}
18	0.571	0.002	0.007	0.991	1.346	0.004	0.859	0.059	0.078
19	1.516	0.487	0.023	0.507	1.202	0.008	0.856	0.059	0.078
20	10.502	0.284	0.047	0.023	1.891	0.050	0.819	0.056	0.075
21	4.500	0.855	0.051	0.047	1.987	0.026	0.840	0.058	0.076
22	3.508	0.635	0.051	0.051	1.130	0.022	0.843	0.058	0.077
23	1.517	0.914	0.020	0.051	1.148	0.009	0.854	0.059	0.078
24	0.000	0.980	0.028	0.020	1.918	0.000	0.862	0.059	0.079
25	0.000	0.972	0.000	0.028	1.057	0.000	0.862	0.059	0.079

Table A3-2: System 3 Experimental Data (contd.) 30 wt% MDEA + 20 wt% DEA + 50 wt% H_2O - 363.15 K							
Measurement	Average Temperature (K)	Average Pressure (bar)	Density of Solvent ρ_m (g/cm^3) at 363.15 K	Measured Volume of Solvent (cm^3)	Amount of CO_2 Charged (mol)	CO_2 Loading (mol CO_2/mol DEA+MDEA)	Partition coefficient
18	361.59	5.054	1.042	14.173	0.003	0.045	1.780
19	361.96	9.957	1.042	14.173	0.008	0.116	2.963
20	361.89	17.235	1.042	14.165	0.044	0.548	0.937
21	362.07	14.946	1.042	14.180	0.020	0.282	1.948
22	362.08	4.962	1.042	14.180	0.023	0.334	2.321
23	362.15	5.109	1.042	14.173	0.010	0.146	2.160
24	361.62	5.432	1.042	14.173	0.000	0	0
25	361.94	14.957	1.042	14.173	0.000	0	0

Table A4-1: System 4 Experimental Data – 30 wt% MDEA + 20 wt% DEA + 50 wt% H_2O - 413.15 K									
Measurement	P_{CO2} (bar)	y_{N2}	y_{CO2}	y_{H2O}	x_{N2} ($x10^8$)	x_{CO2}	x_{H2O}	x_{DEA}	x_{MDEA}
26	0.520	0.418	0.002	0.580	1.352	0.003	0.860	0.059	0.078
27	1.525	0.674	0.149	0.177	1.538	0.005	0.858	0.059	0.078
28	10.500	0.188	0.616	0.196	1.600	0.014	0.850	0.058	0.077
29	1.520	0.004	0.003	0.996	1.085	0.005	0.858	0.059	0.078
30	0.000	0.198	0.000	0.802	1.315	0.000	0.862	0.059	0.079
31	0.000	0.646	0.000	0.354	1.978	0.000	0.862	0.059	0.079
32	3.520	0.214	0.294	0.492	1.751	0.007	0.857	0.059	0.078
33	4.503	0.621	0.290	0.089	1.650	0.008	0.856	0.059	0.078

Table A4-2: System 4 Experimental Data (contd.) 30 wt% MDEA + 20 wt% DEA + 50 wt% H_2O - 413.15 K							
Measurement	Average Temperature (K)	Average Pressure (bar)	Density of Solvent ρ_m (g/cm^3) at 413.15 K	Measured Volume of Solvent (cm^3)	Amount of CO_2 Charged (mol)	CO_2 Loading (mol CO_2/mol DEA+MDEA)	Partition coefficient
26	412.11	4.986	1.038	14.165	0.003	0.042	0.793
27	412.16	15.003	1.038	14.180	0.008	0.094	27.085
28	412.17	15.900	1.038	14.173	0.026	0.301	43.147
29	412.08	5.306	1.038	14.173	0.010	0.155	0.604
30	412.15	5.201	1.038	14.180	0.000	0.000	0.000
31	412.14	14.935	1.038	14.180	0.000	0.000	0.000
32	412.12	5.224	1.038	14.173	0.015	0.209	45.156
33	412.13	15.556	1.038	14.165	0.018	0.236	37.268

Table A5-1: System 5 Experimental Data – 50 wt% DEA + 50 wt% H_2O - 393.15 K									
Measurement	P_{CO2} (bar)	y_{N2}	y_{CO2}	y_{H2O}	x_{N2} ($x10^8$)	x_{CO2}	x_{H2O}	x_{DEA}	x_{MDEA}
34	10.501	0.120	0.829	0.051	1.279	0.039	0.820	0.141	0.000
35	4.504	0.719	0.148	0.133	1.205	0.021	0.835	0.143	0.000
36	1.501	0.912	0.018	0.070	1.504	0.007	0.848	0.145	0.000

Table A5-2: System 5 Experimental Data (contd.) – 50 wt% DEA + 50 wt% H_2O - 393.15 K							
Measurement	Average Temperature (K)	Average Pressure (bar)	Density of Solvent ρ_m (g/cm^3) at 393.15 K	Measured Volume of Solvent (cm^3)	Amount of CO_2 Charged (mol)	CO2 Loading (mol CO_2/mol DEA+MDEA)	Partition coefficient
34	392.11	14.839	1.054	14.165	0.036	0.394	21.241
35	392.13	15.000	1.054	14.173	0.021	0.273	6.911
36	392.13	14.971	1.054	14.187	0.007	0.091	2.735

Partition Coefficient Graphs

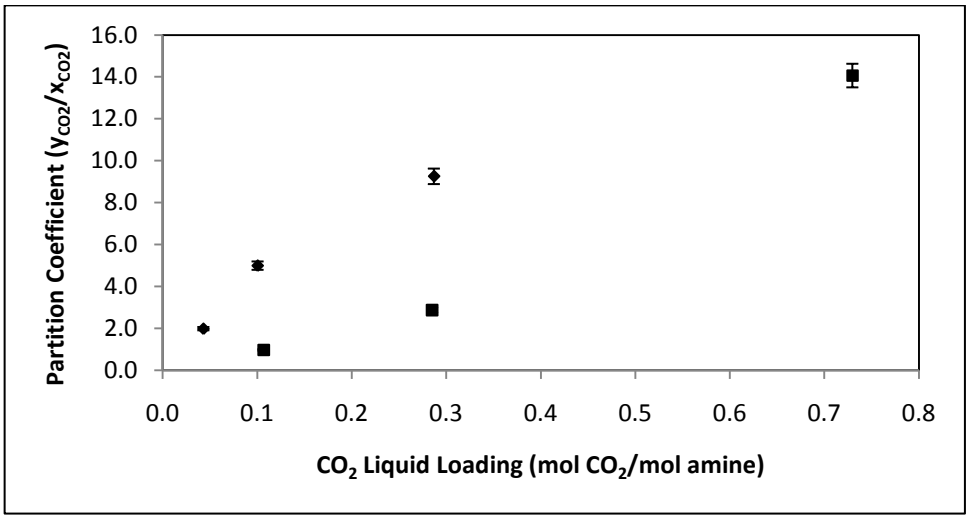

Figure A1: Partition coefficient vs CO_2 liquid loading for System 1: 25 wt% MDEA + 25 wt% DEA + 50wt% H_2O, 363.15 K. ■ – 15 bar pressure; ♦ - 5 bar pressure

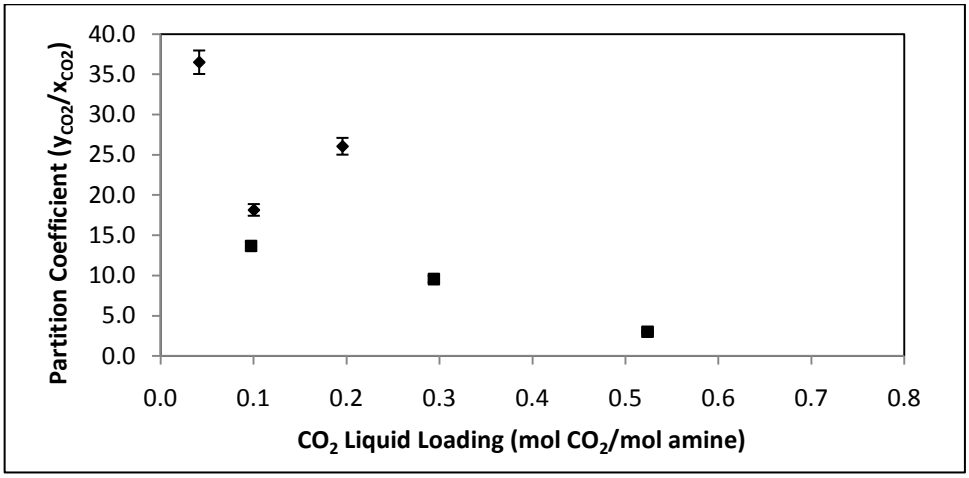

Figure A2: Partition coefficient vs CO_2 liquid loading for System 2: 25 wt% MDEA + 25 wt% DEA + 50 wt% H_2O, 413.15 K. ■ – 15 bar pressure; ♦ - 5 bar pressure

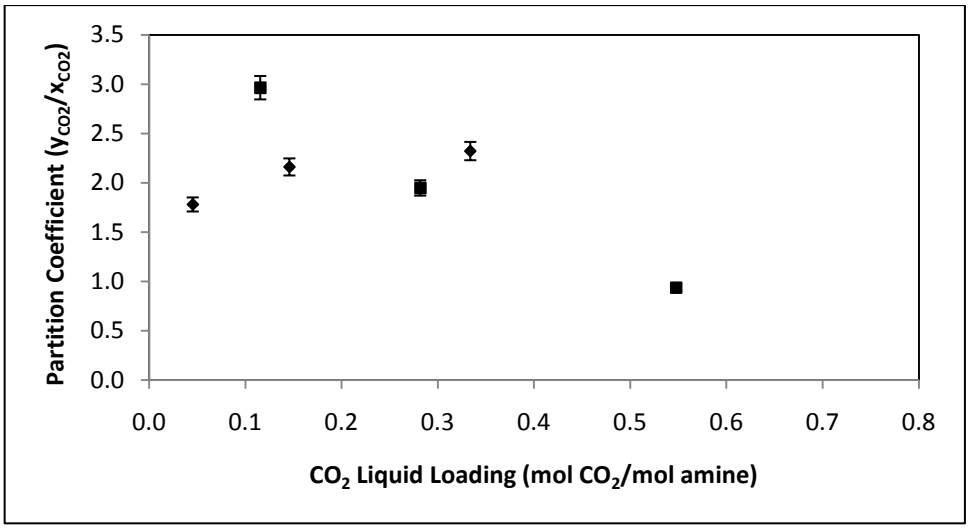

Figure A3: Partition coefficient vs CO_2 liquid loading for System 3: 30 wt% MDEA + 20 wt% DEA + 50 wt% H_2O, 363.16 K. ■ – 15 bar pressure; ♦ - 5 bar pressure

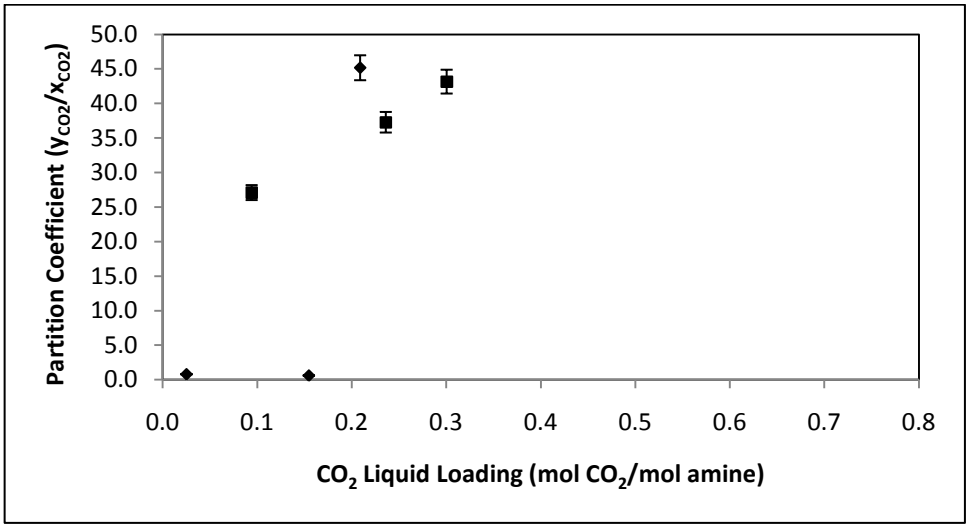

Figure A4: Partition coefficient vs CO_2 liquid loading for System 4: 30 wt% MDEA + 20 wt% DEA + 50 wt% H_2O, 413.15 K. ■ – 15 bar pressure; ♦ - 5 bar pressure

Appendix B: Calibration data

Table B1: N_2 Calibration Data: 50 - 500 µl syringe. N_2 Retention time - 0.22 min									
No.	V (µl)	P (mbar)	T(°C)	Moles (gmol)	Area	First Order Mole Estimate	Error (%)	Second Order Mole Estimate	Error (%)
1	50	1005.49	23.36	2.04E-06	90.22	2.26E-06	9.66	2.01E-06	-1.25
2	50	1005.49	23.41	2.04E-06	89.99	2.25E-06	9.50	2.01E-06	-1.48
3	50	1005.54	23.63	2.04E-06	89.89	2.25E-06	9.48	2.01E-06	-1.52
4	50	1005.54	23.63	2.04E-06	89.95	2.25E-06	9.53	2.01E-06	-1.45
5	50	1005.53	23.6	2.04E-06	90.55	2.26E-06	9.98	2.02E-06	-0.81
1	100	1004.49	23.32	4.08E-06	188.13	4.16E-06	1.97	4.11E-06	0.73
2	100	1005.46	23.5	4.08E-06	188.97	4.17E-06	2.31	4.12E-06	1.13
3	100	1005.46	23.58	4.08E-06	188.67	4.17E-06	2.20	4.12E-06	1.00
4	100	1005.46	23.58	4.08E-06	188.76	4.17E-06	2.25	4.12E-06	1.05
5	100	1005.46	23.58	4.08E-06	187.97	4.15E-06	1.88	4.10E-06	0.64
1	200	1005.19	22.98	8.17E-06	385.22	7.98E-06	-2.32	8.18E-06	0.16
2	200	1005.12	22.97	8.16E-06	384.77	7.97E-06	-2.42	8.17E-06	0.05
3	200	1005.09	23.04	8.16E-06	387.54	8.03E-06	-1.71	8.22E-06	0.76
4	200	1005.09	23.15	8.16E-06	385.19	7.98E-06	-2.25	8.18E-06	0.22
5	200	1005.09	23.17	8.16E-06	381.60	7.91E-06	-3.15	8.10E-06	-0.67
1	300	1005.06	23.38	1.22E-05	590.68	1.20E-05	-2.20	1.22E-05	0.00
2	300	1005.06	23.38	1.22E-05	587.36	1.19E-05	-2.75	1.22E-05	-0.52
3	300	1006.07	23.49	1.22E-05	588.24	1.19E-05	-2.67	1.22E-05	-0.45
4	300	1006.01	23.68	1.22E-05	584.73	1.19E-05	-3.19	1.21E-05	-0.94
5	300	1006.01	23.68	1.22E-05	591.69	1.20E-05	-2.03	1.22E-05	0.17
1	400	1006.23	23.71	1.63E-05	813.07	1.63E-05	-0.16	1.64E-05	0.52
2	400	1006.26	23.72	1.63E-05	809.05	1.62E-05	-0.64	1.63E-05	0.08
3	400	1006.27	23.75	1.63E-05	808.52	1.62E-05	-0.70	1.63E-05	0.03
4	400	1006.26	22.95	1.63E-05	811.34	1.62E-05	-0.63	1.64E-05	0.07
5	400	1006.26	22.95	1.63E-05	812.81	1.63E-05	-0.45	1.64E-05	0.23
1	500	1005.34	23.76	2.04E-05	1034.91	2.06E-05	1.08	2.03E-05	-0.24
2	500	1005.35	23.44	2.04E-05	1045.99	2.08E-05	2.00	2.05E-05	0.58
3	500	1005.49	22.95	2.04E-05	1041.94	2.07E-05	1.45	2.04E-05	0.06
4	500	1005.49	22.95	2.04E-05	1033.23	2.06E-05	0.64	2.03E-05	-0.67
5	500	1005.52	23.03	2.04E-05	1041.54	2.07E-05	1.43	2.04E-05	0.05

Calibration curve obtained using the LNST function in excel:

First order: n_{N2} = 1.9e-8(A) + 5.07e-07

Second order: n_{N2} = -2e-12(A^2) + 2.2e-8(A) + 4.75e-8

Where A = area obtained during integration using WINILAB III software.

Second order calibration was used as it produced less error.

Table B2: CO_2 Calibration Data: 50 - 250 µl syringe. CO_2 Retention time - 0.8 min									
No.	V (µl)	P (mbar)	T(°C)	Moles (gmol)	Area	First Order Mole Estimate	Error (%)	Second Order Mole Estimate	Error (%)
1	50	1000.22	23.07	2.03E-06	104.77	2.02E-06	-0.4	2.02E-06	-0.69
2	50	1000.22	23.07	2.03E-06	106.5	2.06E-06	1.21	2.05E-06	0.94
3	50	1000.22	23.06	2.03E-06	104.73	2.02E-06	-0.4	2.02E-06	-0.73
4	50	1000.22	23.07	2.03E-06	104.77	2.02E-06	-0.4	2.02E-06	-0.69
5	50	1000.22	23.07	2.03E-06	104.98	2.03E-06	-0.2	2.02E-06	-0.49
1	100	1000.13	23.07	4.06E-06	212.66	4.07E-06	0.22	4.08E-06	0.37
2	100	1000.13	23.08	4.06E-06	213.21	4.08E-06	0.48	4.09E-06	0.63
3	100	1000.13	23.09	4.06E-06	212.85	4.07E-06	0.32	4.08E-06	0.46
4	100	1000.15	23.09	4.06E-06	213.04	4.08E-06	0.41	4.08E-06	0.55
5	100	1000.14	23.1	4.06E-06	212.97	4.08E-06	0.38	4.08E-06	0.52
1	150	999.99	23.2	6.09E-06	317.98	6.07E-06	-0.3	6.07E-06	-0.22
2	150	1000.01	23.22	6.09E-06	316.94	6.05E-06	-0.6	6.05E-06	-0.54
3	150	999.99	23.22	6.09E-06	318.06	6.07E-06	-0.3	6.08E-06	-0.19
4	150	999.98	23.21	6.09E-06	317.95	6.07E-06	-0.3	6.07E-06	-0.22
5	150	999.99	23.22	6.09E-06	316.98	6.05E-06	-0.6	6.06E-06	-0.53
1	200	1000.03	23.18	8.12E-06	426.94	8.14E-06	0.22	8.13E-06	0.15
2	200	1000.03	23.17	8.12E-06	425.94	8.12E-06	-0	8.11E-06	-0.08
3	200	1000.04	23.19	8.12E-06	426.5	8.13E-06	0.12	8.12E-06	0.05
4	200	1000.03	23.17	8.12E-06	427.19	8.14E-06	0.28	8.13E-06	0.21
5	200	1000.04	23.17	8.12E-06	426.66	8.13E-06	0.15	8.12E-06	0.08
1	250	1000.21	23.06	1.02E-05	536.24	1.02E-05	0.56	1.02E-05	0.26
2	250	1000.21	23.06	1.02E-05	536.76	1.02E-05	0.65	1.02E-05	0.36
3	250	1000.21	23.06	1.02E-05	538.61	1.03E-05	0.99	1.02E-05	0.70
4	250	1000.21	23.06	1.02E-05	536.74	1.02E-05	0.65	1.02E-05	0.35
5	250	1000.21	23.06	1.02E-05	536.87	1.02E-05	0.67	1.02E-05	0.38

Calibration curve obtained using the LNST function in excel:

First order: n_{CO2} = 1.9e-8(A) + 3.46e-07

Second order: n_{CO2} = -1e-12(A^2) + 1.95e-8(A) – 1.87e-8

Second order calibration was used as it produced less error.

Table B3: H_2O Calibration: 1µl Syringe. Retention time - 5.2 min						
V (µl)	T (°C)	Area	H_2O Density (mol/dm^3)	Moles H_2O Injected	Moles Calculated	Déviation (%)
0.1	23.22	139.22	0.0583	5.83E-06	5.96E-06	2.12
0.1	23.19	140.09	0.0583	5.83E-06	5.99E-06	2.63
0.1	23.19	139.54	0.0583	5.83E-06	5.97E-06	2.31
0.1	23.2	139.68	0.0583	5.83E-06	5.97E-06	2.39
0.1	23.21	140.05	0.0583	5.83E-06	5.98E-06	2.61
0.2	23.22	305.6	0.0583	1.17E-05	1.17E-05	-0.01
0.2	23.91	308.78	0.0583	1.17E-05	1.18E-05	0.94
0.2	23.91	305.95	0.0583	1.17E-05	1.17E-05	0.11
0.2	23.93	310.04	0.0583	1.17E-05	1.18E-05	1.31
0.2	23.91	304.67	0.0583	1.17E-05	1.16E-05	-0.27
0.4	23.77	644.89	0.0583	2.33E-05	2.33E-05	-0.10
0.4	23.78	641.33	0.0583	2.33E-05	2.32E-05	-0.63
0.4	23.78	643.06	0.0583	2.33E-05	2.32E-05	-0.37
0.4	23.78	643.72	0.0583	2.33E-05	2.33E-05	-0.27
0.4	23.78	644.14	0.0583	2.33E-05	2.33E-05	-0.21
0.6	23.11	973.43	0.0583	3.50E-05	3.46E-05	-1.20
0.6	23.17	973.76	0.0583	3.50E-05	3.46E-05	-1.17
0.6	23.17	973.84	0.0583	3.50E-05	3.46E-05	-1.16
0.6	23.17	973.25	0.0583	3.50E-05	3.46E-05	-1.22
0.6	23.17	973.44	0.0583	3.50E-05	3.46E-05	-1.20
0.8	23.07	1336.09	0.0583	4.67E-05	4.70E-05	0.76
0.8	23.34	1330.75	0.0583	4.67E-05	4.68E-05	0.37
0.8	23.34	1331.99	0.0583	4.67E-05	4.69E-05	0.47
0.8	23.32	1333.76	0.0583	4.67E-05	4.69E-05	0.60
0.8	23.32	1332.97	0.0583	4.67E-05	4.69E-05	0.54
1	23.14	1659.32	0.0583	5.83E-05	5.81E-05	-0.38
1	23.73	1673.51	0.0583	5.83E-05	5.86E-05	0.47
1	23.72	1672.97	0.0583	5.83E-05	5.86E-05	0.44
1	23.72	1663.44	0.0583	5.83E-05	5.82E-05	-0.13
1	23.74	1665.48	0.0583	5.83E-05	5.83E-05	-0.01

Calibration curve obtained using the LNST function in excel:

First order: n_{H2O} = 3.43e-8(A) + 1.18e-06

First order calibration was used as it was more applicable.

Table B4: H_2O Calibration: 5µl Syringe. Retention time - 5.2 min						
V (µl)	T (°C)	Area	H_2O Density (mol/dm^3)	Moles H_2O Injected	Moles Calculated	Déviation (%)
1	22.67	1259.76	0.0583	5.83E-05	5.78E-05	-0.82
1	22.7	1260.04	0.0583	5.83E-05	5.79E-05	-0.81
1	22.7	1259.64	0.0583	5.83E-05	5.78E-05	-0.83
1	22.69	1260.4	0.0583	5.83E-05	5.79E-05	-0.79
1	22.69	1259.53	0.0583	5.83E-05	5.78E-05	-0.84
2	22.17	2969.2	0.0583	1.17E-04	1.17E-04	0.56
2	22.19	2971.52	0.0583	1.17E-04	1.17E-04	0.63
2	22.19	2972.22	0.0583	1.17E-04	1.17E-04	0.66
2	22.17	2975.34	0.0583	1.17E-04	1.18E-04	0.75
2	22.18	2975.25	0.0583	1.17E-04	1.18E-04	0.75
3	21.3	4682.8	0.0583	1.75E-04	1.77E-04	1.10
3	21.28	4688.36	0.0583	1.75E-04	1.77E-04	1.21
3	21.28	4688.25	0.0583	1.75E-04	1.77E-04	1.21
3	21.28	4684.11	0.0583	1.75E-04	1.77E-04	1.13
3	21.28	4685.72	0.0583	1.75E-04	1.77E-04	1.16
4	22.01	6191.03	0.0583	2.33E-04	2.29E-04	-1.68
4	22.02	6181.01	0.0583	2.33E-04	2.29E-04	-1.83
4	22.01	6193.43	0.0583	2.33E-04	2.29E-04	-1.64
4	22.01	6191.08	0.0583	2.33E-04	2.29E-04	-1.68
4	22.02	6183.72	0.0583	2.33E-04	2.29E-04	-1.79
5	22.64	8109.19	0.0583	2.92E-04	2.96E-04	1.55
5	22.15	7959.51	0.0583	2.92E-04	2.91E-04	-0.24
5	22.15	7987.72	0.0583	2.92E-04	2.92E-04	0.09
5	22.18	8080.22	0.0583	2.92E-04	2.95E-04	1.20
5	22.15	8004.69	0.0583	2.92E-04	2.92E-04	0.29

Calibration curve obtained using the LNST function in excel:

First order: $n_{H2O} = 3.48e\text{-}8(A) + 1.4e\text{-}05$

First order calibration was used as it was more applicable.

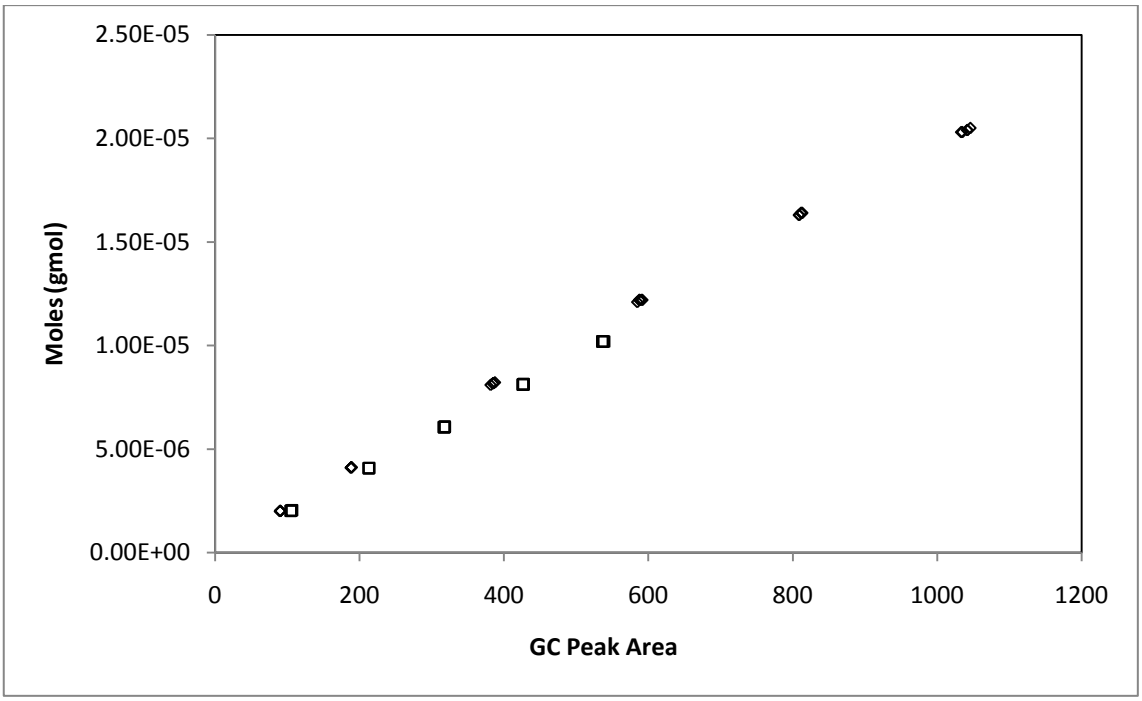

Figure B1: GC Peak Areas for N_2 and CO_2 gas: ◊ - N_2 Gas (50-500 µl Volumes); □ – CO_2 gas (50-250 µl Volumes)

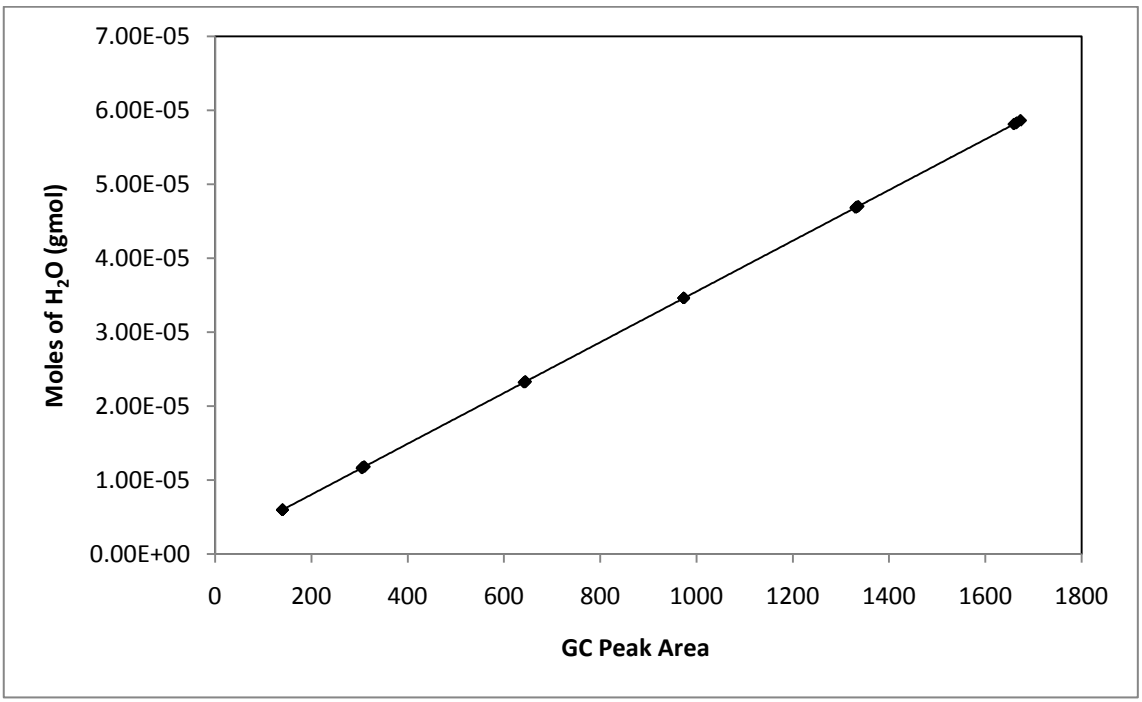

Figure B2: GC Peak Areas for H_2O liquid (1 µl Max. Volume)

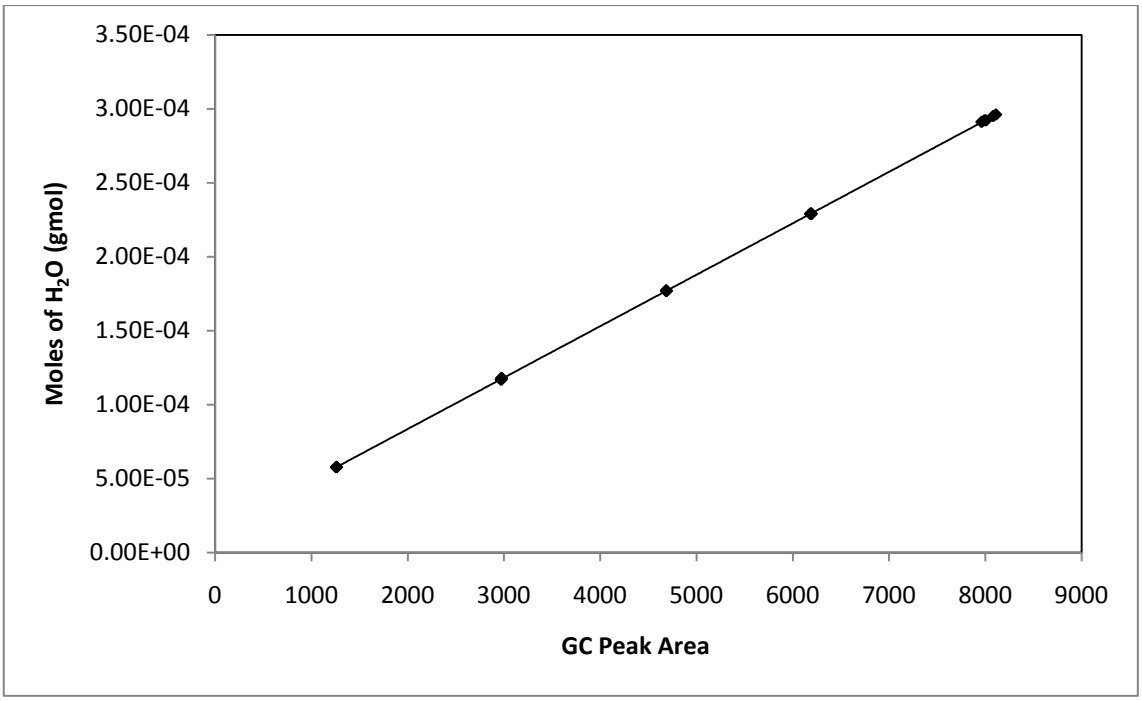

Figure B3: GC Peak Areas for H_2O liquid (5 µl Max. Volume)

Table B5: Density Calibration for MDEA+DEA+H_2O – 25+25+50 wt% Solvent	
Cell Temperature	**Density**
^oC	**g/cm^3**
5.001 (278.151 K)	1.061094
9.998	1.058801
14.996	1.056778
19.996	1.054993
24.997	1.053404
29.996	1.051986
34.996	1.050709
39.996	1.049559
44.997	1.048519
49.995	1.047574
54.994	1.046715
59.996	1.045932
64.996	1.045218
69.998 (343.148 K)	1.044557
2nd Calibration for Consistency	
5.002 (278.152 K)	1.061270
9.998	1.058971
14.996	1.056941
19.996	1.055146
24.995	1.053553
29.995	1.052129
34.996	1.050850
39.995	1.049694
44.996	1.048648
49.995	1.047701
54.995	1.046838
59.996	1.046054
64.997	1.045330
69.998 (343.148 K)	1.044561

The data was plotted in Microsoft Excel 2007 and it was found that it followed an exponential trend. The equation obtained was:

Density = -0.007ln(T) + 1.0738 where T = temperature (^oC). The equation possessed a 96.98 % fit to the data and was used to extrapolate for system temperatures of 363.15 K and 413.15 K.

Table B6: Density Calibration for MDEA+DEA+H_2O – 30+20+50 wt% Solvent	
Cell Temperature	**Density**
^oC	**g/cm^3**
5.002 (278.152 K)	1.059561
9.998	1.057211
14.995	1.055127
19.996	1.053280
24.994	1.051632
29.996	1.050149
34.996	1.048812
39.995	1.047600
44.996	1.046497
49.995	1.045491
54.995	1.044569
59.999	1.043722
64.996	1.042941
69.996 (343.146 K)	1.042222
2nd Calibration for Consistency	
5.001 (278.151 K)	1.059661
9.998	1.057372
14.994	1.055123
19.997	1.054280
24.998	1.051722
29.995	1.050149
34.999	1.049212
39.994	1.047598
44.994	1.046500
49.997	1.045511
54.995	1.044609
59.998	1.043702
64.996	1.043001
69.998 (343.148 K)	1.042252

The data were plotted in Microsoft Excel 2007 and it was found that it followed an exponential trend. The equation obtained was:

Density = -0.007ln(T) + 1.073 where T = temperature (^oC). The equation possessed a 96.85 % fit to the data and was used to extrapolate for system temperatures of 363.15 K and 413.15 K.

Table B7: Density Calibration for DEA+H_2O – 50+50 wt% Solvent	
Cell Temperature	**Density**
^oC	**g/cm^3**
5.001 (278.151 K)	1.067576
9.998	1.065522
14.996	1.063746
19.996	1.062203
24.996	1.060861
29.996	1.059688
34.996	1.058663
39.996	1.057765
44.997	1.056978
49.995	1.056292
54.994	1.055696
59.995	1.055174
64.995	1.054727
69.998 (343.148 K)	1.054345
2nd Calibration for Consistency	
5.001 (278.151 K)	1.067483
9.998	1.065430
14.996	1.063645
19.996	1.062099
24.995	1.060751
29.996	1.059576
34.995	1.058549
39.995	1.057650
44.998	1.056862
49.994	1.056172
54.995	1.055571
59.997	1.055050
64.996	1.054597
69.997 (343.147 K)	1.054210

The data were plotted in Microsoft Excel 2007 and it was found that it followed an exponential trend. The equation obtained was:

Density = -0.005ln(T) + 1.0776 where T = temperature (^oC). The equation possessed a 98.18 % fit to the data and was used to extrapolate for system temperatures of 363.15 K and 413.15 K.

Table B8: Pressure Transducer Calibration Data				
Actual Pressure (bar)	**HP Transducer Pressure (bar)**	**HP ^{2}**	**Pressure Calculated by Calibration (2nd Order) (bar)**	**Error**
1.002	1.078	1.162	1.004	-0.19%
1.002	1.078	1.162	1.004	-0.19%
1.002	1.078	1.162	1.004	-0.19%
3.002	3.071	9.431	3.000	0.27%
3.003	3.072	9.437	3.001	0.24%
4.002	4.073	16.589	4.003	-0.05%
5.003	5.071	25.715	5.002	0.10%
6.002	6.072	36.869	6.004	-0.20%
7.003	7.069	49.971	7.002	0.08%
8.002	8.069	65.109	8.003	-0.13%
9.003	9.065	82.174	9.001	0.25%
10.002	10.066	101.324	10.003	-0.05%
11.002	11.064	122.412	11.002	0.03%
11.003	11.063	122.390	11.001	0.20%
13.002	13.065	170.694	13.005	-0.29%
15.003	15.058	226.743	15.000	0.26%
17.002	17.059	291.009	17.003	-0.12%
19.003	19.055	363.093	19.001	0.12%
21.002	21.054	443.271	21.002	-0.03%
23.002	23.052	531.395	23.002	-0.03%
23.003	23.050	531.303	23.000	0.21%
25.002	25.052	627.603	25.004	-0.23%
27.002	27.049	731.648	27.003	-0.11%
27.003	27.046	731.486	27.000	0.23%
29.003	29.044	843.554	29.000	0.23%
31.002	31.048	963.978	31.006	-0.38%
33.002	33.042	1091.774	33.002	0.06%
35.002	35.045	1228.152	35.007	-0.44%
37.002	37.037	1371.739	37.000	0.21%
41.003	41.032	1683.625	40.999	0.38%
51.003	51.033	2604.367	51.007	-0.49%
61.003	61.019	3723.318	61.000	0.25%

Calibration curve obtained using the LNST function in excel:

Second order: Actual Pressure (bar) = -4.998e-6(HP^2) + 1.001(HP) – 0.075

Second order calibration was used as it was more applicable (produced the lowest error).

Appendix C: CO_2 loading calculation of measured results

This Appendix contains the calculation procedure for CO_2 loading using the VLE data measured, described in Section 2.8. The results of this calculation procedure are tabulated in Appendix A and discussed in Section 4.1.

The quantities measured experimentally are the liquid and vapour mole fractions of CO_2, H_2O, N_2, MDEA and DEA. The system temperature (K) and pressure (bar), the volume of the solvent charged (cm^3) and the solvent density (g/cm^3) is also measured. Liquid mole fractions of components in the prepared solvent were also known by preparation. Refer to the Nomenclature section of this thesis for relevant symbols.

Calculation Procedure:

Mass of charged solvent $m_s = \rho_S V_S$

Thus $n_{MDEA} = (x_{MDEA})(m_s)/(M_{MDEA})$

Similarly

$$n_{DEA} = (x_{DEA})(m_s)/(M_{DEA})$$

$$n_{H2O} = (x_{H2O})(m_s)/(M_{H2O})$$

$$n_{total} = n_{MDEA} + n_{DEA} + n_{H2O}$$

$$n_{amine} = n_{MDEA} + n_{DEA}$$

The amount of CO_2 charged into the cell was controlled by pressure difference under constant temperature. The CO_2 tank was used according to pressure difference.

Initial CO_2 Pressure in tank (P_{CO2}^1) was measured using pressure transducer, at constant temperature T_{CO2}. Final CO_2 Pressure in tank (P_{CO2}^2) after charging was also measured.

ρ_{CO2}^1 of CO_2 in tank before charging was obtained using ALLPROPS Property Package (developed by the Centre of Applied Thermodynamic Studies, University of Idaho, Moscow). (Taken at P_{CO2}^1 , T_{CO2})

ρ_{CO2}^2 of CO_2 in tank after charging was obtained using ALLPROPS Property Package (Taken at P_{CO2}^2, T_{CO2})

$$\Delta\rho_{CO2} = \rho_{CO2}^1 - \rho_{CO2}^2$$

The total volume of the CO_2 tank (V_{CO2}) was 101.692 cm^3

Thus moles taken from the CO_2 tank and loaded into the cell $n_{CO2} = \Delta\rho_{CO2} [\frac{mol}{dm^3}] \times V_{CO2} [dm^3]$

Total moles dissolved in solvent = $n_{MDEA} \times \frac{x_{CO2}}{x_{MDEA}}$

$V_C = V_C^{\ L} + V_C^{\ V}$ (assume swelling due to the addition of CO_2 is negligible)

Hence $V_C^{\ V} = V_C - V_C^{\ L}$

For CO_2, the molar balance is as follows:

$$n_{CO2} = n_{CO2}^L + n_{CO2}^V$$

In the vapor phase, the mole number of CO_2 is calculated considering the vapor phase composition.

$$n_{CO2}^V = \frac{V_C^{\ V}}{v_T^V} y_{CO2}$$

The molar volumes (v_i^v) of pure gases were used at T, and P to calculate molar volumes (v_T^v). The ALLPROPS Property Package was used to obtain molar volumes at the system temperature system pressure.

$$v_T^V \approx \sum_i y_i v_i^V = (y_{CO2})(v_{CO2}^{\ V}) + (y_{N2})(v_{N2}^{\ V}) + (y_{H2O})(v_{H2O}^{\ V})$$

Thus

$$n_{CO2}^V = \frac{V_C^{\ V}}{v_T^V} y_{CO2}$$

Finally, liquid loadings for CO_2 can be defined as

$$L_{CO_2} = \frac{n_{CO_2} - n_{CO_2}^V}{n_{MDEA} + n_{DEA}} = [mol\, CO_2 / mol \text{ amine}]$$

Appendix D: Modelling results

This appendix contains data relevant to the modelling done in Matlab R2009b. The two models programmed were the Posey-Tapperson-Rochelle model and the Deshmukh-Mather model (Deshmukh and Mather (1981)).

Table D1: Comparison of Experimental Results to Posey-Tapperson-Rochelle Model Predictions

System	Data Point	CO_2 Loading (mol CO_2/mol Amine)	P_{CO2} (Experimental) (bar)	P_{CO2} (Calculated) (bar)	Relative Error (%)
1	1	0	0	0	0
	2	0	0	0	0
	3	0	0	0	0
	6	0.1068	1.5	1.619	-0.079
	4	0.0431	0.611	0.699	-0.144
	5	0.1005	1.492	1.262	0.154
	7	0.285	4.496	4.091	0.090
	8	0.287	3.508	3.939	-0.123
	9	0.7297	10.51	10.509	9.51E-05
2	10	0	0	0	0
	12	0.0417	0.494	0.414	0.162
	13	0.0975	1.509	1.759	-0.166
	16	0.2944	4.5	4.727	-0.050
	14	0.1005	1.6	1.6	0
	11	0	0	0	0
	17	0.5244	11.529	11.509	0.002
	15	0.196	3.506	3.103	0.115
3	20	0.0453	0.571	0.818	-0.433
	21	0.1154	1.516	1.491	0.016
	25	0.5472	10.502	10.468	0.003
	23	0.2815	4.5	3.687	0.181
	24	0.3335	3.508	4.264	-0.216
	22	0.1457	1.517	1.493	0.016
	19	0	0	0	0
	18	0	0	0	0
4	28	0.0423	0.52	0.438	0.158
	29	0.0941	1.525	1.612	-0.057
	33	0.3002	10.5	10.485	0.001
	30	0.1544	1.52	1.626	-0.070
	26	0	0	0	0
	27	0	0	0	0
	31	0.2087	3.52	3.211	0.088
	32	0.2359	4.503	4.688	-0.041

Table D2: Regressed Posey-Tapperson-Rochelle Model Parameters for Systems 1 - 4					
System	**Regressed Parameters**				**Sum of Least Squares Error (bar)**
	A	**B**	**C**	**D**	
Original Posey et al.(1996)	32.0	-7440.0	33.0	-18.5	
1	-1360.20	495870.0	-33.662	6.064	0.0724
2	-4250.20	1755200.0	-35.379	10.261	0.0665
3	-548.74	201590.0	-37.918	11.251	0.1423
4	1903.30	-780670.0	12.838	-2.403	0.0493

Table D3: Comparison of Experimental Absorption data with Deshmukh-Mather Predictions				
System 1				
Data Point	**Experimental CO_2 loading (mol CO_2/mol Amine)**	**Predicted CO_2 loading (mol CO_2/mol Amine)**	**P_{CO2} (bar)**	**CO_2 Loading Error (%)**
1	0	0	0	0
2	0	0	0	0
3	0	0	0	0
4	0.1068	0.1068	1.5	3.65E-14
5	0.0431	0.0431	0.611	-2.96E-14
6	0.1005	0.1005	1.492	2.82E-14
7	0.285	0.285	4.496	3.89E-15
8	0.287	0.287	3.508	8.90E-15
9	0.7297	0.7297	10.51	9.13E-16
System 2				
Data Point	**Experimental CO_2 loading (mol CO_2/mol Amine)**	**Predicted CO_2 loading (mol CO_2/mol Amine)**	**P_{CO2} (bar)**	**CO_2 Loading Error (%)**
10	0	0	0	0
11	0.0417	0.0417	0.494	1.61E-13
12	0.0975	0.0975	1.509	1.57E-15
13	0.2944	0.2944	4.5	2.64E-15
14	0.1005	0.1005	1.6	3.96E-14
15	0	0	0	0
16	0.5244	0.5244	11.529	-2.33E-15
17	0.196	0.196	3.506	-8.64E-15
System 3				
Data Point	**Experimental CO_2 loading (mol CO_2/mol Amine)**	**Predicted CO_2 loading (mol CO_2/mol Amine)**	**P_{CO2} (bar)**	**CO_2 Loading Error (%)**
18	0.0453	0.0433	0.571	4.19E-02
19	0.1154	0.1213	1.516	-5.11E-02
20	0.5472	0.5475	10.502	-5.48E-04
21	0.2815	0.2791	4.5	8.53E-03
22	0.3335	0.3389	3.508	-1.62E-02
23	0.1457	0.1399	1.517	3.98E-02
24	0	0	0	0
25	0	0	0	0
System 4				
Data Point	**Experimental CO_2 loading (mol CO_2/mol Amine)**	**Predicted CO_2 loading (mol CO_2/mol Amine)**	**P_{CO2} (bar)**	**CO_2 Loading Error (%)**
26	0.0423	0.0418	0.52	1.18E-02
27	0.0941	0.0942	1.525	-1.06E-03
28	0.3002	0.3002	10.5	0.00E+00
29	0.1544	0.1503	1.52	2.66E-02
30	0	0	0	0
31	0	0	0	0
32	0.2087	0.2177	3.52	-4.31E-02
33	0.2359	0.2301	4.503	2.46E-02

Table D4: Binary Interaction Parameters: Regressed Values for System 1 - 4 Using Deshmukh-Mather Model. Literature Estimates Included					
a_{ij} [L/mol]	**System 1**	**System 2**	**System 3**	**System 4**	**Literature (Benamor and Aroua (2005))**
DEAH-DEA	0.1361	0.0773	0.006	-1.4668	8.01E-04
DEAH-CO_2	0.8549	-2.9919	-1.3964	7.6496	0.398
DEAH-$DEACOO^-$	26.2723	9.8808	-23.2358	-116.8301	4.7
DEAH-HCO_3^-	-0.6288	-0.5568	-0.1465	3.1311	0.377
DEA-DEA	0.4102	-23.1325	10.9029	-22.8453	0.703
DEA-CO_2	-0.0025	0.1959	7.03E-06	-0.0433	8.05E-06
DEA-$DEACOO^-$	-2.5769	-74.4943	-4.2209	68.6306	1.919
DEA-HCO_3^-	9.0506	-91.5338	12.6228	18.9861	4.521
CO_2-$DEACOO^-$	1.34E-05	0.0051	-4.25E-06	0.5914	1.84E-06
CO_2-HCO_3^-	3.3455	-5.98E+04	1.6631	9.10E+04	6.61E-04
MDEAH-CO_2	0.0178	1.0683	0.0004	0.0691	6.17E-05
MDEAH-HCO_3^-	0.9626	15.3728	-12.0634	-5.6645	1.024
MDEAH-CO_3^{2-}	-158.8	7.51E+04	4.9896	2.42E+03	0.725
MDEA-CO_2	-0.0017	-2.0881	0.0002	-0.0588	3.35E-05
MDEA-HCO_3^-	0.4036	1.7856	0.5962	3.8336	0.172
MDEA-CO_3^{2-}	-35.8346	5.73E+06	6.4842	-1.54E+06	0.972
CO_2-HCO_3^-	0.8116	0.086	-5.9981	0.7489	0.178
CO_2-CO_3^{2-}	-2.73E-05	-0.2806	0.002	-0.0158	9.58E-04
DEAH-MDEA	0.0052	5.34E+03	-0.01	110.6601	6.18E-04
DEA-$MDEA^+$	0.0002	-4.626	0.0007	4.2562	3.17E-05
DEA-MDEA	-4.18E-05	-0.9026	-0.0001	1.1224	3.44E-06
MDEAH-$DEACOO^-$	-0.1479	3.2685	1.072	17.0618	0.89
MDEA-$DEACOO^-$	1.2301	12.8166	1.7795	-41.5728	0.416
bij [L.K/mol]					
DEAH-DEA	0.001	-9.76E-04	0.0006	-0.003	-1.50E-04
DEAH-CO_3	6.45E-07	5.63E-04	-4.55E-08	2.04E-05	-1.99E-09
DEAH-$DEACOO^-$	0.0053	-0.0031	0.0768	0.3369	-0.012
DEAH-HCO_3^-	-4.96E-11	2.50E-06	2.43E-11	-7.68E-07	-6.78E-13
DEA-DEA	-2.98E-06	-5.70E-03	-5.04E-08	0.0903	-3.16E-08
DEA-CO_3	-1.19E-05	7.60E-04	-2.76E-06	-1.37E-04	-1.30E-07
DEA-$DEACOO^-$	-0.0076	0.0888	-0.0513	-0.2826	-0.005
DEA-HCO_3^-	-0.0174	2.13E-01	-0.0402	-0.0584	-0.013
CO_2-$DEACOO^-$	1.83E-06	0.00019084	1.24E-06	-0.0017	-6.51E-08
CO_2-HCO_3^-	6.40E-06	0.3328	-1.95E-06	-0.2861	-6.79E-04
MDEAH-CO_3	-9.68E-06	-0.0015	5.75E-06	2.41E-04	-1.93E-07
MDEAH-HCO_3^-	-0.0013	-0.0487	-0.0175	0.0516	-0.003
MDEAH-CO_3^{2-}	0.3168	-1.24E+05	-0.0202	0.6373	-0.003
MDEA-CO_3	-0.0001	-0.009	1.73E-06	-3.02E-04	-2.71E-07
MDEA-HCO_3^-	0.0002	0.0028	5.01E-06	-2.77E-04	-4.67E-06
MDEA-CO_3^{2-}	-0.3438	674.749	-0.0175	0.1742	-0.003
CO_2-HCO_3^-	-1.31E-06	6.96E-05	-3.36E-07	-1.97E-04	-4.39E-08
CO_2-CO_3^{2-}	0.0013	0.0017	-0.0002	-0.0019	-4.70E-05
DEAH-MDEA	-0.013	-12.9284	-0.3944	-0.072	-0.018
DEA-$MDEA^+$	-4.89E-07	0.0142	2.65E-07	-0.0036	-1.32E-08
DEA-MDEA	-0.0126	0.1059	-0.4183	-0.1388	-0.019
MDEAH-$DEACOO^-$	1.38E-07	-3.73E-07	-6.65E-08	-1.01E-04	-1.37E-08
MDEA-$DEACOO^-$	-0.0542	-0.0663	-0.3628	-0.0418	-0.018

Table D5: Equilibrium Constant and Henry Constant Parameters (Benamor and Aroua (2005))					
Constant (mol/L)	**a_i**	**b_i**	**c_i**	**d_i**	**Range of Validity (K)**
$K_{1,DEA}$	-3071.15	6.776904	0	-48.7594	273.13 – 353.15
$K_{1,MDEA}$	-8483.95	-13.8328	0	87.39717	393.15 – 333.15
K_2	-17067.2	-66.8007	0	439.709	313.15 – 331.15
K_3	-12092.1	-36.7816	0	235.482	273.15 – 498.15
K_4	-12431.7	-35.4819	0	220.067	273.15 – 499.15
K_5	-13445.9	-22.4773	0	140.932	273.15 – 500.15
H_{CO2}	-6789.04	-11.4519	-0.010454	94.4914	273.15 – 501.15

Appendix E: Matlab programme descriptions for modelling of experimental data

E1) Function: Data_Bank.m

This function contains all experimental data acquired for all 4 Systems that were studied. It is accessed by programmes using the Posey model (E3) and the Deshmukh Mather Model (E6).

E2) Function: Amine_Var.m

This function provides the Posey Model Parameter Estimates. It is where parameter regression occurs. The function is repeatedly utilised by Program (E3) until parameters that provide good loading estimates are achieved and error is minimised. Parameters A,B,C, and D for equation (2-1) repeated here:

$$\text{Ln}(K_{CO2}) = a + \frac{b}{T} + cL_T C^O{}_{AMINE} + d(L_T C^O{}_{AMINE})^{0.5} \text{.....(2-1)}$$

E3) Programme: Posey_Model.m

This program caters for the modelling of experimental data using the simple model contrived by Posey et al. (1996). The model calculates actual CO_2 loading by using the experimental data stored in the function Data_Bank (E1) and the calculation procedure described in Appendix C. It then calculates the CO_2 loading using measured data and thereafter uses this data to regress parameters for the Posey-Tapperson-Rochelle model using the function Amine_Var (Program (E2)). The accuracy of CO_2 loading predictions achieved by the regressed parameters are outputted and compared to the measured CO_2 loading graphically.

E4) Function: Newton_Raphson2.m

This function is used to calculate the H^+ concentration in the system, known in the function as Hconc, to satisfy the conditions of equation (2-15):

$$A[H^+]^6 + B[H^+]^5 + C[H^+]^4 + D[H^+]^3 + E[H^+]^2 + F[H^+] + G = 0 \text{.....(2-15)}$$

A-G are calculated in the Program Deshmukh12 (E6). Thereafter this function is called. Refer to the program Deshmukh12 (E6) to get a clear understanding of this.

E5) Function: Amine_Var_Desmukh7.m

This function is where the regression of the binary interaction parameters of the Deshmukh-

Mather model is done. Each binary interaction parameter was assigned an initial value, taken from Benamor and Aroua (2005) and thereafter modified to produce the lowest overall system error for all data points of a particular system. A least squares error value was sought to be minimised, as shown in the code.

Equilibrium constant values were modified in the process, due to the change in interaction prameters, according to the calculation procedure described in Benamor and Aroua (2005) and re-explained in the "Modelling of Experimental Data" section of this report (Equations 2-3 to 2-8). This enabled correct values of activity coefficients to be found, and good CO_2 Loading estimates to be achieved.

E6) Programme: Deshmukh12.m

This is the main programme for the Deshmukh-Mather modelling of the data investigated in this work. The programme accepts experimental data by calling the Data_Bank (E1) function and calculates actual CO_2 loading using the calculation procedure described in Appendix C. It provides first estimates for equilibrium and Henry constants using parameters found in Benamor and Aroua (2005) and charge estimates from Weiland et al. (1993). Initial binary interaction parameter estimates from Benamor and Aroua (2005), as well as calculations of Activity coefficients and other species concentrations are handled in this programme.

The programme utilises the fminsearch function and Amine_Var_Deshmukh7 (E5) for the interaction parameter regression. Input of desired system to investigate and output of binary interaction parameters and CO_2 loading estimates are handled in this programme as well.

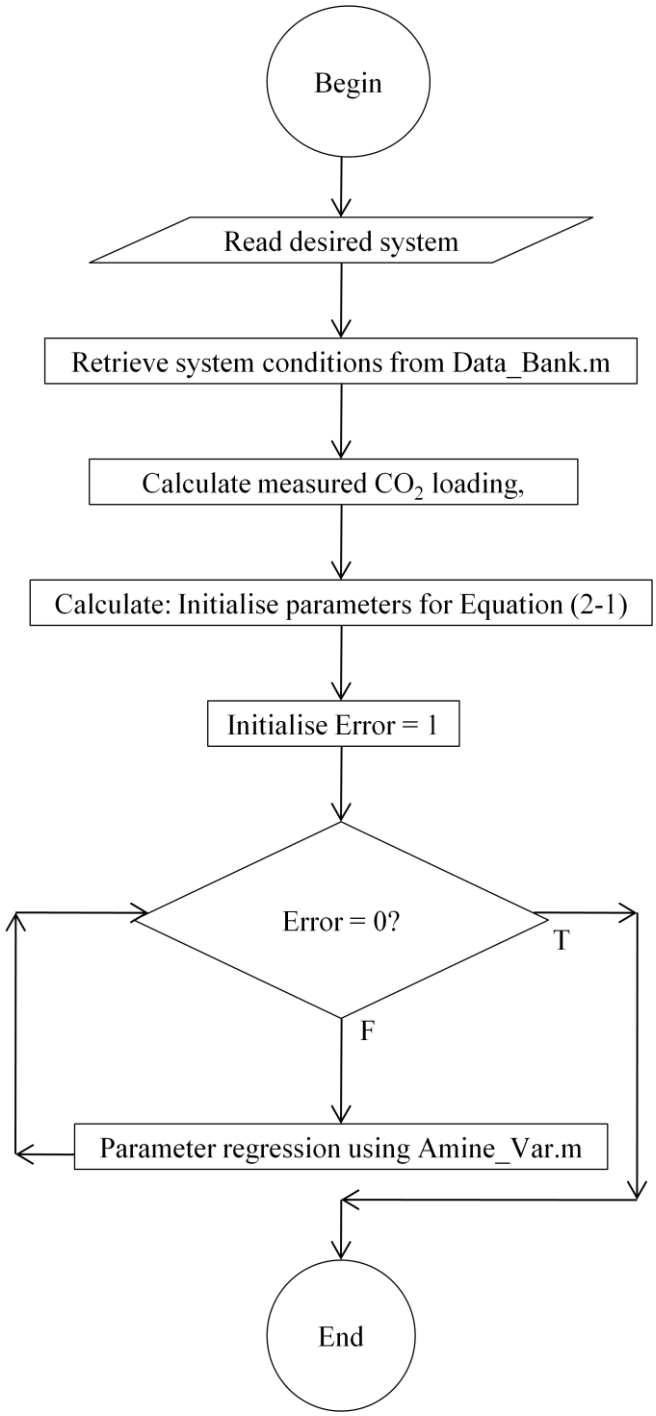

Figure E-1: Flowchart of Programme - Posey_Model.m

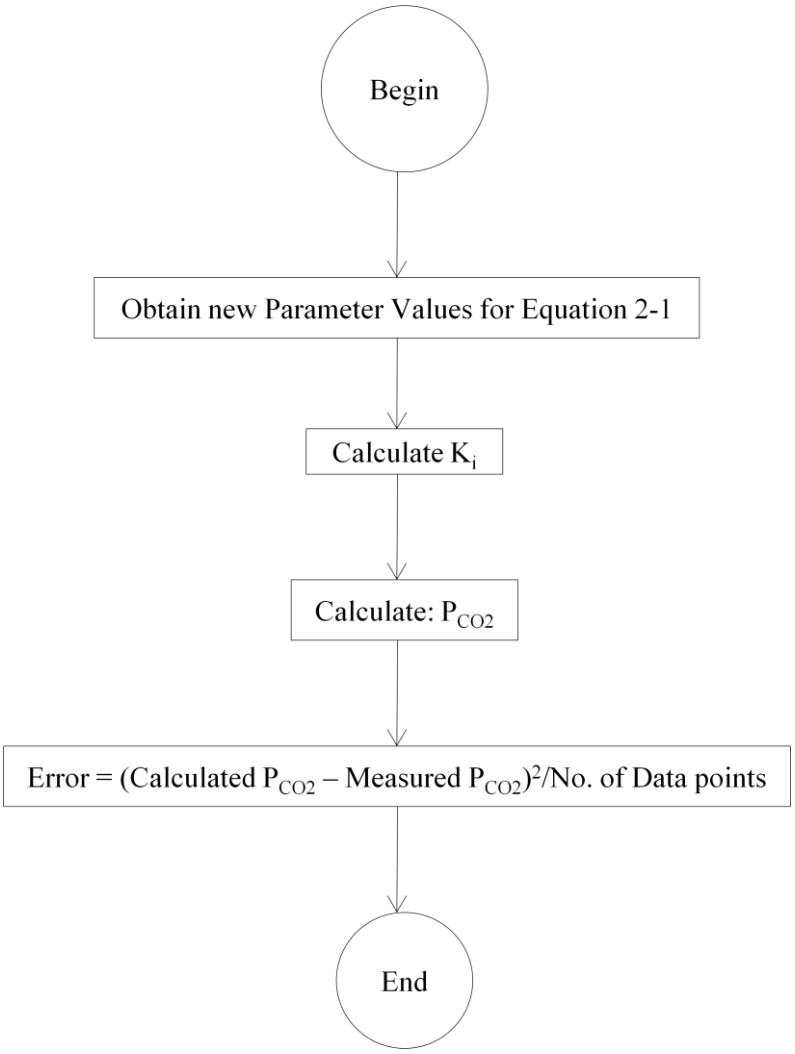

Figure E-2: Flowchart of Function Amine_Var.m

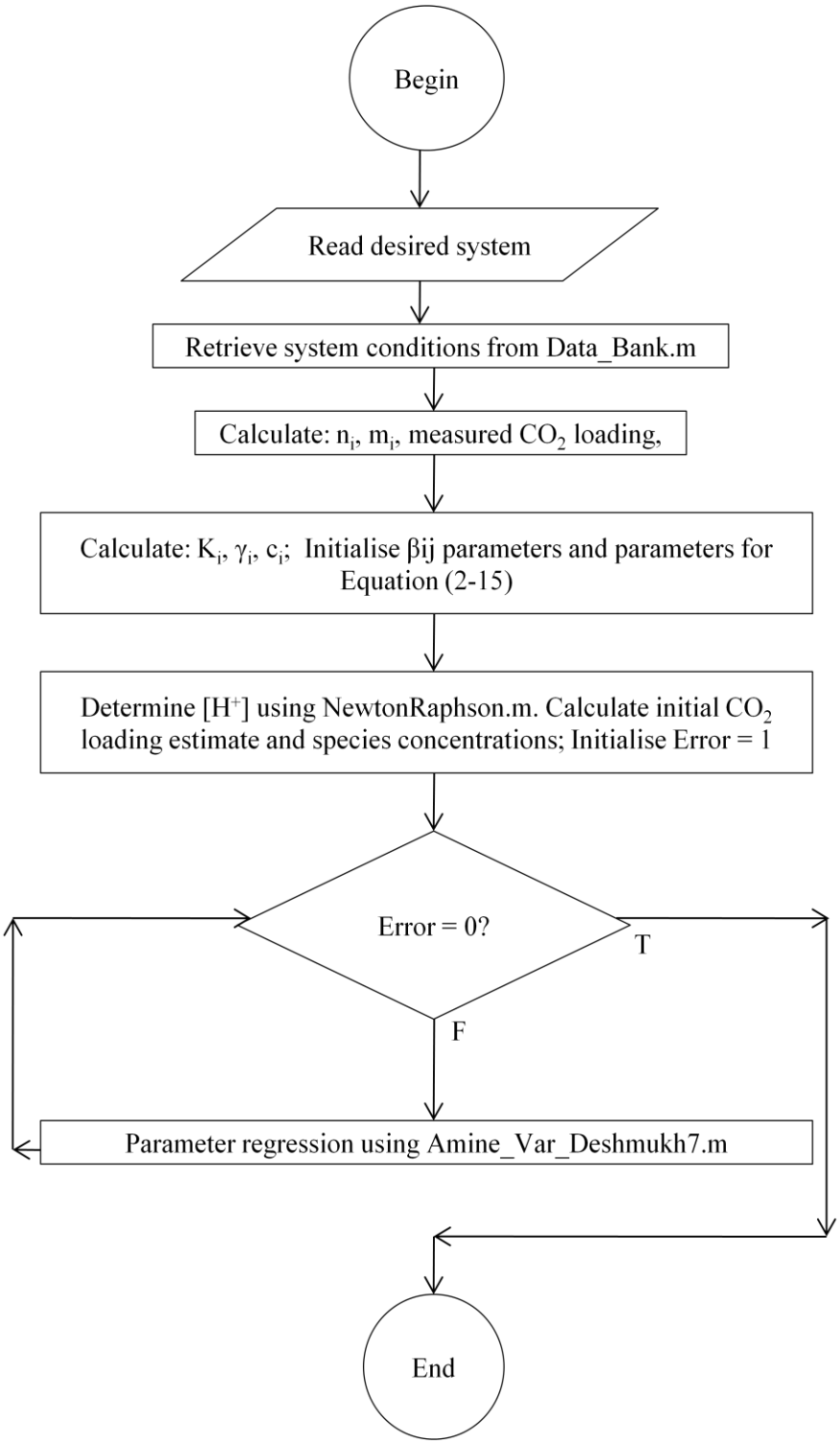

Figure E-3: Flowchart of Programme Deshmukh12.m

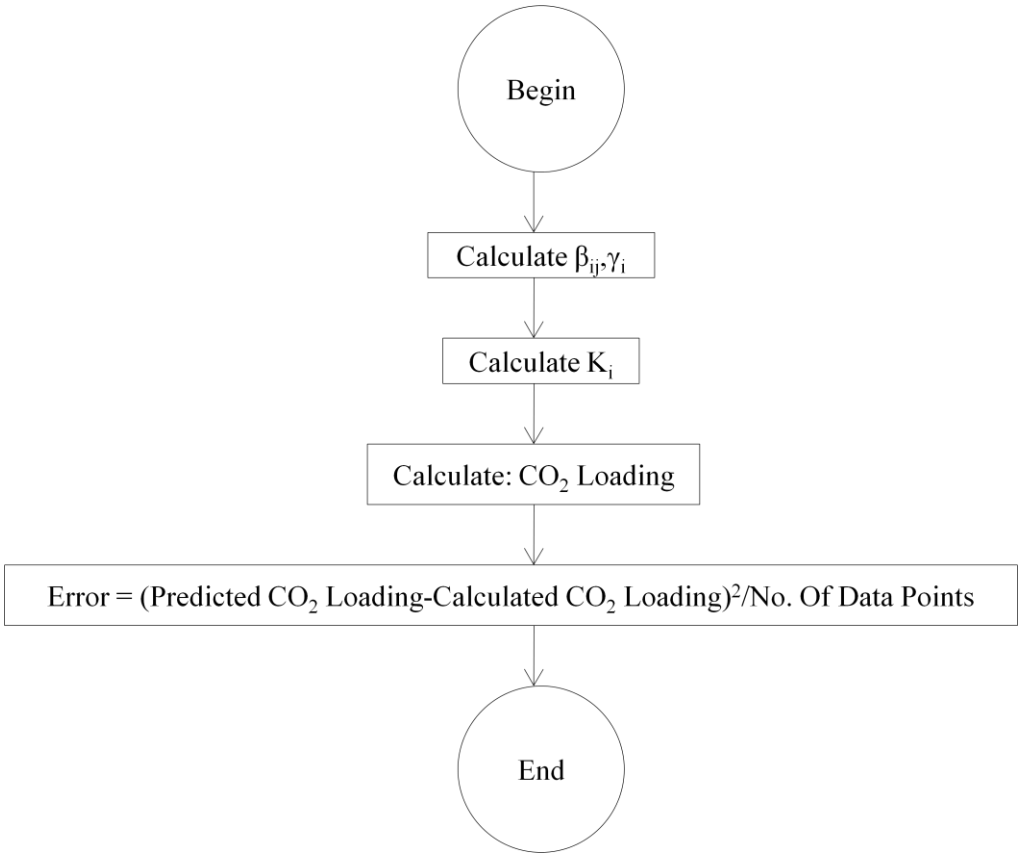

Figure E-4: Flowchart of Function - Amine_Var_Deshmukh7.m

Appendix F: Aspen simulation results

Table F1: Regressed Binary Interaction Parameter Estimates for Elec-NRTL Model Using Aspen Plus								
Species i	**Species j**	**a_{ij}**	**a_{ji}**	**b_{ij}**	**b_{ji}**	**c_{ij}**	**T_{lower} (K)**	**T_{upper} (K)**
CO_2	H_2O	10.064	10.064	18000.000	-5882.643	0.2	-273.15	473.15
MDEA	CO_2	-8.240	0	18000.000	0	0.3	-273.15	726.85
MDEA	H_2O	0	0	2680.094	0	0.3	-273.15	726.85
MDEA	N_2	0	0	1.413	0	0.3	-273.15	726.85
DEA	CO_2	-0.079	0	18000.000	0	0.3	-273.15	726.85
DEA	H_2O	0	0	-590.336	0	0.3	-273.15	726.85
DEA	N_2	0	0	-0.300	0	0.3	-273.15	726.85
CO_2	N_2	0	0	-0.013	0	0.3	-273.15	726.85
H_2O	N_2	0	0	-0.330	0	0.3	-273.15	726.85
MDEA	DEA	0	292.685	5278.482	269.118	0.3	-273.15	726.85
MDEA	$DEAH^+$	0	0	0	0	0.3	-273.15	726.85
DEA	$MDEAH^+$	0	0	0	0	0.3	-273.15	726.85
MDEA	$DEACOO^-$	0	0	0	0	0.3	-273.15	726.85
$MDEAH^+$	$DEACOO^-$	0	0	0	0	0.3	-273.15	726.85
DEA	$DEACOO^-$	0	0	0	0	0.3	-273.15	726.85
$DEAH^+$	$DEACOO^-$	0	0	0	0	0.3	-273.15	726.85
CO_2	$DEACOO^-$	0	0	0	0	0.3	-273.15	726.85
$DEAH^+$	HCO_3^-	0	0	0	0	0.3	-273.15	726.85
DEA	HCO_3^-	0	0	0	0	0.3	-273.15	726.85
CO_2	HCO_3^-	0	0	0	0	0.3	-273.15	726.85
$MDEAH^+$	HCO_3^-	0	0	0	0	0.3	-273.15	726.85
MDEA	HCO_3^-	0	0	0	0	0.3	-273.15	726.85
d_{ij}, e_{ij} and f_{ij} were all found to be zero, by Aspen regression routines								

Table F2: Observed Results drawn from Aspen Simulation data (no recycle)									
Data Pnt.	**CO_2 In Flue Gas (kmol/s)**	**N_2 In Flue Gas (kmol/s)**	**CO_2 Vapor Purity In Flue Gas (%)**	**Solvent into Absorber (kmol/s)**	**Potential CO_2 Loading (mol CO_2/mol Amine)**	**CO_2 Loading in Solvent 3 (kmol/s)**	**CO_2 Lost to stack (kmol/s)**	**CO_2 Recovery From the Absorber (%)**	**N_2 in Stack (kmol/s)**
4	1.038	9.34	10.00	29.31	0.035	0.033	0.064	93.785	7.32
5	1.359	9.01	13.11	29.31	0.046	0.015	0.934	31.299	8.43
6	3.175	7.21	30.58	29.31	0.108	0.035	2.155	32.140	6.72
7	3.134	7.26	30.14	29.31	0.107	0.094	0.359	88.549	5.73
8	7.326	3.10	70.29	29.31	0.250	0.077	5.033	31.295	2.88
9	6.444	3.93	62.11	29.31	0.220	0.197	0.666	89.662	3.00
11	0.955	9.42	9.20	29.31	0.033	0.003	0.857	10.272	9.06
12	1.058	9.32	10.20	29.31	0.036	0.007	0.845	20.155	8.37
13	3.092	7.28	29.80	29.31	0.106	0.022	2.460	20.446	6.52
14	2.418	7.96	23.30	29.31	0.082	0.009	2.161	10.608	7.59
16	7.191	3.19	69.30	29.31	0.245	0.055	5.585	22.340	2.81
17	6.807	3.57	65.60	29.31	0.232	0.024	6.118	10.127	3.43
18	1.173	9.20	11.30	28.99	0.040	0.014	0.769	34.406	8.55
19	1.577	8.80	15.20	28.99	0.054	0.035	0.567	64.028	7.55
20	6.319	4.06	60.90	28.99	0.218	0.197	0.595	90.585	3.09
21	3.123	7.25	30.10	28.99	0.108	0.094	0.388	87.580	5.73
22	7.336	3.04	70.70	28.99	0.253	0.077	5.105	30.419	2.83
23	3.082	7.29	29.70	28.99	0.106	0.035	2.065	32.990	6.78
26	1.079	9.30	10.40	28.99	0.037	0.004	0.971	9.999	8.96
27	1.058	9.32	10.20	28.99	0.037	0.007	0.848	19.865	8.36
28	6.849	3.53	66.00	28.99	0.236	0.049	5.424	20.797	3.14
29	2.968	7.41	28.60	28.99	0.102	0.01	2.672	9.956	7.13
32	6.994	3.38	67.40	28.99	0.241	0.024	6.305	9.850	3.26
33	2.999	7.38	28.90	28.99	0.103	0.021	2.384	20.518	6.59

Table F3: Observed Results drawn from Aspen Simulation data (no recycle) (Continued)								
Point	**Amine lost to Stack (kmol/s)**	**H_2O lost to Stack (kmol/s)**	**Amine lost from Stripping (kmol/s)**	**H_2O lost from Stripping (kmol/s)**	**CO_2 Recovered from Stripping (kmol/s)**	**N_2 lost from Stripping (kmol/s)**	**CO_2 Recovery from the Total Process (%)**	**CO_2 Vapor Purity from Stripper (%)**
4	0.0001	0.322	0.0027	2.398	0.971	4.03	93.613	19.404
5	0.0004	1.414	0.0572	45.463	0.430	3.20	31.628	11.832
6	0.0003	1.320	0.0385	33.097	1.015	3.09	31.977	24.714
7	0.0001	0.277	0.0034	3.019	2.750	3.54	87.758	43.690
8	0.0003	1.260	0.0452	37.452	2.247	2.82	30.672	44.369
9	0.0000	0.161	0.0041	3.475	5.765	2.80	89.466	67.313
11	0.0094	12.309	0.0131	12.001	0.098	2.95	10.272	3.219
12	0.0022	2.558	0.0017	1.538	0.213	2.98	20.100	6.658
13	0.0021	2.494	0.0018	1.583	0.630	2.77	20.384	18.549
14	0.0065	8.190	0.0072	6.473	0.256	2.90	10.608	8.136
16	0.0020	2.189	0.0018	1.570	1.598	2.27	22.220	41.362
17	0.0096	12.434	0.0160	14.353	0.689	2.72	10.127	20.199
18	0.0004	1.251	0.0266	22.188	0.403	3.25	34.406	11.051
19	0.0002	0.544	0.0051	4.197	1.010	3.60	64.024	21.894
20	0.0001	0.156	0.0044	3.391	5.710	2.83	90.358	66.861
21	0.0001	0.277	0.0038	3.004	2.732	3.54	87.466	43.541
22	0.0004	1.261	0.0512	38.116	2.232	2.81	30.419	44.224
23	0.0004	1.249	0.0304	24.746	1.017	3.11	32.990	24.636
26	0.0115	13.735	0.0197	16.055	0.108	2.94	9.999	3.542
27	0.0024	2.526	0.0019	1.514	0.210	2.98	19.814	6.571
28	0.0023	2.344	0.0021	1.631	1.419	2.34	20.724	37.743
29	0.0108	12.600	0.0163	13.383	0.295	2.87	9.956	9.335
32	0.0111	12.871	0.0196	15.758	0.689	2.72	9.850	20.213
33	0.0023	2.406	0.0019	1.522	0.613	2.77	20.453	18.109

Table F4: Results of Aspen Absorption Simulation With Recycle									
Data Pnt.	**CO_2 In Flue Gas (kmol/s)**	**N_2 In Flue Gas (kmol/s)**	**CO_2 Vapor Purity In Flue Gas (%)**	**Solvent into Absorber (kmol/s)**	**Potential CO_2 Loading (mol CO_2/mol Amine)**	**CO_2 Loading in Solvent 3 (kmol/s)**	**CO_2 Lost to stack (kmol/s)**	**CO_2 Recovery From the Absorber (%)**	**N_2 in Stack (kmol/s)**
4	1.038	9.339	10.00	58.7341	0.0177	0.0173	0.0210	97.971	6.6282
5	1.359	9.017	13.10	58.7394	0.0231	0.0097	0.7911	41.804	8.2796
6	3.175	7.201	30.60	58.7393	0.0541	0.0238	1.7756	44.080	6.5650
7	3.134	7.243	30.20	58.7344	0.0534	0.0530	0.0225	99.283	4.9852
8	7.326	3.051	70.60	58.7393	0.1247	0.0578	3.9326	46.319	2.7583
9	6.444	3.933	62.10	58.7335	0.1097	0.1097	0.0001	99.999	2.0200
11	0.955	9.422	9.20	58.7290	0.0163	0.0022	0.8250	13.584	9.0253
12	1.058	9.318	10.20	58.7320	0.0180	0.0058	0.7170	32.255	8.0762
13	3.092	7.284	29.80	58.7320	0.0527	0.0177	2.0540	33.576	6.2607
14	2.418	7.959	23.30	58.7324	0.0412	0.0065	2.0344	15.855	7.5260
16	7.191	3.186	69.30	58.7315	0.1224	0.0478	4.3852	39.019	2.6419
17	6.807	3.570	65.60	58.7292	0.1159	0.0159	5.8762	13.676	3.4171
18	1.173	9.204	11.30	58.0557	0.0202	0.0091	0.6452	44.972	8.3788
19	1.577	8.799	15.20	58.0531	0.0272	0.0214	0.3376	78.593	7.1409
20	6.319	4.057	60.90	58.0489	0.1089	0.1089	0.0001	99.999	2.0829
21	3.123	7.253	30.10	58.0501	0.0538	0.0533	0.0274	99.122	5.0102
22	7.336	3.040	70.70	58.0557	0.1264	0.0574	4.0055	45.402	2.7525
23	3.082	7.295	29.70	58.0556	0.0531	0.0239	1.6920	45.098	6.6229
26	1.079	9.298	10.40	58.0422	0.0186	0.0023	0.9435	12.573	8.9401
27	1.058	9.318	10.20	58.0474	0.0182	0.0058	0.7239	31.608	8.0718
28	6.849	3.528	66.00	58.0472	0.1180	0.0422	4.3984	35.776	2.9727
29	2.968	7.409	28.60	58.0440	0.0511	0.0067	2.5811	13.028	7.1035
32	6.994	3.383	67.40	58.0438	0.1205	0.0157	6.0840	13.010	3.2435
33	2.999	7.378	28.90	58.0472	0.0517	0.0173	1.9962	33.436	6.3173

Table F5: Results of Aspen Absorption Simulation With Recycle (Continued)								
Data Point	Amine lost to Stack (kmol/s)	H_2O lost to Stack (kmol/s)	Amine lost from Stripping (kmol/s)	H_2O lost from Stripping (kmol/s)	CO_2 Recovered from Stripping (kmol/s)	N_2 lost from Stripping (kmol/s)	CO_2 Recovery from the Total Process (%)	CO_2 Vapor Purity from Stripper (%)
4	0.0001	0.286	0.0075	151.332	1.0166	2.711	97.971	27.275
5	0.0003	1.344	0.0020	161.935	0.5683	0.738	41.804	43.510
6	0.0003	1.191	0.0021	161.713	1.3996	0.637	44.080	68.740
7	0.0001	0.217	0.0072	151.259	3.1113	2.258	99.283	57.949
8	0.0003	0.981	0.0021	162.356	3.3934	0.292	46.320	92.064
9	0.0000	0.077	0.0082	149.601	6.4439	1.913	99.999	77.111
11	0.0103	13.060	0.0024	151.080	0.1297	0.397	13.584	24.632
12	0.0020	2.402	0.0076	150.052	0.3414	1.242	32.257	21.559
13	0.0019	2.249	0.0078	149.860	1.0383	1.024	33.576	50.350
14	0.0062	7.897	0.0031	153.027	0.3834	0.433	15.856	46.961
16	0.0015	1.752	0.0086	148.943	2.8059	0.544	39.020	83.767
17	0.0101	12.802	0.0024	151.456	0.9309	0.153	13.676	85.922
18	0.0003	1.190	0.0025	160.944	0.5273	0.825	44.972	38.983
19	0.0001	0.484	0.0052	155.291	1.2396	1.659	78.594	42.773
20	0.0000	0.077	0.0096	149.277	6.3193	1.974	99.999	76.195
21	0.0001	0.217	0.0083	151.121	3.0960	2.243	99.123	57.986
22	0.0003	0.990	0.0025	162.381	3.3309	0.288	45.403	92.044
23	0.0003	1.126	0.0025	161.158	1.3899	0.672	45.098	67.410
26	0.0136	15.521	0.0026	149.865	0.1357	0.357	12.573	27.514
27	0.0022	2.374	0.0089	149.841	0.3346	1.247	31.610	21.160
28	0.0019	1.936	0.0094	149.260	2.4502	0.555	35.777	81.522
29	0.0117	13.348	0.0028	151.010	0.3866	0.306	13.028	55.859
32	0.0119	13.511	0.0027	151.116	0.9099	0.139	13.010	86.719
33	1.9965	2.173	0.0093	149.497	1.0027	1.061	33.436	48.598

Table F6: Heat Duties of Absorption Process with Recycle						
Data Pnt.	**HEX 1 Duty (kW)**	**HEX2 Duty (kW)**	**Stripper Condenser Duty (kW)**	**Stripper Reboiler Duty (kW)**	**Maximum Duty Required (MW)**	**Energy Penalty (GJ/ton CO_2)**
4	2252022	-3446000	-5091000	14207000	7922	173.47
5	2587060	-2107000	-5722000	12325000	7083	118.40
6	2617599	-2149000	-5729000	12390000	7130	51.02
7	2261622	-3436000	-5150000	14236000	7912	57.37
8	2875295	-2178000	-5809000	12310000	7198	22.33
9	2278357	-3630000	-5156000	14509000	8001	28.21
11	1037739	-1306000	-5280000	12164000	6616	157.46
12	648909	-2365000	-4976000	14058000	7366	158.13
13	640054	-2390000	-4980000	14114000	7384	54.26
14	866661	-1490000	-5292000	12708000	6793	63.84
16	618539	-2525000	-4961000	14330000	7463	23.58
17	1093823	-1301000	-5316000	12143000	6620	22.10
18	2471960	-2190000	-5667000	12512000	7127	138.11
19	2298775	-2913000	-5333000	13565000	7618	109.74
20	2308426	-3693000	-5137000	14544000	8022	28.85
21	2287415	-3469000	-5144000	14245000	7919	57.61
22	2906945	-2186000	-5809000	12286000	7198	22.29
23	2560551	-2194000	-5699000	12483000	7151	52.72
26	1119685	-1253000	-5258000	11934000	6543	137.76
27	653507	-2389000	-4966000	14082000	7381	158.44
28	631050	-2468000	-4977000	14243000	7429	24.65
29	1075920	-1288000	-5289000	12107000	6606	50.58
32	1130546	-1279000	-5310000	12060000	6602	21.45
33	644358	-2440000	-4958000	14166000	7412	56.16

Appendix G: Preliminary design specifications of equipment

Table G1: Absorber Specifications	
Number of Trays in Design	29
Tray Type	Sieve Tray
Tray Spacing (m)	0.61
Column Diameter (m)	14.63
Design pressure (bar)	15.65
Design temperature (K)	400.15
Material used	Carbon Steel

Table G2: Stripper Specifications	
Number of Trays in Design	6
Tray Type	Sieve Tray
Tray Spacing (m)	0.61
Column Diameter (m)	20
Design pressure (bar)	15.65
Design temperature (K)	536.15
Material	Carbon Steel

Table G3: HEX1 Specifications	
Heat Exchanger Type	U Tube
No. of Shell Passes	1
No. of Tube Passes	2
Tube length (m)	6
Heat Transfer Area (m^2)	62997
Tube Design temp. (K)	465.15
Tube design pressure (bar)	10.13
Shell design pressure (bar)	15.705
Shell design temp. (K)	455.15
Tube Material	Unspecified

Table G4: HEX2 Specifications	
Heat Exchanger Type	U Tube
No. of Shell Passes	1
No. of Tube Passes	2
Tube length (m)	6
Heat Transfer Area (m^2)	32960
Tube Design temp. (K)	537.15
Tube design pressure (bar)	10.13
Shell design pressure (bar)	15.705
Shell design temp. (K)	537.15
Tube Material	Unspecified

Table G5: Stream results for Designed Aspen Flowsheet based on Data Point 4 (Solvent: 25 wt% + 25wt% + 50wt% - MDEA + DEA + H_2O, System Temperature of 90°C, System Pressure of 15 bar, P_{CO2} = 1.5 bar)						
	Stream					
	SOLVENT2	FLUEGAS	STACK	SOLVENT3	SOLVENT4	CO_2
Mole Flow (kmol/s)						
DEA	15.63	0	1.07E-05	31.25	31.25	0
MDEA	13.74	0	6.60E-05	27.48	27.48	0.01
CO_2	0	1.04	0.02	1.02	1.02	1.02
N_2	0	9.34	6.63	2.71	2.71	2.71
H_2O	181.67	0	0.29	211.44	211.44	151.33
Total Flow (kmol/s)	211.04	10.38	6.94	273.90	273.90	155.07
Total Flow (kg/s)	6553.6	307.3	191.8	10490.4	10490.4	2847.8
Total Flow (m^3/s)	6.68	20.78	13.90	10.84	19.46	381.31
Temperature (K)	362.17	362.17	362.27	362.68	428.15	470.40
Pressure (bar)	15	15	15	15	15	15
Vapor Fraction	0	1	1	0	0.013	1
Liquid Fraction	1	0	0	1	0.987	0
Enthalpy (J/kmol)	-3.06E+08	-3.75E+07	-9.37E+06	-3.18E+08	-3.09E+08	-2.33E+08
Enthalpy (J/kg)	-9.86E+06	-1.27E+06	-3.39E+05	-8.29E+06	-8.08E+06	-1.27E+07
Enthalpy (W)	-6.46E+10	-3.89E+08	-6.50E+07	-8.70E+10	-8.47E+10	-3.62E+10
Density (kmol/m^3)	31.61	0.50	0.50	25.27	14.07	0.41
Density (kg/m^3)	981.48	14.79	13.80	967.85	539.04	7.47
Average MW (kg/kmol)	31.05	29.61	27.65	38.30	38.30	18.37

Table G5 (Contd.): Stream results for Designed Aspen Flowsheet based on Data Point 4				
	Stream			
	SOLVENT1	1	RECYCLE	SOLVENT5
Mole Flow (kmol/s)				
DEA	31.25	31.25	15.63	15.63
MDEA	27.47	27.47	13.74	13.74
CO_2	0.00	0.00	0.00	0.00
N_2	0.00	0.00	0.00	0.00
H_2O	60.11	60.11	30.05	30.05
Total Flow (kmol/s)	118.83	118.83	59.42	59.42
Total Flow (kg/s)	7642.6	7642.6	3821.3	3821.3
Total Flow (m^3/s)	9.23	7.70	3.85	3.85
Temperature (K)	509.39	362.17	362.17	362.17
Pressure (bar)	15	15	15	15
Vapor Fraction	0	0	0	0
Liquid Fraction	1	1	1	1
Enthalpy (J/kmol)	-3.42E+08	-3.71E+08	-3.71E+08	-3.71E+08
Enthalpy (J/kg)	-5.31E+06	-5.76E+06	-5.76E+06	-5.76E+06
Enthalpy (W)	-4.06E+10	-4.40E+10	-2.20E+10	-2.20E+10
Density (kmol/m^3)	12.87	15.43	15.43	15.43
Density (kg/m^3)	827.61	992.51	992.51	992.51
Average MW (kg/kmol)	64.31	64.31	64.31	64.31

Appendix H: Costing table

Table H1: Estimated Capital Costs		
Unit	**Cost (R) (2008)**	**Cost (R) (2010)**
Absorber	79437813	88970351
Tower	78519420	87941750
Pumparound	918393	1028600
Stripper	52881833	59227652
Tower	23555826	26382525
Pumparound	2156704	2415508
Condenser	12741554	14270540
Reflux Pump	6988695	7827338
Reboiler	7439054	8331740
HEX1	11051117	12377251
HEX2	6590654	7381532
Capital Cost	181288233	203042821